

UNCLASSIFIED

AD NUMBER

ADB015295

LIMITATION CHANGES

TO:

Approved for public release; distribution is unlimited.

FROM:

Distribution authorized to U.S. Gov't. agencies only; Test and Evaluation; 22 MAR 1976. Other requests shall be referred to Air Force Avionics Laboratory, Air Force Systems Command, Attn: AFAL/RWI, Wright-Patterson AFB, OH 45433.

AUTHORITY

AFWAL ltr, 18 Sep 1981

THIS PAGE IS UNCLASSIFIED

THIS REPORT HAS BEEN DELIMITED
AND CLEARED FOR PUBLIC RELEASE
UNDER DOD DIRECTIVE 5200.20 AND
NO RESTRICTIONS ARE IMPOSED UPON
ITS USE AND DISCLOSURE.

DISTRIBUTION STATEMENT A

APPROVED FOR PUBLIC RELEASE;
DISTRIBUTION UNLIMITED.

4 (2)

AD B O I 5 2 9 5

FLIR HIGH FREQUENCY STABILIZATION STUDY PROGRAM

AEROJET ELECTROSYSTEMS COMPANY
1100 W. HOLLYVALE STREET
AZUSA, CALIFORNIA 91702

AUGUST 1976

FINAL REPORT 31 MARCH 1975 THROUGH 22 JANUARY 1976

DDC
RECEIVED
NOV 30 1976
B

AD No. _____
DDC FILE COPY

Distribution limited to U.S. Government agencies only; test and evaluation; 22 March 1976. Other requests for this document must be referred to Air Force Avionics Laboratory, Air Force Systems Command, Wright-Patterson Air Force Base, Ohio 45433 AFAL/RWI

Prepared For:
AIR FORCE AVIONICS LABORATORY
AIR FORCE WRIGHT AERONAUTICAL LABORATORIES
AIR FORCE SYSTEMS COMMAND
WRIGHT-PATTERSON AIR FORCE BASE, OHIO 45433

COPY AVAILABLE TO DDC DOES NOT PERMIT FULLY LEGIBLE PRODUCTION

This final report was submitted by Aerojet ElectroSystems Company, 1100 W. Hollyvale St., Azusa, California in accordance with Contract Data Requirements List Sequence No. A005, Data Item DI-S-3591/S-117-1/M of Contract F33615-75-C-1128 with Air Force Avionics Laboratory, Air Force Systems Command, Wright-Patterson Air Force Base, Ohio.

Distribution limited to U.S. Government agencies only; test and evaluation; 22 March 1976. Other requests for this document must be referred to Air Force Avionics Laboratory, Air Force Systems Command, Wright-Patterson Air Force Base, Ohio.

This technical report has been reviewed and is approved for publication.


ROBERT E. DEAL, ACTING CHIEF
Electro-Optics & Reconnaissance Branch
Reconnaissance and Weapon Delivery Division

ACCESSION for	
NTIS	White Section <input type="checkbox"/>
DDC	Bull Section <input checked="" type="checkbox"/>
UNANNOUNCED	<input type="checkbox"/>
JUSTIFICATION.....	
BY.....	
DISTRIBUTION/AVAILABILITY CODES	
Digi.	AVAIL. and/or SPECIAL
B	

When Government drawings, specifications, or other data are used for any purpose other than in connection with a definitely related Government procurement operation, the United States Government thereby incurs no responsibility nor any obligation whatsoever; and the fact that the government may have formulated, furnished, or in any way supplied the said drawings, specifications, or other data, is not to be regarded by implication or otherwise as in any manner licensing the holder or any other person or corporation, or conveying any rights or permission to manufacture, use, or sell any patented invention that may in any way be related thereto.

Copies of this report should not be returned unless return is required by security considerations, contractual obligations, or notice on a specific document.

UNCLASSIFIED

SECURITY CLASSIFICATION OF THIS PAGE (When Data Entered)

19 REPORT DOCUMENTATION PAGE		READ INSTRUCTIONS BEFORE COMPLETING FORM
18 1. REPORT NUMBER AFAL-TR-76-78 ✓	2. GOVT ACCESSION NO.	3. RECIPIENT'S CATALOG NUMBER
6 4. TITLE (and Subtitle) FLIR HIGH FREQUENCY STABILIZATION STUDY PROGRAM.		5. TYPE OF REPORT & PERIOD COVERED Final--31 March 1975 through 22 January 1976
7. AUTHOR(s) 10 H. B. Ellis		6. PERFORMING ORG. REPORT NUMBER 14 AESC-5281 ✓
9. PERFORMING ORGANIZATION NAME AND ADDRESS Aerojet ElectroSystems Company ✓ 1100 W. Hollyvale Street Azusa, California 91702		8. CONTRACT OR GRANT NUMBER(s) 15 F33615-75-C-1128 <i>new</i>
11. CONTROLLING OFFICE NAME AND ADDRESS Air Force Avionics Laboratory (AFAL RWI) Air Force Wright Aeronautical Laboratories Air Force Systems Command Wright-Patterson Air Force Base, Ohio 45433		10. PROGRAM ELEMENT, PROJECT, TASK AREA & WORK UNIT NUMBERS Project No 2004/06/03 16 17
14. MONITORING AGENCY NAME & ADDRESS (if different from Controlling Office) Wright-Patterson Air Force Base, Ohio		12. REPORT DATE 11 Aug 1976
16. DISTRIBUTION STATEMENT (of this Report) Distribution limited to U.S. Government agencies only; test and evaluation; 22 March 1976. Other requests for this document must be referred to Air Force Avionics Laboratory, Air Force Systems Command, Wright-Patterson Air Force Base, Ohio AFAL/RWI		13. NUMBER OF PAGES 110
17. DISTRIBUTION STATEMENT (of the abstract entered in Block 20, if different from Report) 9 Final rept. 31 Mar 75 - 22 Jan 76		15. SECURITY CLASS. (of this report) Unclassified
18. SUPPLEMENTARY NOTES		
19. KEY WORDS (Continue on reverse side if necessary and identify by block number) high frequency, line-of-sight stabilization, internal optical internal optical line-of-sight stabilization stabilization folding mirror module		
20. ABSTRACT (Continue on reverse side if necessary and identify by block number) A Forward Looking Infrared (FLIR) High Frequency Stabilization Study was conducted to investigate cost-effective techniques for achieving internal optical line-of-sight stabilization in an AN/AAQ9 XA1 or XA2 type FLIR. A stabilization technique which command-stabilizes a gimballed folding mirror in the FLIR IR optical system was selected. Tests verified the stabilization performance of the laboratory demonstration breadboard model. Vibration attenuations of over 27 dB were achieved in the spectrum between 20 and 100 Hz. System noise levels were sufficiently low to achieve the desired 7-microradian line-of-sight stabilization level.		

406260 *net*

PREFACE

Without a line-of-sight stabilization capability, mechanical vibrations of FLIRs installed in aircraft can degrade the image quality of the FLIR to an extent that seriously restricts the utility of the unit. As a consequence, the Air Force Avionics Laboratory, Wright-Patterson Air Force Base, Ohio, sponsored a study of high frequency line-of-sight stabilization in the AN/AAQ-9 XA1 and XA2 type FLIRs. This study concluded with a laboratory demonstration which proved the feasibility of the selected stabilization concept. In this concept line-of-sight stabilization was achieved by applying compensating motions to the folding mirror in the FLIR optical system. This report details the investigation conducted and the results obtained.

TABLE OF CONTENTS

Section		Page
I	INTRODUCTION AND SUMMARY	1
II	ACCOMPLISHMENTS	7
III	EVALUATION OF STABILIZATION TECHNIQUES	13
	1. Stabilization Requirements	13
	2. FLIR Response to a Linear Vibration Environment	13
	3. Review of Stabilization Techniques	22
	4. Technique Selection for Laboratory Demonstration Breadboard Model	34
IV	LABORATORY DEMONSTRATION BREADBOARD MODEL DESIGN	39
	1. Gimballed Mirror	39
	2. Mirror Driver	47
	3. FLIR Motion Sensor	59
	4. Electronics	59
V	STABILIZATION PERFORMANCE VERIFICATION	69
VI	CONCLUSIONS AND RECOMMENDATIONS	77

FIGURES

Figure		Page
1	Line-of-Sight Attenuation Versus Frequency with S-D Angular Displacement Sensor	2
2	Folding Mirror Stabilization Module Concept in AN/AAQ9 XA1 FLIR	4
3	Folding Mirror Stabilization Module Concept in AN/AAQ9 XA2 FLIR	5
4	Assembly of Laboratory Breadboard Stabilization Mirror Unit . .	6
5	Stabilization Mirror Performance Test Setup	8
6	Component Parts of Laboratory Breadboard Stabilization Mirror Unit	9
7	S-D Angular Displacement Sensor Noise Spectrum	11
8	Line-of-Sight Stabilization Spectrum With S-D Sensor	12
9	Sinusoidal and Random Vibration	14
10	FLIR Vibration MTF	16
11	Model of FLIR Sensor Vibrational Motion	18
12	Projected FLIR Angular Vibrational Response Envelope	20
13	Required Attenuation	21
14	FLIR Optical Systems	24
15	Gimbaled Folding Mirror	25
16	Gimbaled Doublet Lenses	26
17	Oscillating Skew Plate	27
18	Variable Angle Prism	28
19	Gimbaled Prism	30
20	Display Stabilization	31
21	Vidicon Focal Plane Stabilization	33
22	Scan Stabilization By An Optical Skew Plate	35
23	Sectional View--Ball and Socket Pivot Mounting of the Mirror. .	41
24	Replicated Plano Mirror	44
25	Mirror Surface Interferometer Pattern	45
26	Mirror Surface Interferometer Pattern Within One Fringe	46
27	Mirror/Driver System Dynamic Characteristics	48
28	Laboratory Breadboard Stabilization Mirror Unit	50
29	Displacement Sensitivity Versus D-C Electric Field Strength in Ceramic	53

FIGURES (cont.)

Figure		Page
30	Figure Displacement Sensitivity Versus A-C Electric Field Strength in Ceramic	54
31	Stabilization Mirror Unit Voice Coil Drive	55
32	Simplified Side View of Trilaminar Bender	57
33	Line-Of-Sight Stabilization Spectrum With S-D Sensor	60
34	Gain Versus Frequency Characteristics Gyro Compensation	61
35	Combined Gain Versus Frequency Noise Amplification Characteristics	62
36	Mirror Stabilization System Noise Spectrum With Integrating Rate Gyro	63
37	System Block Diagram	64
38	McIntosh MI-75 Amplifier Characteristics	67
39	Breadboard Stabilization Mirror Stabilization Performance Tests	70
40	Test Setup Block Diagrams	71
41	General View of Line-Of-Sight Stabilization Test Installation	73
42	Close-Up View of Stabilization Mirror Unit	74
43	Close-Up View of Stabilization Mirror Unit	75

TABLES

Table		Page
1	EVALUATION SUMMARY	37
2	RELATIVE MERIT OF MIRROR MATERIALS	42

APPENDIX

Section		Page
I	SENSITIVITY TO APPLIED VIBRATIONS	81
1.	INDUCED MIRROR ANGULAR VIBRATIONS	81
2.	MIRROR POSITION TRANSLATION	81
3.	MIRROR UNIFORMITY TESTS	81
II	LINE-OF-SIGHT STABILIZATION TESTS	83
1.	SCOPE OF TESTS	83
2.	PRELIMINARY EVALUATION TESTS	83
3.	SCHEDULED TESTS	83
4.	ADDITIONAL TESTS	84

SECTION I

INTRODUCTION AND SUMMARY

The purpose of the Forward Looking Infrared (FLIR) High Frequency Stabilization Study Program was to investigate cost-effective techniques for achieving internal optical line-of-sight stabilization in an AN/AAQ9 XA1 or XA2 type of FLIR. The program was composed of the following three main tasks:

- Evaluation of techniques for achieving internal optical line-of-sight stabilization, and selection of a recommended technique, with Air Force concurrence
- Design and fabrication of a laboratory demonstration breadboard model
- Demonstration, by tests, of the stabilization capabilities of the breadboard model (in one dimension).

A stabilization technique which command-stabilizes a gimballed folding mirror in the FLIR IR optical system was selected. This technique is readily applicable to both FLIRs, as it requires only substitution of a stabilization mirror module for one of the normal FLIR folding mirrors. No change in optics design nor degradation in performance results, and the technique readily accommodates step zoom field-of-view changes by a simple scale-factor change in the electronics.

The stabilization performance of the laboratory demonstration breadboard model is shown in Figure 1. This figure shows vibration attenuation as a function of sinusoidal vibration frequency, and demonstrates that an attenuation of from 20 to over 27 dB was achieved in the spectrum between 20 and 100 Hz. The test results also showed system noise levels to be sufficiently low to permit the desired 7-microradian line-of-sight stabilization level to be achieved.

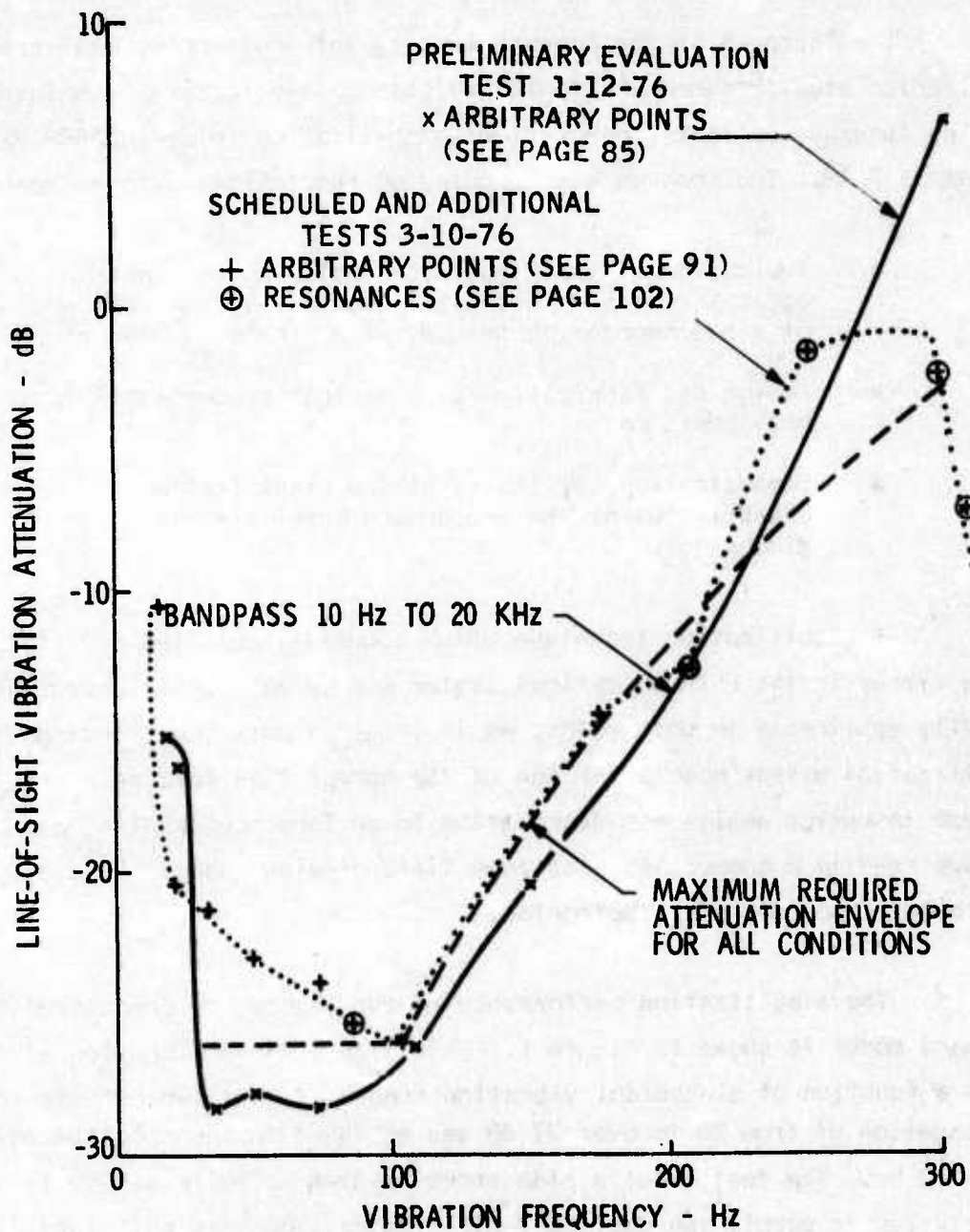


Figure 1 Line-Of-Sight Attenuation Versus Frequency With S-D Angular Displacement Sensor

Sketches illustrating the mechanical configurations of stabilization folding mirror modules applicable to the AN/AAQ9 XA1 and XA2 are shown in Figures 2 and 3. These sketches are based on the design of the laboratory demonstration breadboard, which made use of an aluminum honeycomb structure with a replicated plano-optical mirror surface. The mirror was driven independently about two axes by piezoelectric drivers. The completed laboratory demonstration breadboard model is shown in Figure 4.

Aerojet ElectroSystems Company (AESC) recommends a follow-on program to apply the experience gained from this study program to the design of a cost-effective stabilization system for a selected aircraft-mounted FLIR/gimbal configuration.

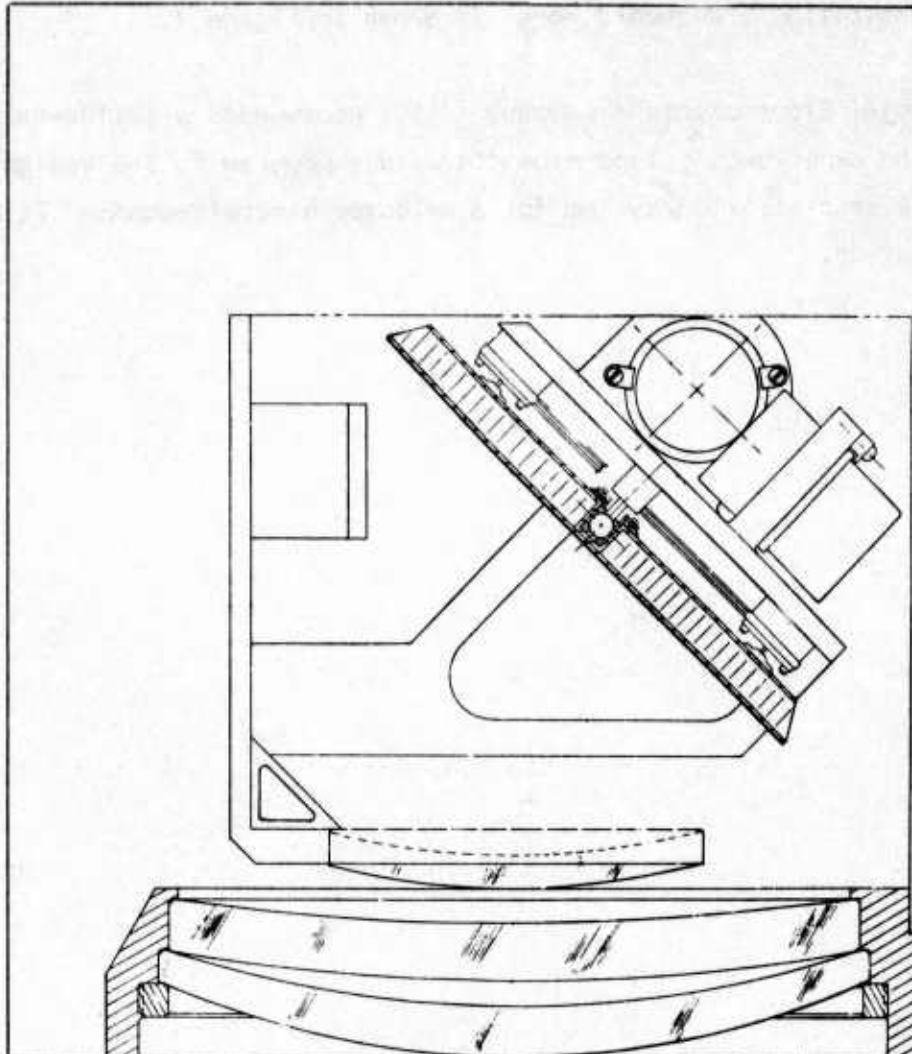


Figure 2 Folding Mirror Stabilization Module Concept
in AN/AAQ9 XA1 FLIR

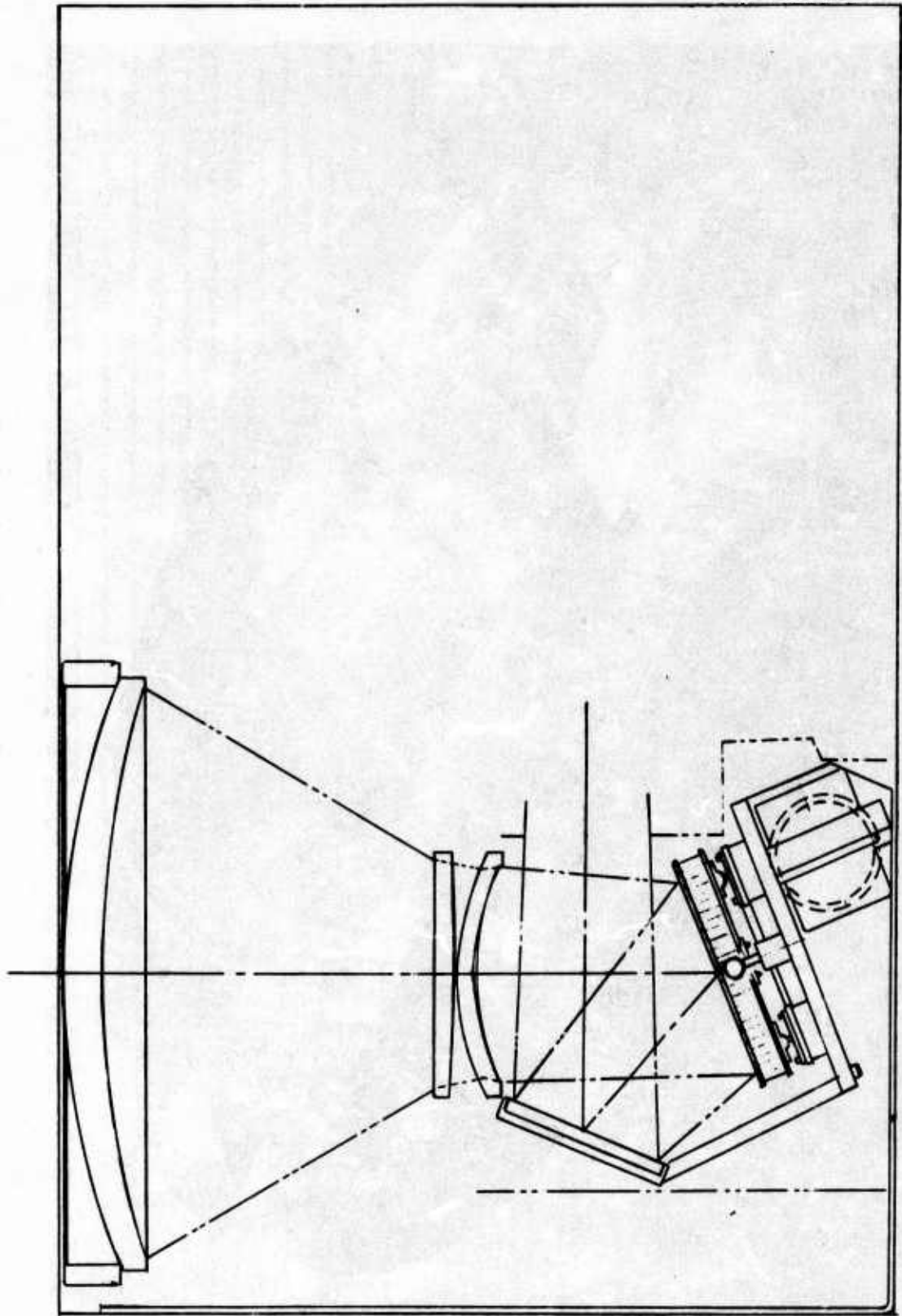


Figure 3 Folding Mirror Stabilization Module Concept
in AN/AAQ9 XA2 FLIR

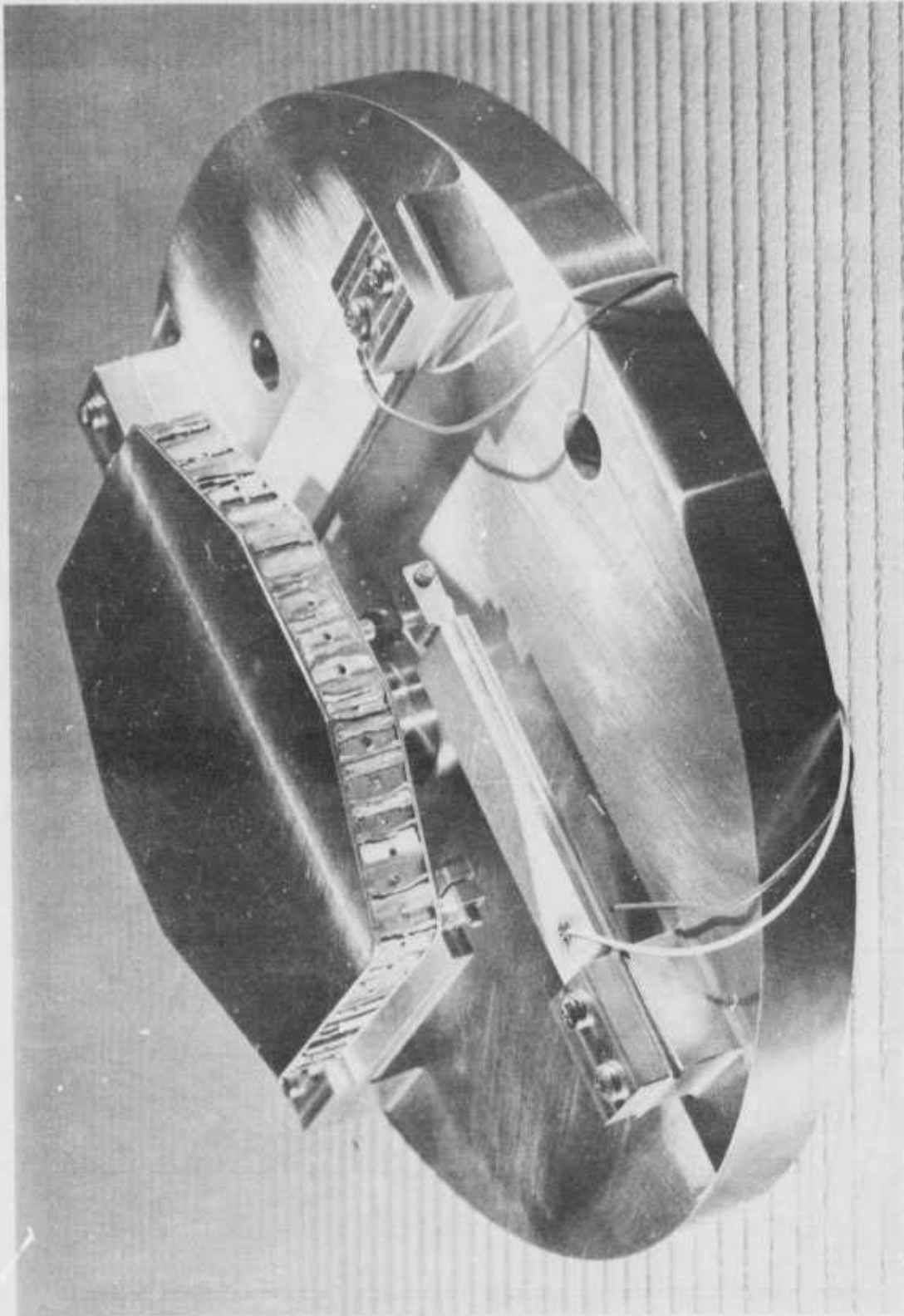


Figure 4 Assembly of Laboratory Breadboard Stabilization Mirror Unit

SECTION II

ACCOMPLISHMENTS

The FLIR High Frequency Stabilization Study Program successfully accomplished the program objectives of high-frequency internal stabilization to existing or modular FLIR systems. Significant accomplishments included

- Demonstration of satisfactory line-of-sight stabilization from 30 to over 300 Hz by a gimballed stabilization mirror
- Design of a low-cost stabilization mirror with a 500-Hz natural frequency that is suitable for use in relatively severe three-axes translational vibration environments
- Demonstration of stabilization mirror drive systems with linear characteristics and low noise levels throughout a bandwidth of 30 Hz to 1 kHz.

The demonstration of satisfactory line-of-sight stabilization was made by subjecting the stabilization mirror to applied rotational vibrations and by measuring angular deflection of the mirror using a laser and detector. A general view of the test setup is shown in Figure 5. The rotational vibrations were applied about a single axis (vertical), were sinusoidal in form, and were representative of the expected aircraft environment.

The design of the low-cost stabilization mirror made use of an aluminum honeycomb substrate for a replicated plano mirror, piezoelectric drivers, and a ball/socket pivot at the mirror center of gravity. These component parts for the laboratory demonstration breadboard are shown in Figure 6. By using already developed aluminum honeycomb structures for the mirror substrate, both the mirror stiffness and moment of inertia requirements

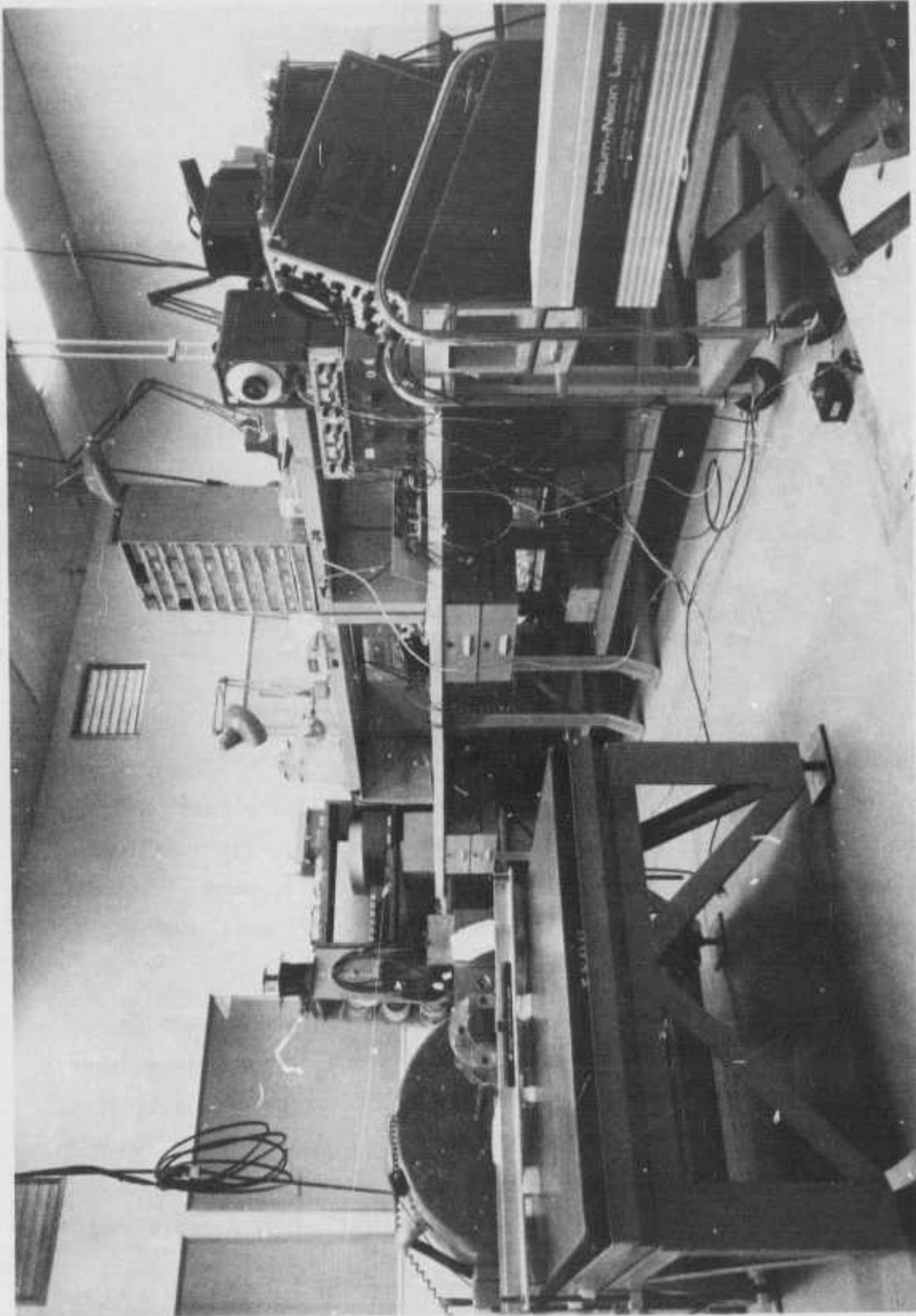


Figure 5 Stabilization Mirror Performance Test Setup

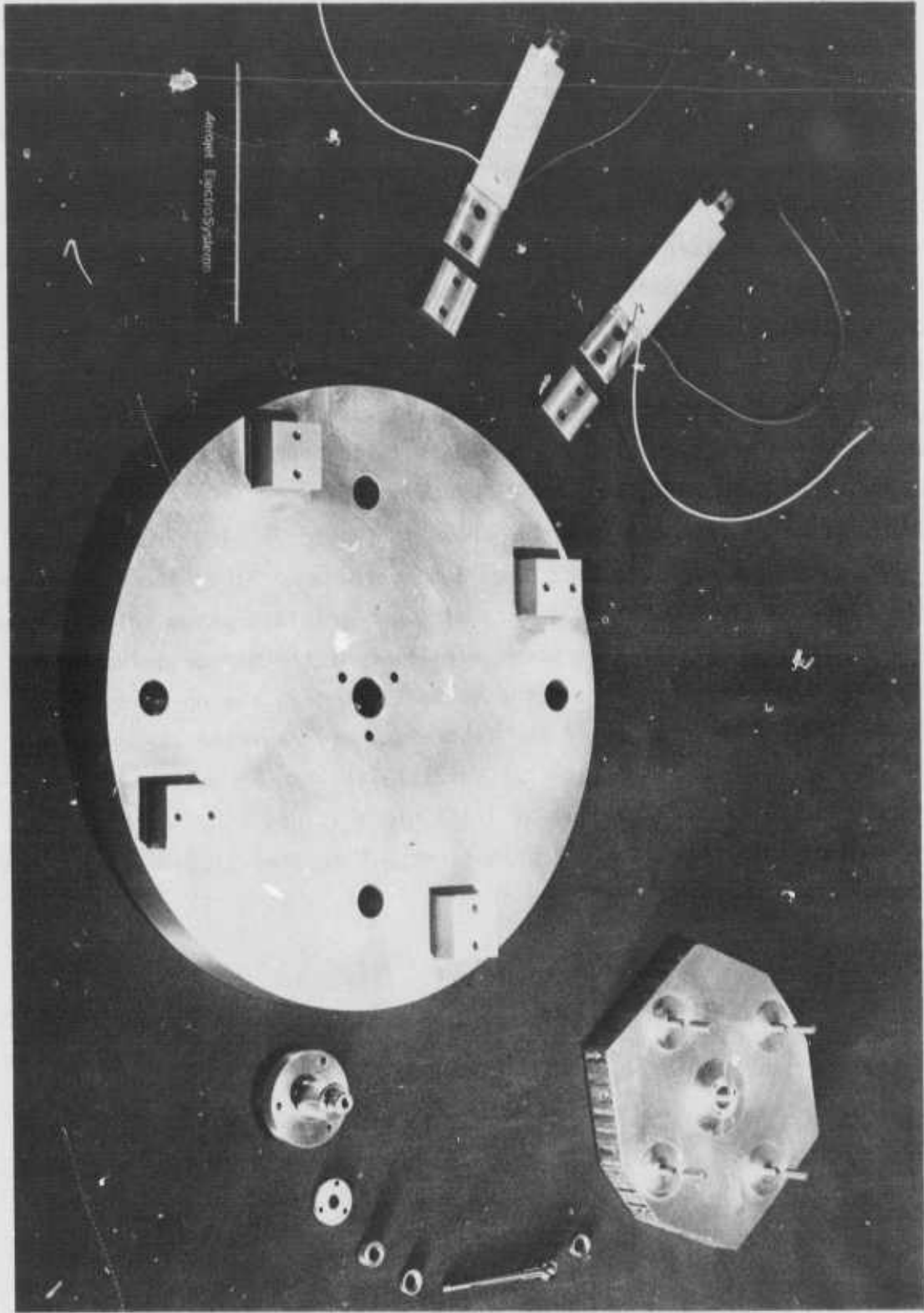


Figure 6 Component Parts Of Laboratory Breadboard Stabilization Mirror Unit

could be met. To avoid degradation of the FLIR optical performance, the mirror must be sufficiently stiff to keep the mirror surface deflections within acceptable limits when exposed to linear vibration environments. The peak severity of the linear vibration environment for this study was 20 g and 105 Hz. To obtain a relatively high (500 Hz or higher) natural frequency of the mirror/driver system, a low mirror moment of Inertia is required, limited by the driver characteristics. With the pivot at the mirror center of gravity, the three-dimensional linear vibration environment has no effect upon the mirror position or motion. This decouples the mirror stabilization drive system from the linear vibration environment.

The demonstration of the stabilization mirror drive system, with linear characteristics and low noise levels throughout a bandwidth of 30 Hz to 1 kHz, required a suitable angular displacement sensor. The noise spectrum characteristics of such a sensor are shown in Figure 7. The broadband (30 Hz to 1 kHz) rms noise level is less than 1 microradian. Since the sensor output is linear between 30 Hz and 1 kHz, with a negligible phase shift, it can be used directly to control the power amplifier of the mirror driver. The mirror stabilization system broadband noise (including the noise spikes at multiples of 60 Hz attributed to the laboratory environment) was approximately 5 microradians. This level is sufficiently low to achieve the desired line-of-sight stabilization value of 7-1/2 microradians rms, under applied vibration amplitudes of 150 microradians rms. A typical line-of-sight stabilization spectrum is shown in Figure 8.

276-1193

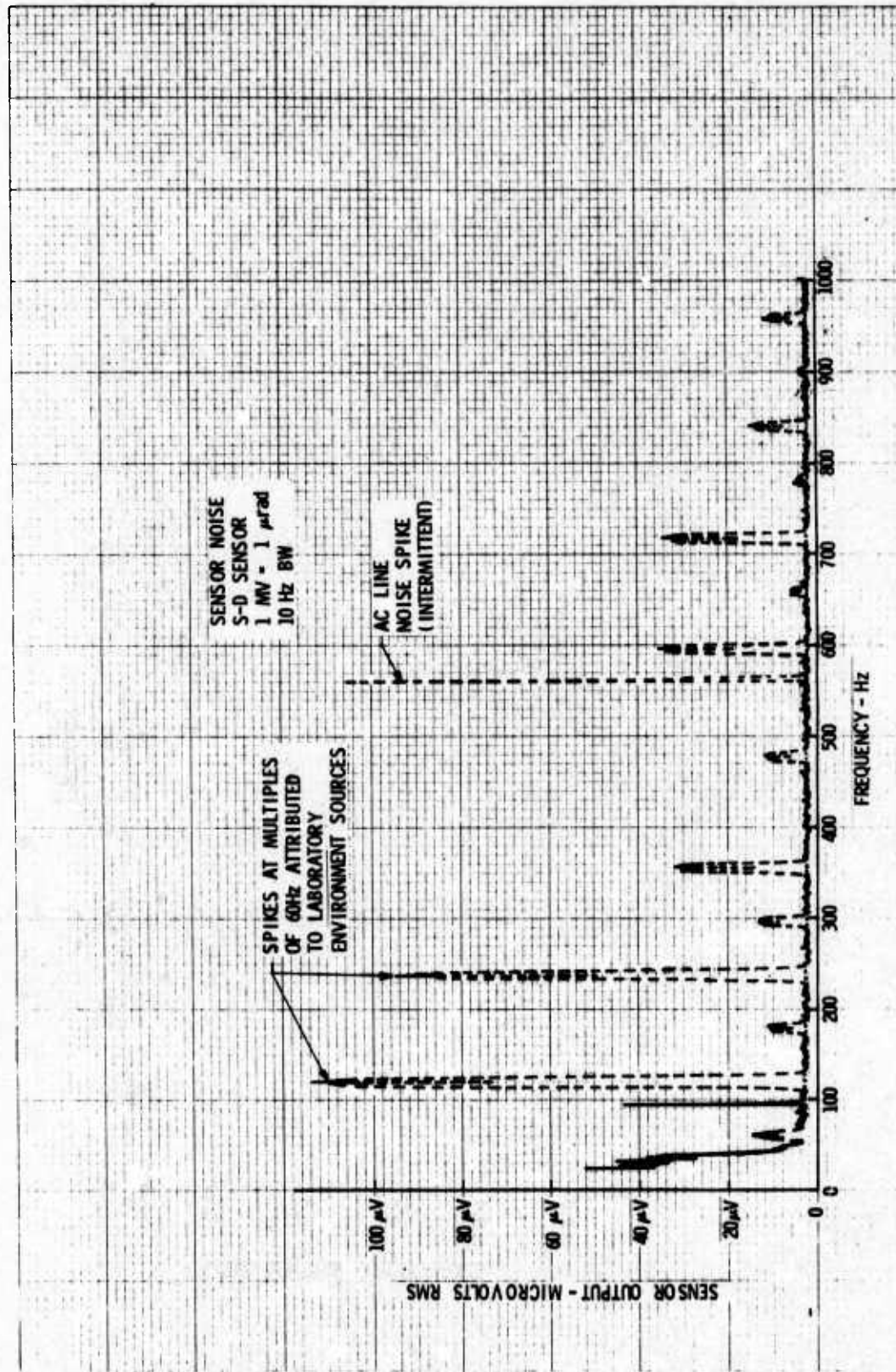


Figure 7 S-D Angular Displacement Sensor Noise Spectrum

276-1195

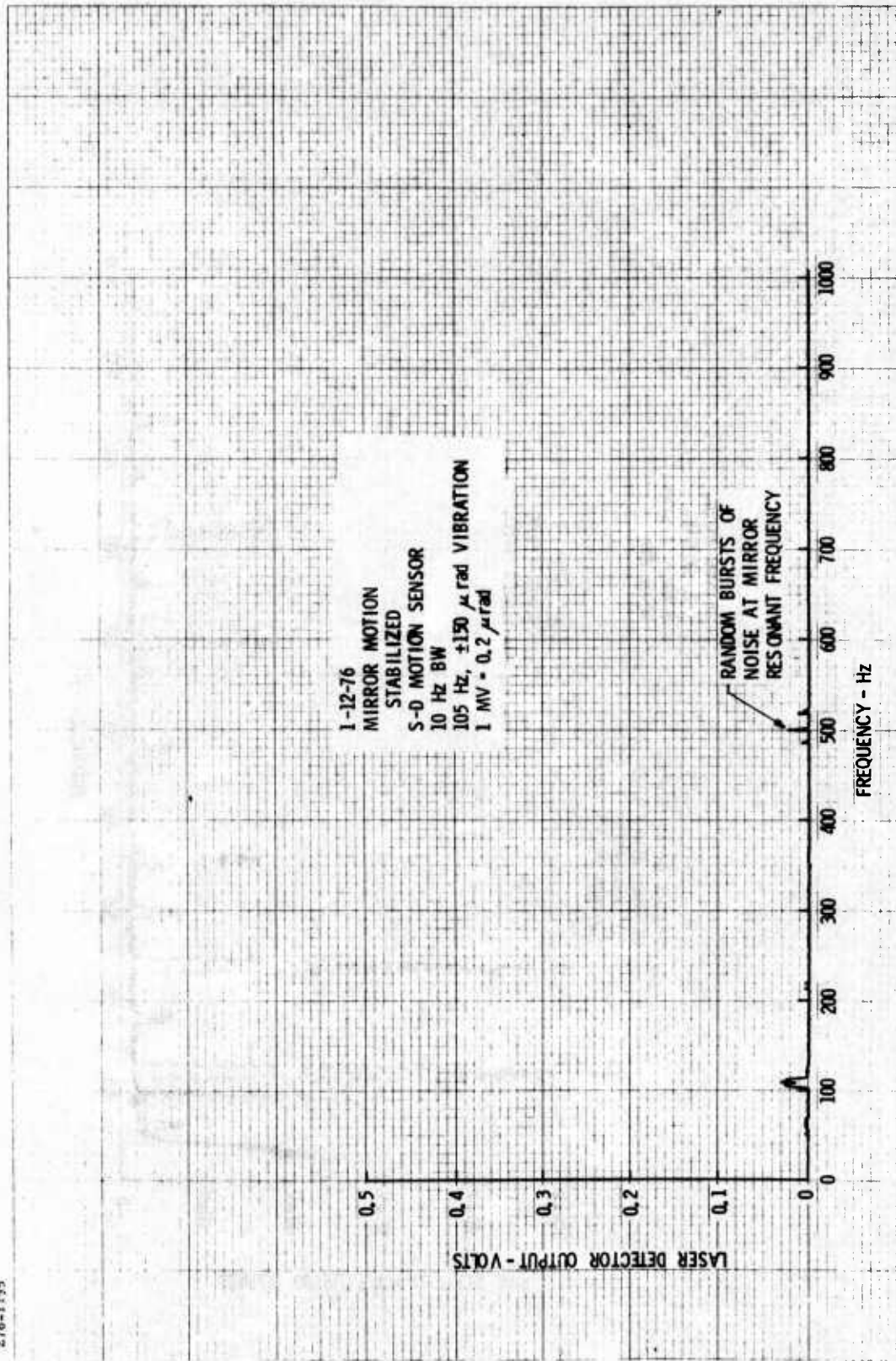


Figure 8 Line-Of-Sight Stabilization Spectrum With S-D Sensor

SECTION III

EVALUATION OF STABILIZATION TECHNIQUES

1. STABILIZATION REQUIREMENTS

Stabilization requirements are summarized below.

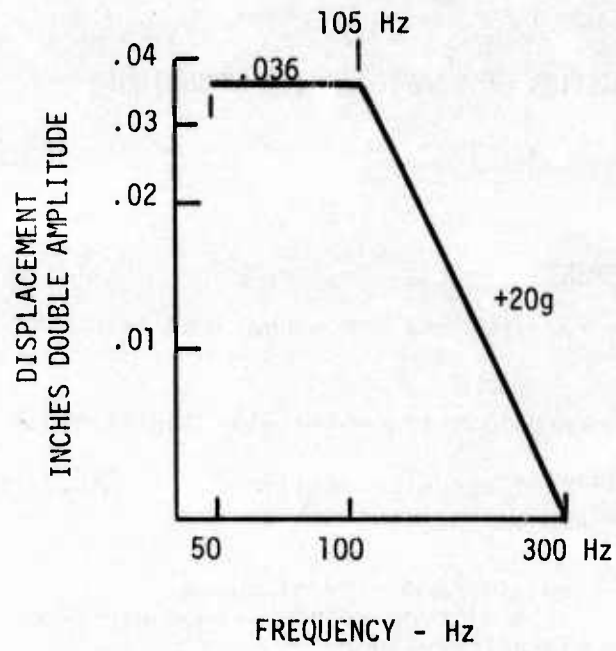
- Seven microradians line-of-sight stabilization
- No significant boresight shift between stabilized and unstabilized operational state
- Vibration environment--translational sinusoidal amplitude versus frequency--Figure 9A random vibration--Figure 9B
- Temperature environment
 - within specification 0 to +44°C
 - Startup -54 to +44°C
 - Thermal shock 3 degrees/second
 - Minimum telescope modifications
 - Compatibility with two FLIRS

Low-frequency stabilization from DC up to the 5 to 10 Hz region would be provided by the FLIR gimbal system.

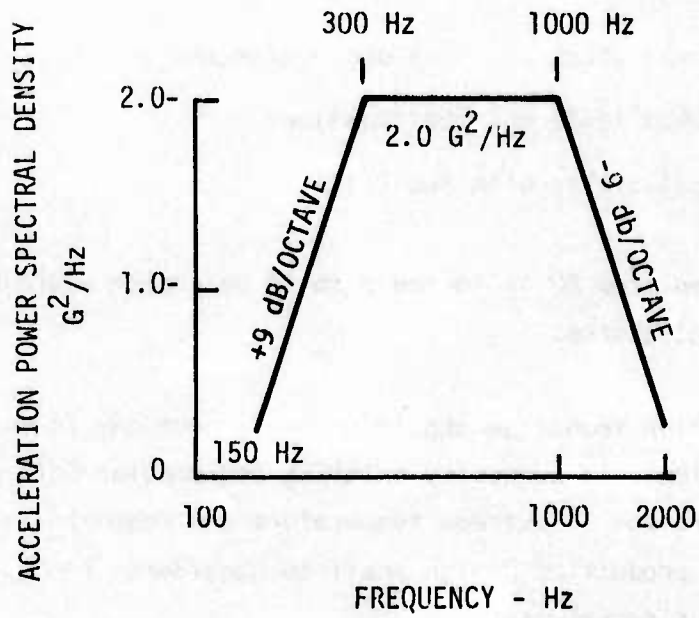
The stabilization technique should emphasize economy in materials, fabrication, and integration with currently existing and modular FLIR designs. Assurance of reliable operation in extreme temperature environments is essential. An economical production design shall be considered in implementing the design-to-cost considerations.

2. FLIR RESPONSE TO A LINEAR VIBRATION ENVIRONMENT

When a Forward Looking Infrared (FLIR) system is mounted on an aircraft, the FLIR sensor becomes subject to applied vibrations. This results



A - Sinusoidal vibration



B - Random vibration

Figure 9 Sinusoidal And Random Vibration

In angular vibratory movements of the FLIR sensor. The effect of such vibrations on the FLIR modulation transfer function (MTF) has been described by the following equation:

$$MTF = e^{-\left(\frac{\pi \alpha}{1.4 \theta}\right)^2}, \quad \Omega = \frac{1}{2\theta} \quad (1)$$

where

α = rms amplitude of random rotational vibration (radian)

θ = IR detector angular subtense (radian)

Ω = FLIR nominal spatial frequency, cycles/radian

The resulting MTF degradation for different FLIR resolution values is shown in Figure 10. This figure clearly illustrates the requirement for increased stabilization of the FLIR as the resolution increases. Ten microradian rms stabilization with 0.1 microradian resolution provides an MTF degradation of 5 percent, while 7 microradian stabilization provides 3 percent MTF degradation with 0.1 microradian FLIR.

The disturbing motions that degrade picture quality through angular motion of the line of sight stem from several sources. The lower frequencies are dominated by aircraft motions stemming from turbulence and from aerodynamic oscillations. These low frequencies are generally compensated for by the servo system. In the midfrequency range, the disturbances are dominated by the angular vibration of the aircraft structure, and by interactions between linear structural vibration, the FLIR mounting structure, and the gimbal system. Higher-frequency disturbances generally result from some internal disturbance within the sensor, such as mass unbalance of a motor or rotor, or are structurally transmitted harmonics from some part of the aircraft.

The aircraft vibrational environment is generally given in terms of a translatory vibration. Clearly, translational motion of the line of sight, in itself, does not adversely affect the FLIR imagery. However, such a translatory vibration applied to a FLIR mounting structure can cause

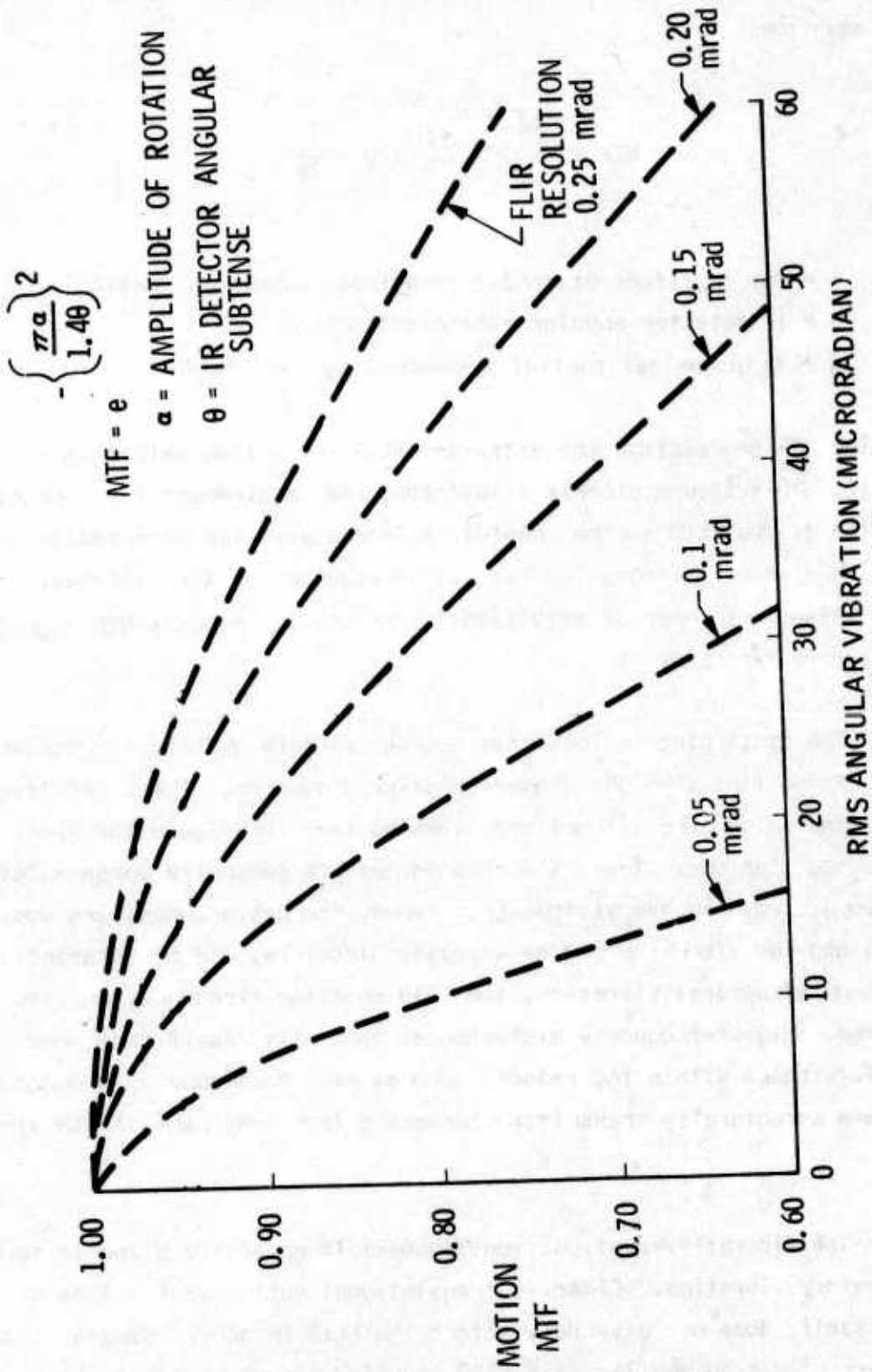


Figure 10 FLIR Vibration MTF

rotational vibratory movements to appear; these movements adversely affect the FLIR imagery, and must be attenuated. To establish rotational coupling levels and, therefore, the attenuation performance required of a FLIR high-frequency stabilization system, the model presented in Figure 11 is used. This model establishes a rotational coupling to the applied translational vibration by treating the FLIR as though it were mounted on the free end of a weightless, inertia-less cantilevered beam with the input translatory vibration environment, applied to the "fixed" end of the cantilevered beam. The resultant FLIR rotation is the sum of

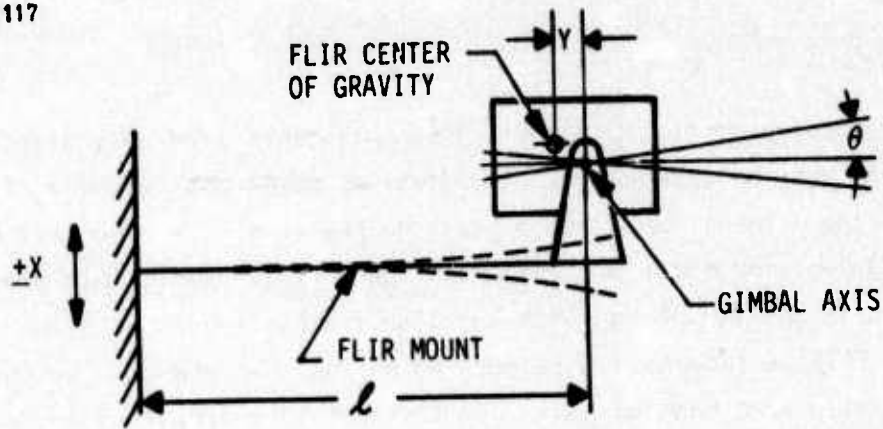
- (1) the rotational response to the FLIR mass-unbalance about the gimbal axis;
- (2) the forced rotation of the FLIR about the gimbal axis resulting from the angular rotation of the "free" end of the deflected antilever beam acting through the FLIR servo system.

The equation developed to express the FLIR angular motion response to an applied linear vibration included both of these two causes of rotation and the effects of the pertinent parameters within each. Dominant factors include the polar moment of inertia of the FLIR, the magnitude of the FLIR mass unbalance about the gimbal axis, and the length of the equivalent cantilever beam of the FLIR gimbal mount. The equation is given below:

$$\theta = \frac{X \left\{ - \left(\frac{3}{2l} U_2^2 - 4 \zeta_1 \zeta_2 U_1 U_2 \right) - \frac{Y}{r_g} U_1^2 + j \left[- \frac{3}{2l} \left(2\zeta_1 U_1 U_2^2 - 2\zeta_2 U_2 \right) - \frac{Y}{r_g} \left(2\zeta_2 U_1^2 U_2 \right) \right] \right\}}{\left(1 - U_1^2 + j 2\zeta_1 U_1 \right) \left(1 - U_2^2 + j 2\zeta_2 U_2 \right)} \quad (2)$$

The parameters in this equation are:

- θ = angular amplitude of the FLIR vibration
- X = amplitude of the applied linear vibration
- U_1 = ratio of applied linear vibration frequency to the natural frequency of the gimbal axis (f/f_1)
- U_2 = ratio of applied linear vibration frequency to the natural frequency of the gimbal mount (f/f_2)



MODEL PARAMETERS*

FLIR

MASS	M
RADIUS OF GYRATION	r_g
NATURAL FREQUENCY ON GIMBAL AXIS	f_1
CRITICAL DAMPING	ζ_1
CG OFFSET FROM GIMBAL AXIS	Y

FLIR MOUNT-CANTILEVERED BEAM

WEIGHT	-0-
MOMENT OF INERTIA	-0-
NATURAL FREQUENCY	f_2
CRITICAL DAMPING	ζ_2
LENGTH	l

INPUT VIBRATION

TRANSLATORY AMPLITUDE (PEAK)	+X
FREQUENCY	f

OUTPUT VIBRATION

ROTATIONAL AMPLITUDE (PEAK)	θ
FREQUENCY	f

*Symbols are explained following Equation (2).

Figure 11 Model Of FLIR Sensor Vibrational Motion

ζ_1 = per-unit critical damping of the gimbal servo
 ζ_2 = per-unit critical damping of cantilever FLIR mount
 l = length of the cantilever FLIR mount
 r_g = radius of gyration of the FLIR about the gimbal axis
 Y = offset of FLIR center of gravity from gimbal axis
 $j = \sqrt{-I}$

To establish rotational coupling levels and the required attenuation performance (Equation 2), the following "typical" values for the various "fixed" parameters of a FLIR installation were selected based upon AESC experience:

$$f_1 = 0.87 \text{ Hz}$$

$$\zeta_1 = 0.5$$

$$\zeta_2 = 0.10$$

$$l = 2.0 \text{ ft}$$

$$r_g = 0.71 \text{ ft}$$

$$Y = 0.01 \text{ ft}$$

The value of FLIR mass used was $1.55 \text{ lb sec}^2/\text{ft}$

The variable parameters in the formula were the applied linear vibration amplitude (X) and frequency (f) and the gimbal mount natural frequency (f_2). The values used in calculating the FLIR angular vibration amplitude and the attenuation performance required of the high frequency stabilization system were:

Applied vibration - X and f

$\pm 0.018 \text{ in.}$ to 105 Hz
 20 g 105 to 300 Hz

FLIR mount natural frequency (f_2)

20 to 300 Hz.

The results, derived to set baseline design requirements for the high-frequency stabilization system, are plotted in Figures 12 and 13.

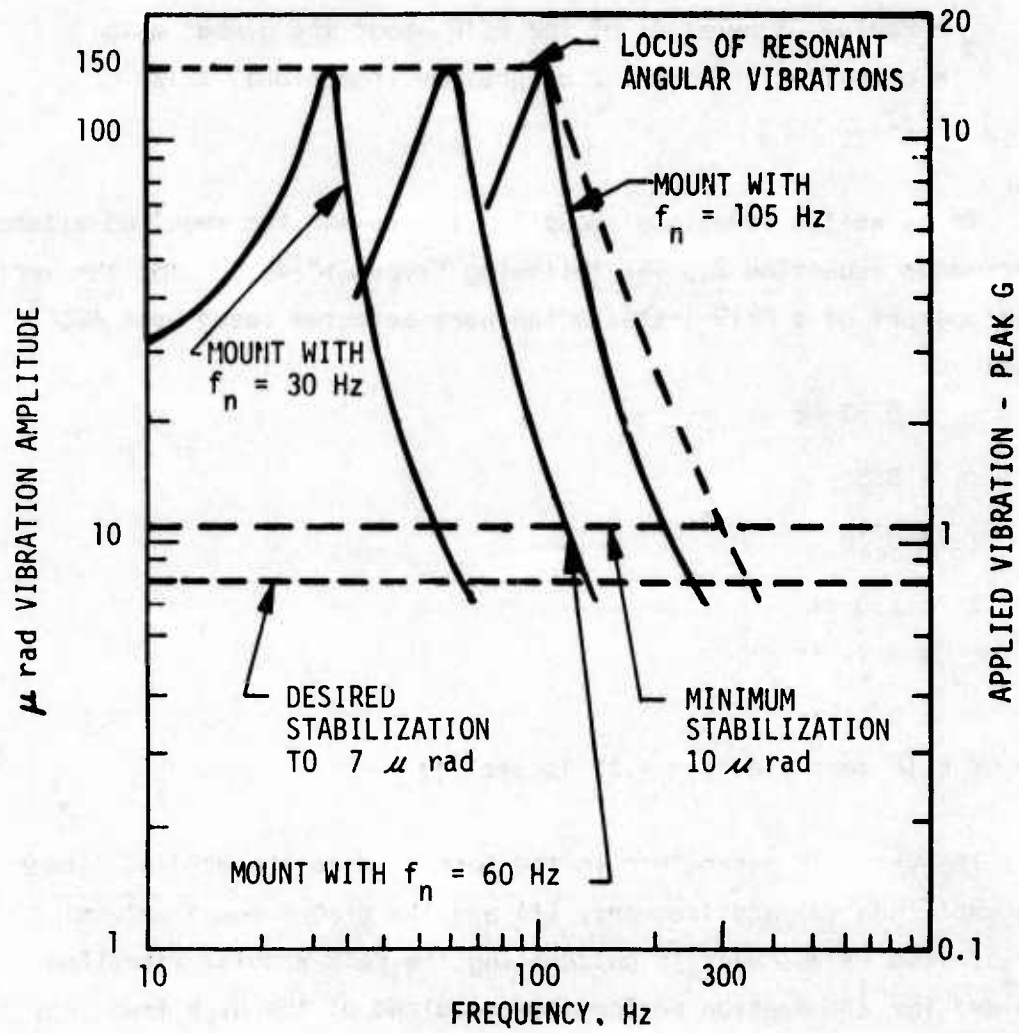


Figure 12 Projected FLIR Angular Vibrational Response Envelope

1174-1119

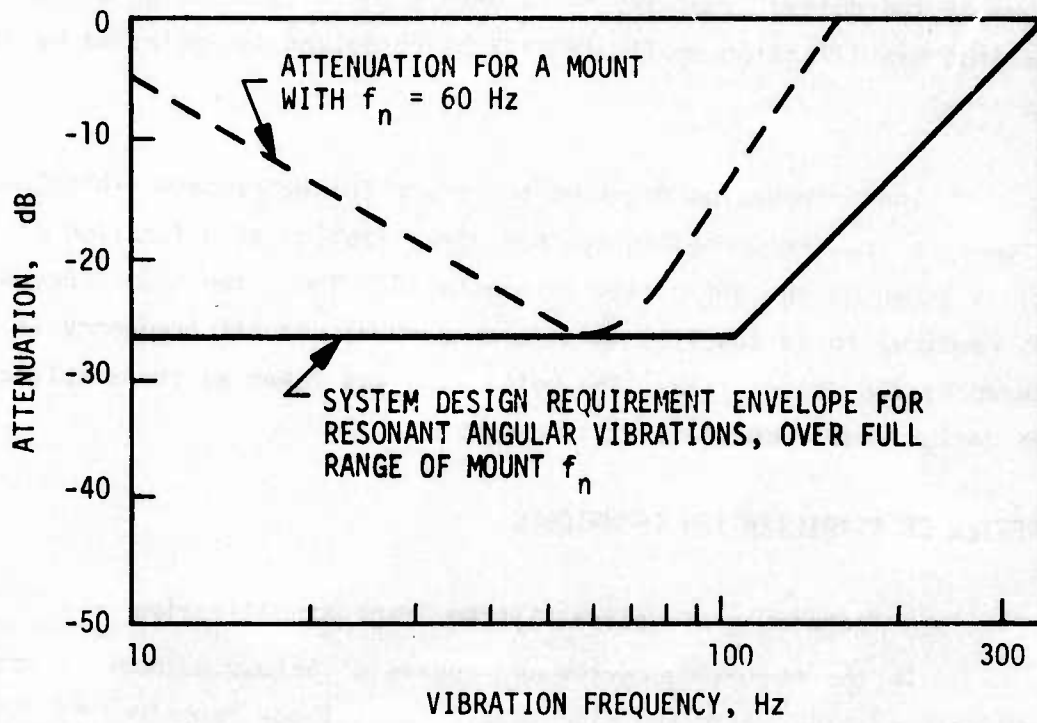


Figure 13 Required Attenuation

Amplitudes versus applied frequencies were calculated for three different natural frequency mounts, namely, 30 Hz, 60 Hz, and 105 Hz. These amplitudes are shown by the three solid-line curves in Figure 12. Since the design and natural frequency of the actual FLIR mount has not been established, it was assumed that it may be anywhere between 20 and 300 Hz. Consequently, the stabilization design requirements were established as the locus of the vibrational amplitudes at the mount resonant frequencies, throughout the possible range of mount natural frequencies from 20 to 300 Hz. This locus is shown by the dotted line, and represents a worst-case design criteria. The desired stabilization amplitude of 7 microradians is indicated by the dashed line.

The attenuation required to reduce the worst-case vibrational amplitudes to the 7-microradian desired stabilization as a function of frequency is shown by the solid line in Figure 13. The attenuation versus frequency required for a specific mount with a 60-Hz natural frequency is indicated by the dashed line. The solid line was taken as the stabilization system design requirements for this program.

3. REVIEW OF STABILIZATION TECHNIQUES

a. Techniques of Optical System Image Stabilization

In the following review and analysis various methods of optical system image stabilization are discussed. The methods described may be applied to either the IR optics or the vidicon visual optics.

(1) Gimbaled Folding Mirrors

Gimbaled folding mirrors are prime candidates for providing the required stabilization. This technique is the simplest, and has the most universal application potential since all candidate FLIRs have folding mirrors located somewhere in their optical systems. Thus, an image motion compensating mirror may be substituted for the normal folding mirror, or included in the main scanning mirror system, without affecting the optical system. No aberrations are introduced and no change in the other optical elements is required. Recent developments in the art of replicated plano mirrors on

aluminum honeycomb substrates offer an inexpensive lightweight mirror construction. The mirror mass properties combined with the small required motion permit the use of piezoelectric drivers with their small size and high natural frequency. Potential applications to two FLIR optical systems are illustrated in Figure 14. The principal of the gimbaleed folding mirror is shown in Figure 15.

(2) Doublet Lens

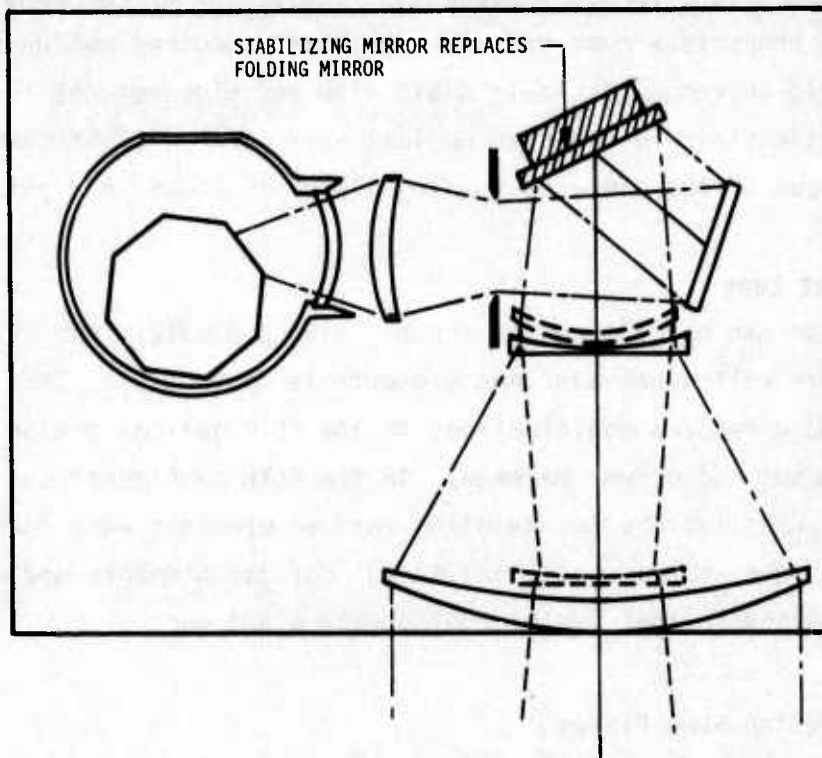
Image motion can be compensated for by using a doublet lens (Figure 16) wherein the relative motion between lens elements is controlled. This technique, however, would require modifications to the FLIR optical design to accept the optical element and driver package. In the FLIR configurations considered, no simple substitutions for existing optical elements were identified. Thus, this technique would require additional optical elements and a modification of the present optical system configuration and parts.

(3) Oscillating Skew Plates

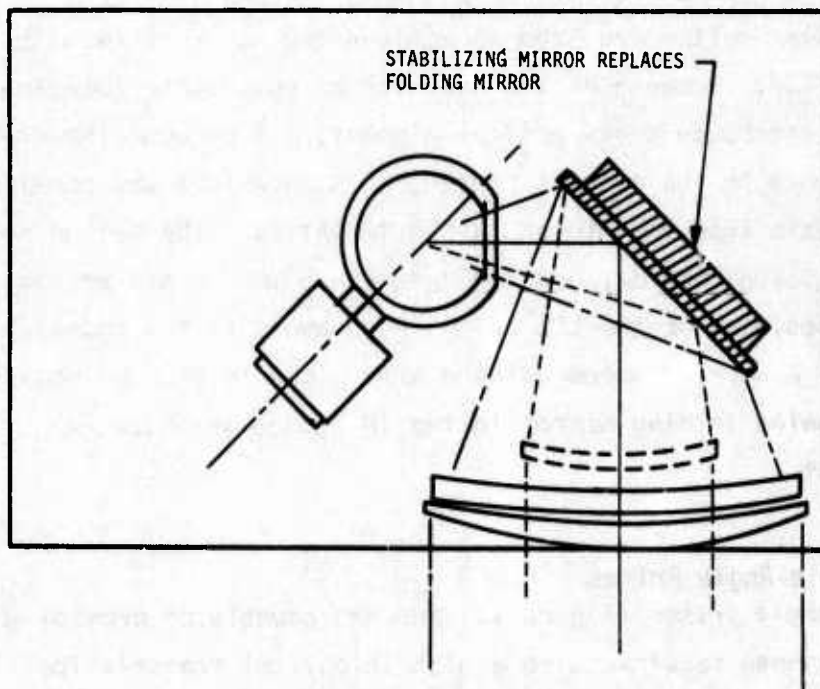
Oscillating plano skew plates (Figure 17) can produce movement of the image. The basic problem in the IR optics is the magnitude of the thickness and the angular motion required to achieve the required level of image motion compensation. Because of the need for an accessible location in the optical system to introduce a new optical element, and because the skew plate can add aberrations in the optical system, this technique was considered a less suitable candidate than the mirror in the IR optics. The method becomes feasible in the visual optics, however, wherein a skew plate may be used to vary the apparent position of the LED units in response to the commands from a motion sensor. A hybrid system using a skew plate in the LED optics, and a single-axis gimbaleed folding mirror in the IR optics was studied as an alternate concept.

(4) Variable-Angle Prisms

Variable-angle prisms (Figure 18) are not capable of providing the high-frequency response required with a high IR optical transmission efficiency. Their use would require modifications to the existing optical systems to accept the new optical element and to permit adjustments for

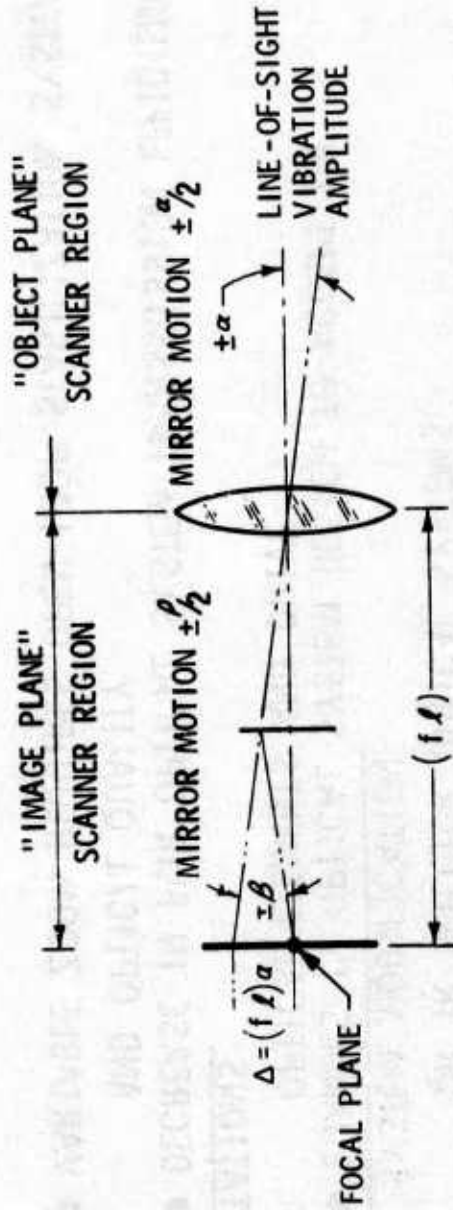


SYSTEM A



SYSTEM B

Figure 14 FLIR Optical Systems



DESIRABLE FEATURES

- GYRO CONTROL THROUGH ELECTRONIC DRIVERS CAN BE READILY PROGRAMMED

FOR ZOOM RATIOS

APPLICATION

- TO BOTH FLIRS

FLIR SYSTEM MODIFICATIONS

- MINIMAL-GIMBALED FOLDING MIRROR SUBSTITUTED FOR EXISTING FIXED

FOLDING MIRROR

LIMITATIONS

- MIRROR/DRIVE NATURAL FREQUENCY RESPONSE
- OPEN LOOP STABILIZATION SYSTEM

Figure 15 Gimbaled Folding Mirror



DESIRABLE FEATURES

- CAN BE DIRECTLY CONTROLLED BY FREE GYROS OR BY ELECTRONIC DRIVERS

APPLICATION

- PRIMARILY TO SMALL DIAMETER SECTIONS OF THE OPTICAL SYSTEM RAY BUNDLES TO EITHER THE VIEWING VIDICON OR IR DETECTOR OPTICAL SYSTEMS

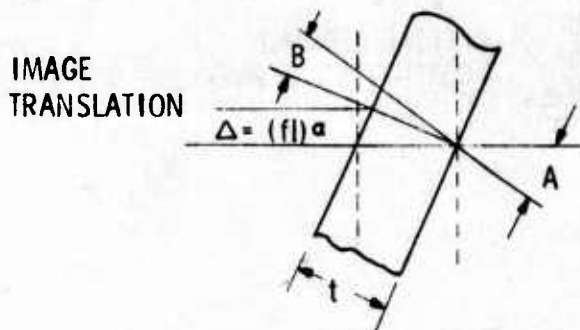
FLIR SYSTEM MODIFICATION

- CHANGES IN OPTICAL SYSTEM DESIGN TO ACCEPT THE OPTICAL ELEMENTS AND DRIVE

LIMITATIONS

- DECREASE IN FLIR OPTICAL SYSTEM TRANSMISSION EFFICIENCY AND OPTICAL QUALITY
- VARIABLE ZOOM REQUIRES OPEN LOOP STABILIZATION SYSTEM

Figure 16 Gimbaled Doublet Lenses



$$\Delta = [\sin(A-B)] \frac{t}{\cos B}$$

A = SKEW PLATE ROTATIONAL AMPLITUDE

t = SKEW PLATE THICKNESS

$$B = \sin^{-1} \left(\frac{\sin A}{n} \right)$$

n = SKEW PLATE INDEX OF REFRACTION

DESIRABLE FEATURES

- GYROSCOPIC CONTROL THROUGH ELECTRONIC DRIVERS CAN BE READILY PROGRAMMED FOR DIFFERENT ZOOM RATIOS

APPLICATION

- PRIMARILY TO SMALL DIAMETER SECTIONS OF THE OPTICAL SYSTEM RAY BUNDLES TO EITHER THE VIEWING VIDICON OR IR DETECTOR OPTICAL SYSTEMS IN CONVERGING BUNDLE

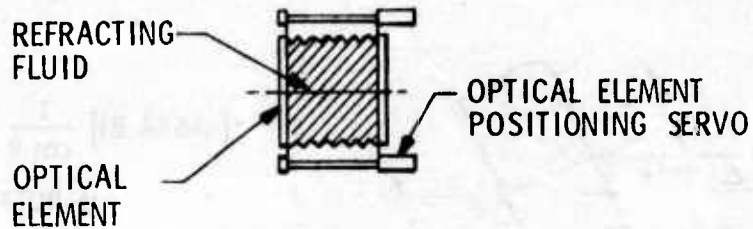
FLIR SYSTEM MODIFICATIONS

- CHANGES IN OPTICAL SYSTEM DESIGN AND PACKAGING CONFIGURATION REQUIRED TO ACCEPT THE OPTICAL ELEMENTS AND THEIR DRIVERS

LIMITATIONS

- DECREASE IN FLIR OPTICAL SYSTEM TRANSMISSION EFFICIENCY AND OPTICAL QUALITY
- OPEN LOOP STABILIZATION SYSTEM

Figure 17 Oscillating Skew Plate



DESIRABLE FEATURES

- GYRO CONTROL THROUGH ELECTRONIC DRIVERS CAN BE READILY PROGRAMMED FOR ZOOM CONTROL

APPLICATION

- PRIMARILY TO SMALL DIAMETER SECTIONS OF THE OPTICAL SYSTEM RAY BUNDLES TO EITHER THE VIEWING VIDICON OR IR OPTICAL SYSTEMS

FLIR SYSTEM MODIFICATIONS

- CHANGES IN OPTICAL SYSTEM DESIGN TO ACCEPT THE OPTICAL SYSTEM AND DRIVE

LIMITATIONS

- FREQUENCY RESPONSE LIMITED
- DECREASE IN FLIR OPTICAL SYSTEM TRANSMISSION EFFICIENCY AND OPTICAL QUALITY
- OPEN LOOP STABILIZATION SYSTEM

Figure 18 Variable Angle Prism

changes in the overall system optical path length. Consequently, this method was considered less desirable than the oscillating mirror.

(5) Inertially Stabilized Optical Elements

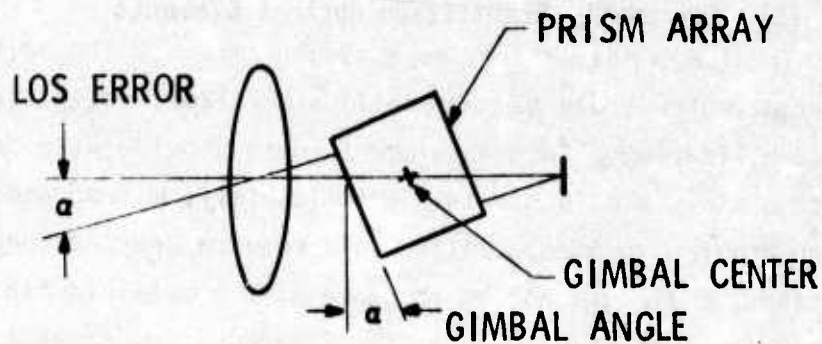
The ideal method for image stabilization would be the use of an optical element which could be inertially stabilized, using its own inertia to aid in stabilization. Such an element would provide wide bandwidth stabilization with a minimum of controls. Unfortunately, mirror and prism techniques which provide this capability would require drastic changes in the optical systems, and would not be amenable with a multiple field-of-view sensor. An example of this type is the gimballed prism shown in Figure 19.

b. Techniques of Electronic Stabilization

(1) Display Stabilization

Display stabilization may be achieved using standard TV display, as shown in Figure 20. In this method, the pulse phase of the horizontal and vertical sync pulses is varied in response to FLIR angular motions sensed by a gyro. There is a frequency response limit in this system. The horizontal line rate of 15,750 Hz is high enough to achieve adequate horizontal stabilization; however, the 60-Hz vertical field rate precludes stabilization at frequencies higher than about 30 Hz in the vertical direction. Thus, a serial scan FLIR would require an optical, line-of-sight stabilization system in the vertical direction.

A parallel scan FLIR, with light-emitting diode (LED) or digital scan conversion to TV format, could not use TV display stabilization because the vidicon scan format differs from the FLIR scan format. Because the scan converters display the scene slightly later than real time, any sensing of sensor motion and application of direct stabilization correction to the display will provide an erroneous stabilization value. Thus, for the parallel scan system, stabilization must be provided prior to the vidicon.



DESIRABLE FEATURES

- INERTIAL STABILIZATION
- CLOSED LOOP STABILIZATION SYSTEM

APPLICATION

- IR OR VIDICON OPTICAL SYSTEMS

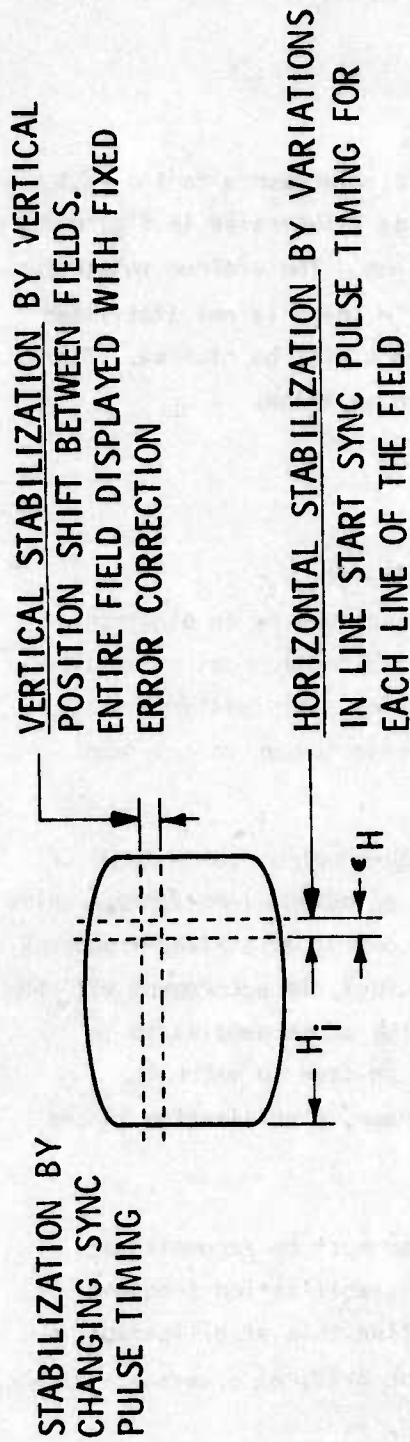
FLIR SYSTEM MODIFICATIONS

- CHANGES IN OPTICAL SYSTEM DESIGN TO ACCEPT OPTICAL ELEMENT AND GIMBAL

LIMITATIONS

- VARIABLE ZOOM PRISM MUST BE MOVED IN THE OPTICAL SYSTEM
- DECREASE IN FLIR OPTICAL SYSTEM TRANSMISSION EFFICIENCY AND OPTICAL QUALITY

Figure 19 Gimbaleed Prism



DESIRABLE FEATURES

- SIMPLE GYRO CONTROL OF TV MONITOR FORMAT HORIZONTAL LINE POSITION
- READILY ADJUSTABLE TO VARIABLE ZOOM RATIOS

APPLICATION

- DIRECT IR SERIAL SCAN FLIR SYSTEMS

FLIR SYSTEM MODIFICATIONS

- SIMPLE ELECTRONIC CIRCUITS ADDED TO DISPLAY MONITOR

LIMITATIONS

- APPLICABLE ONLY TO SERIAL SCAN FLIRS
- VERTICAL STABILIZATION LIMITED TO 30 Hz
- OPEN LOOP STABILIZATION SYSTEM

Figure 20 Display Stabilization

(2) Vidicon Focal Plane Stabilization

Stabilization by applying corrective displacements to the instantaneous sampling position on the vidicon target, as illustrated in Figure 21, will not accomplish FLIR line-of-sight stabilization. The vidicon integrates the scene on the vidicon target plane; thus, if the image is not stabilized prior to the vidicon, the resultant integrated image will be blurred. There is no reasonable processing method to de-blur such an image.

c. Hybrid Stabilization Techniques

(1) Electronic Scan Converter Stabilization

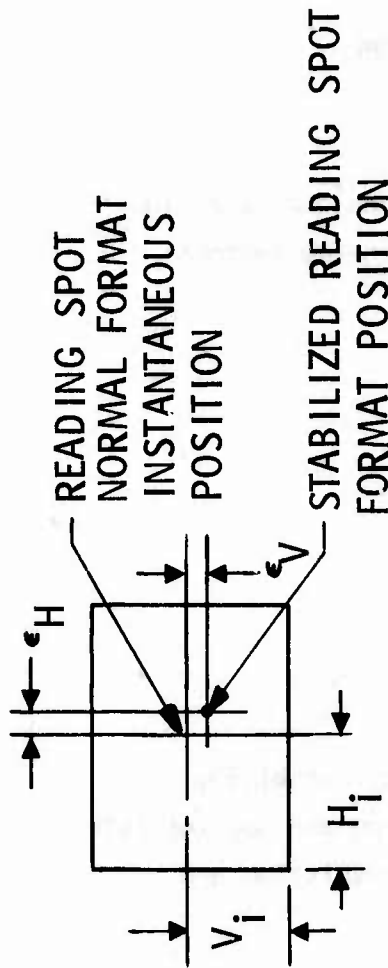
If the LED/vidicon scan converter is replaced by an electronic scan converter, stabilization parallel to the scan direction can be obtained by phase modulating the scan converter sampling rate. This system would be used in combination with optical stabilization perpendicular to the scan direction.

Electronic scan converters using charge-coupled device (CCD) or digital techniques normally strobe the outputs of detectors into storage units at a predetermined rate. This rate is under the control of a fixed-frequency oscillator. By phase modulating the oscillator output, in accordance with the FLIR line-of-sight displacement, the position of the scene samples to be stored in the CCD or digital storage array can be shifted to match the instantaneous line-of-sight position. In this manner, stabilization in the direction of scan may be accomplished.

Stabilization perpendicular to the scan must be accomplished optically because the maximum electronic vertical stabilization frequency is limited by the TV frame rate of 30 Hz. To accomplish this stabilization, the folding mirror may be gimballed and driven about one axis, as previously discussed.

(2) LED-Vidicon Scan Converter Stabilization

In this configuration, stabilization parallel to the scan direction can be obtained by optical means in the LED-vidicon optics, and stabilization perpendicular to the scan can be obtained by optical means in the IR optics. This can be accomplished by using a single-axis gimballed skew plate



DESIRABLE FEATURES

- SIMPLE GYRO CONTROL OF VIDICON FORMAT HORIZONTAL AND VERTICAL SWEEP POSITIONS
- READILY ADJUSTABLE TO ZOOM RATIOS

APPLICATION

- LIMITED TO ELECTROSTATIC CONTROLLED VIDICON VIEWED IR IMAGE SCAN CONVERSION SYSTEMS

FLIR SYSTEM MODIFICATIONS

- SIMPLE ELECTRONIC CIRCUITS ADDED TO VIDICON

LIMITATION

- INTEGRATION TIME OF VIDICON BLURS IMAGE PRIOR TO STABILIZATION

Figure 21 Vidicon Focal Plane Stabilization

In the visual optic system and a single-axis gimbaled folding mirror in the IR optic system, as illustrated in Figure 22.

4. TECHNIQUE SELECTION FOR LABORATORY DEMONSTRATION BREADBOARD MODEL

a. Selection Criteria

In the evaluation of the candidate techniques for high-frequency stabilization, consideration was given to the following factors:

- Applicability
- Zoom adaptability
- FLIR modifications
- Optical system degradation
- Stabilization performance
- Type of system

Primary weight in the evaluation was given to

- Adequate stabilization performance capability
- Universal applicability to existing and modular FLIR
- Feasibility and ease of adding to existing and modular FLIRs
- Cost

In the evaluation of applicability, if the technique was only applicable to a serial scan or to a parallel scan FLIR, but not to both, it was not considered to be an acceptable candidate.

Because the FLIRs involved have a step zoom or a potential variable-zoom capability, it was important that the stabilization technique be readily adaptable to the zoom requirements.

The extent of the modifications necessary to integrate the stabilization technique into the FLIR was considered to be of prime importance.

276-1594

276-1594

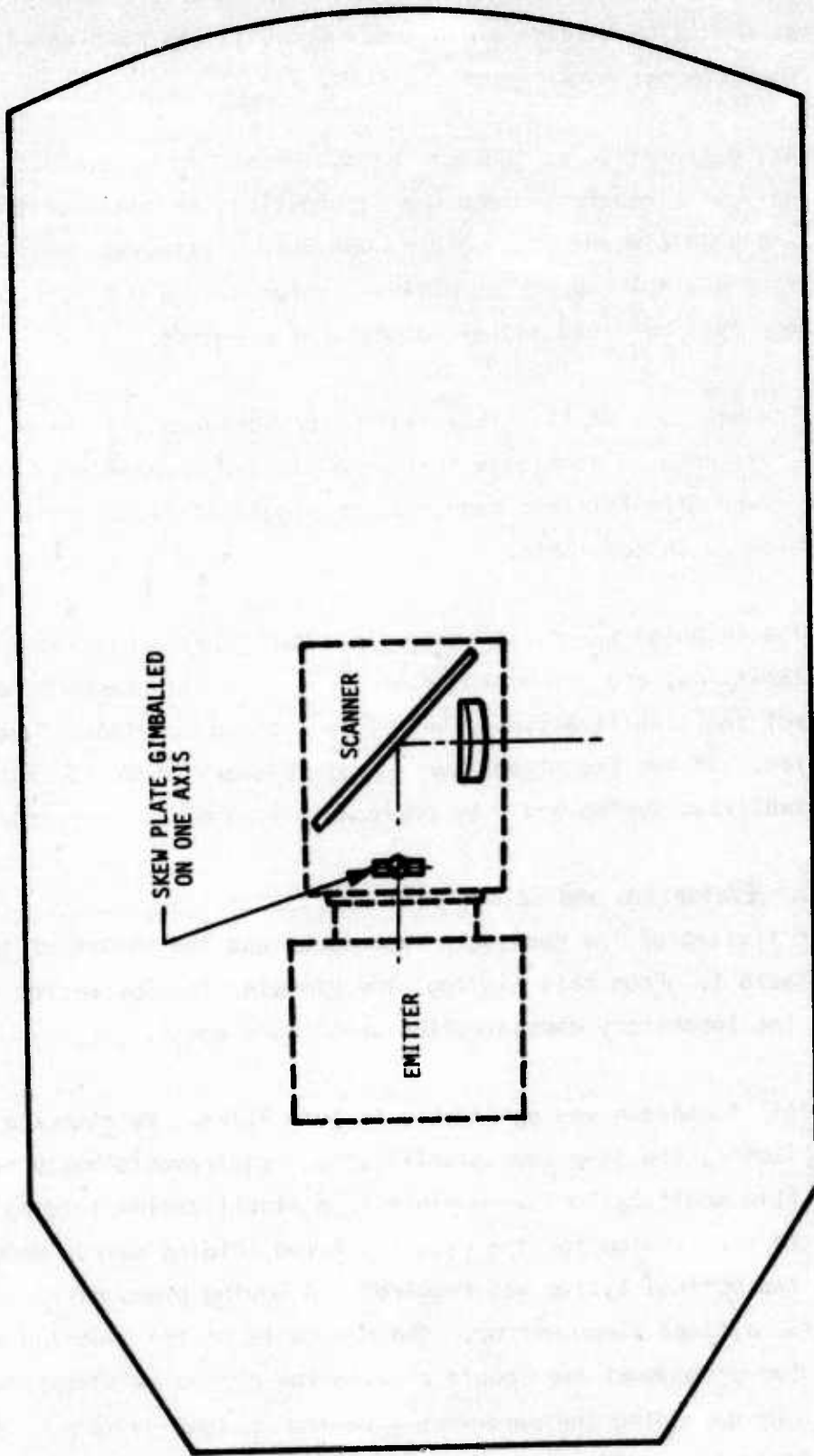


Figure 22 Scan Stabilization By An Optical Skew Plate

Any redesign of other parts or modules of the FLIR to accommodate the stabilization system should be held to a minimum. Also, it was considered important to maintain the external envelope of the FLIR.

Any degradation of the optical system was to be avoided. The addition of optical elements would cause degradations in image quality or sensitivity and possibly introduce other undesirable effects. Consequently, a technique that did not change the optical system design was considered better than one that required additional optical elements.

The adequacy of the stabilization performance was the primary criterion in this area. Techniques that were limited in frequency or by quantization steps of sufficient magnitude to significantly degrade the image MTF were considered unacceptable.

The techniques were separated into two types: one was inherently inertially stabilized, and the other required driving with respect to inertial space to effect the stabilization. The latter type was called a "feed-forward" system. If two techniques were equal in every other respect, the inertially stabilized system would be preferable to the feed-forward system.

b. Evaluation and Selection

A listing of the candidate techniques and the rating of the factors is given in Table 1. From this listing, the gimbaled folding mirror was selected for the laboratory demonstration breadboard model.

This technique was applicable to both FLIRs. By changing the mirror driver scale factor, the step zoom stabilization requirements could readily be met. The FLIR modifications were minimal; a stabilization folding mirror module could be substituted for the existing fixed folding mirror modules. No change in the optical system was required. A moving plano mirror could be substituted for a fixed plano mirror. The movements of the gimbaled folding mirror about two orthogonal axes could provide the degree of stabilization required without degrading the performance of the optical systems. The system is a "feed-forward" system, but the stability characteristics of the

TABLE 1. EVALUATION SUMMARY

Candidate stabilization technique	Applicability	Zoom adaptability	FLIR modifications	Optical system degradation	Stabilization performance	Type system	Relative rating
<u>Optical</u>							
Gimbaled folding mirror	Both FLIRs	Simple - scale factor	Simple - replacement of folding mirror	None	Adequate	Feed Forward	1
Gimbaled doublet lens	Both FLIRs	Simple - scale factor	Major - design changes optical and mechanical	Image quality and transmission	Adequate	Feed Forward	
Gimbaled skew plate	Both FLIRs	Simple - scale factor	Major - design changes optical and mechanical	Image quality and transmission	Adequate	Feed Forward	
Variable-angle prism	Both FLIRs	Simple - scale factor	Major - design changes optical and mechanical	Image quality and transmission	Frequency limited	Feed Forward	
Gimbaled prism	Both FLIRs	Complex - position change	Major - design changes optical and mechanical	Image quality and transmission	Good	Inertial	
<u>Electronic</u>							
Display	IR-serial scan only	Simple - scale factor	None - simple addition to display	None	Inadequate 30 Hz vertical	Feed Forward	2
Vidicon focal plane	E/O scan converter configurations	Simple - scale factor	None - simple addition to vidicon	None	Inadequate - vidicon image blurred before stabilization	Feed Forward	
Hybrid electronic scan converter	Both FLIRs	Simple - scale factor	Simple - replacement of folding mirror add scan converter	None	Adequate	Feed Forward	
LED-vidicon scan converter	IR parallel scan only	Simple - scale factor	Simple - replacement of folding mirror add 1 axis skew plate	Minor image quality and transmission	Adequate	Feed Forward	

electronic components indicated acceptable stability in the overall system performance. Feedback measurements of the stabilization mirror motions could be made. However, such measurements would be subject to the same type of variations as the mirror drive system itself, due to electronic component stability characteristics. Consequently, it was recommended that the initial performance tests be made without any feedback in the stabilization system.

SECTION IV

LABORATORY DEMONSTRATION BREADBOARD MODEL DESIGN

The laboratory demonstration breadboard model was a stabilized-mirror system comprising the following major parts:

- Gimbaled mirror
- Mirror driver
- FLIR motion sensor
- Electronics

The gimbaled mirror/driver was configured for ease in fabrication and suitability for mounting in the laboratory test fixture. The motion sensor was an available prototype that, although not optimized for this specific application, had suitable characteristics. The electronics comprised available laboratory equipment that had acceptable characteristics.

These major parts are discussed in more detail ~~in the following~~ paragraphs.

1. GIMBALED MIRROR

The primary requirements for the gimbaled mirror included:

a. Mirror Structure

- (a) Adequate stiffness to maintain the required optical flatness under dynamic loads imposed by the vibration environment as well as those from the stabilization driver
- (b) Sufficiently low moment of inertia so the mirror/driver system would have a natural frequency of approximately 500 Hz or higher

- (3) Adequate geometric stability over a wide temperature range.

(2) Mirror Pivot

- (a) Gimbal axes on the center of gravity of the mirror so the linear vibration environment would cause no mirror rotation
- (b) Sufficient stiffness in the gimbal pivot so the mirror surface would not change position in the optical system under the linear vibration environment
- (c) Low friction in the gimbal pivots.

(3) Cost

- (a) Low development cost
- (b) Low production cost.

a. Mirror Structure

An aluminum honeycomb substrate with a plano replicated optical mirror surface and a ball and socket pivot mounting was selected as best meeting the mirror structure requirements. This design is illustrated in Figure 23.

In evaluating the mirror material and construction, the following factors were considered:

<u>Factor</u>	<u>Design Requirement</u>
Stiffness versus moment of inertia	High stiffness High natural frequency mirror/drive
Thermal diffusivity	Low temperature effects
Basic material cost	Low production cost
Fabrication technique status of development	Low development cost

1275-1252

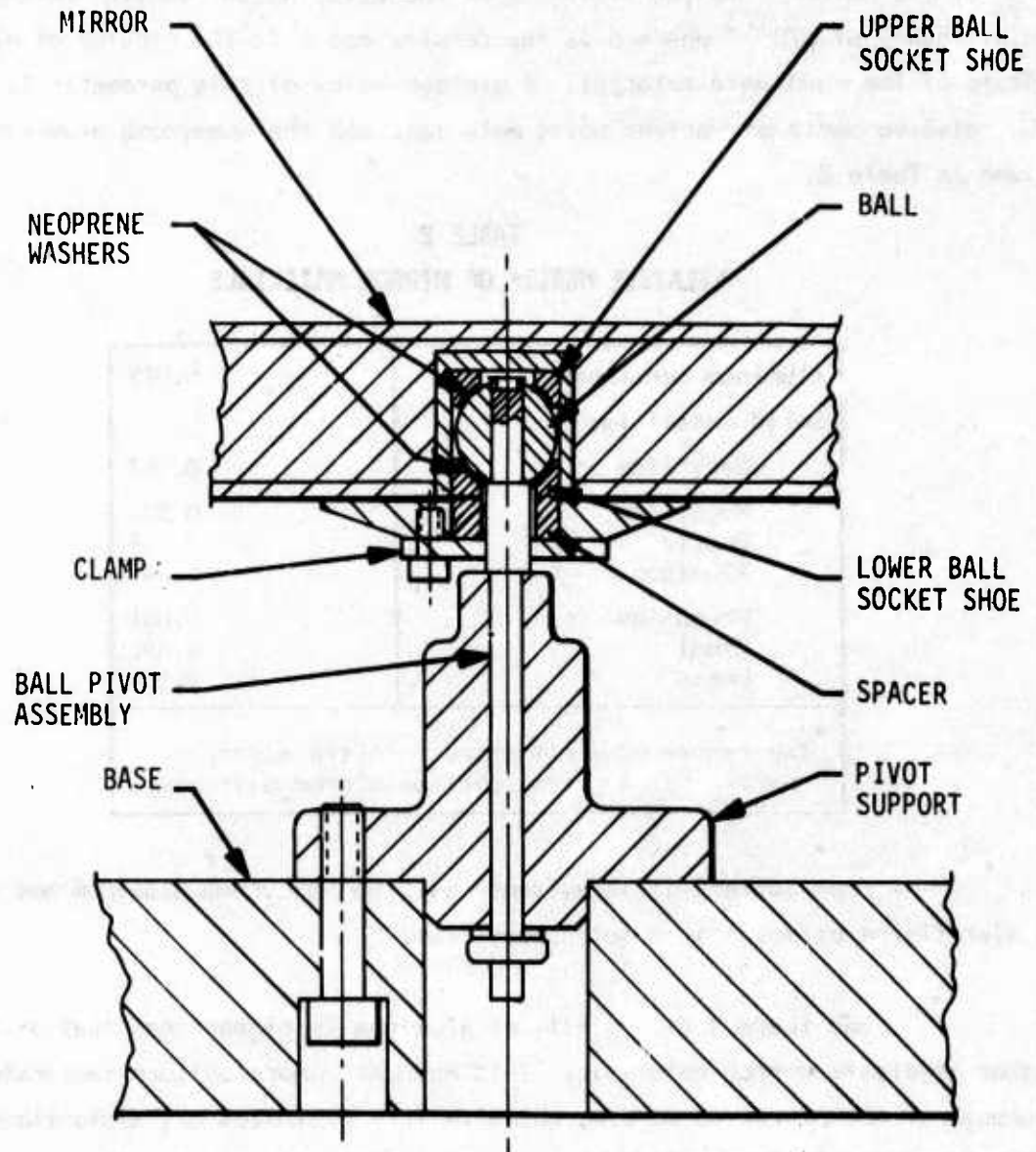


Figure 23 Section View-Ball and Socket Pivot Mounting Of The Mirror

A figure of merit was used for evaluating the stiffness versus moment of inertia. This consisted of the ratio of the inertia of a solid beam of the material to the stiffness of the beam, which resulted in the relationship of $\rho/E^{1/3}$ where ρ is the density and E is the modulus of elasticity of the candidate material. A minimum value of this parameter is desired. The relative merit of various solid materials and the honeycomb aluminum is given in Table 2.

TABLE 2
RELATIVE MERIT* OF MIRROR MATERIALS

Aluminum honeycomb	0.015
Solid materials:	
Beryllium	0.019
Magnesium	0.034
Quartz	0.037
Aluminum	0.045
Germanium	0.081
Steel	0.096
Brass	0.124
* The figure of merit represents the mirror inertia for a given level of mirror stiffness.	

From Table 2 it is evident that the honeycomb aluminum has a better figure of merit than solid beryllium.

The thermal diffusivity of aluminum is higher than that of the other candidate mirror materials. This assures a more uniform temperature throughout the mirror structure, which in turn minimizes any distortions of the mirror due to temperature changes and transients. Temperature cycling tests of aluminum honeycomb substrates with replicated mirror optical surfaces between 0° and 150°C have shown no degradation of the optical surface.

The techniques of fabricating the honeycomb substrates, as well as the techniques of applying the replicated optical surface, have been developed. This was demonstrated during the procurement of the mirror for

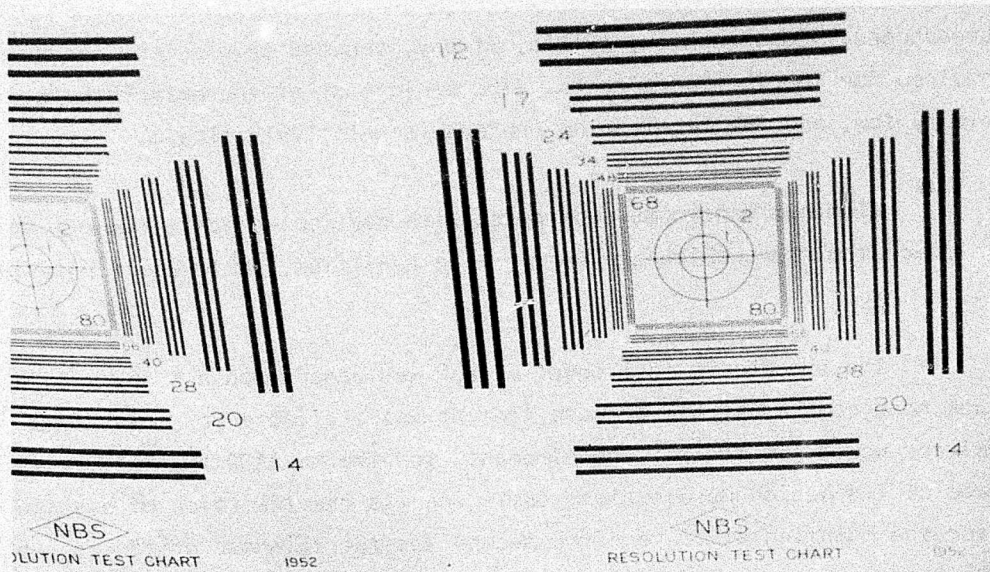
the breadboard. Consequently, little, if any, process development costs would be required for fabricating mirrors. The basic cost of the materials is relatively low, and the fabrication process is relatively simple.

Aluminum honeycomb substrates with replicated optical surfaces offer low-cost mirrors which are better than beryllium, in terms of relative merit.

The breadboard test model mirror was based upon a 4 in. x 4 in. aluminum honeycomb substrate because tooling was available for this size. This mirror would fit the size requirements for the AN/AAQ9 XA2 FLIR. Two features of its design were exploratory. One was the insertion of a solid core for the mounting pivot, and the second was the thinness of the top and bottom plates. They were made intentionally thin to reduce the moment of inertia. The question was whether or not the internal structure of the central core and the honeycomb pattern would show through the replicated plano optical mirror surface.

The replicated surface of the mirror had an excellent optical quality, as indicated by Figure 24 which shows the reflection of a NBS resolution chart. Photographs of interferometer patterns showing the flatness of the mirror surface are presented in Figure 25. The patterns along both the XX axis and the YY axis are 90 degrees from each other. The mirror flatness is within one fringe throughout the oval footprint of the optical ray bundle of the FLIR optical system.

To determine the extent that the honeycomb core of the mirror substrate and the solid boss for the pivot showed through, the mirror surface plane was adjusted so that the entire surface was within one interference fringe. The honeycomb core was not apparent, and the surface variation over the solid pivot boss was negligible, as indicated by the photograph in Figure 26.



NBS
RESOLUTION TEST CHART

1952

NBS
RESOLUTION TEST CHART

1955

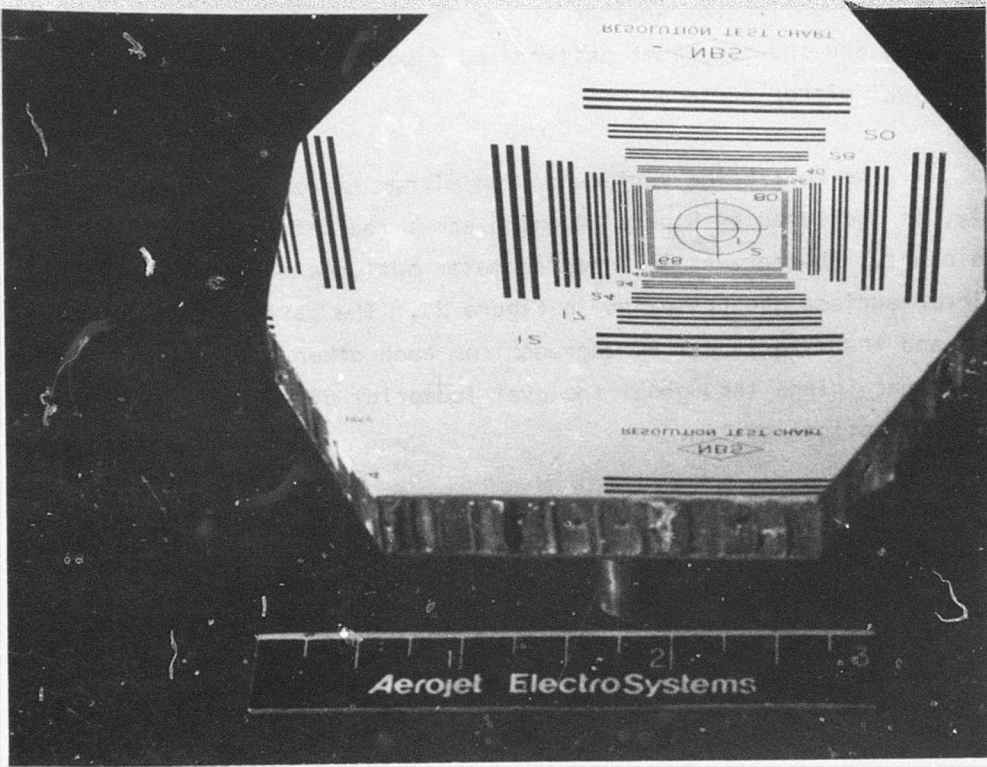
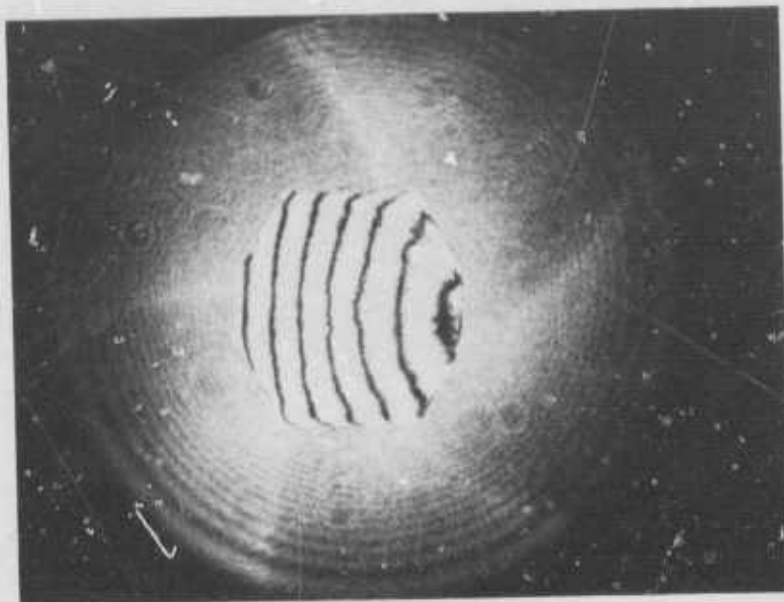
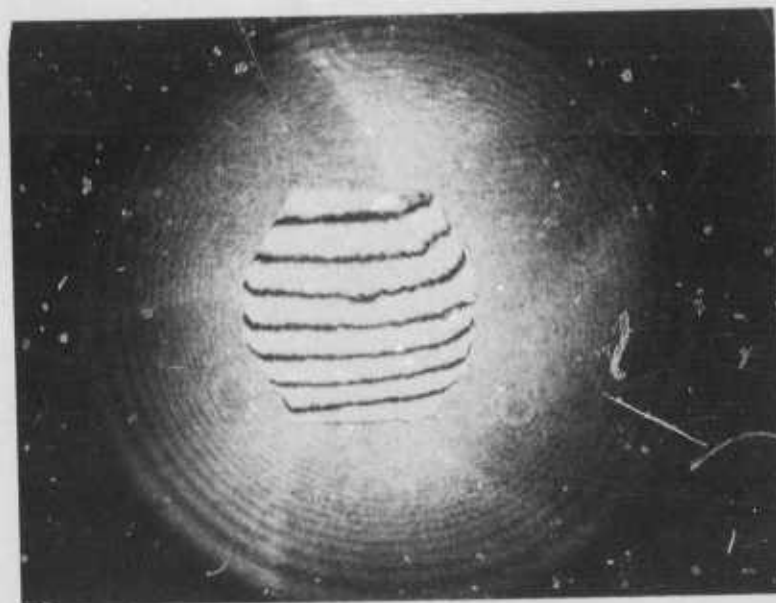


Figure 24 Replicated Plano Mirror



A. Along XX Axis



B. Along YY Axis

Figure 25 Mirror Surface Interferometer Pattern

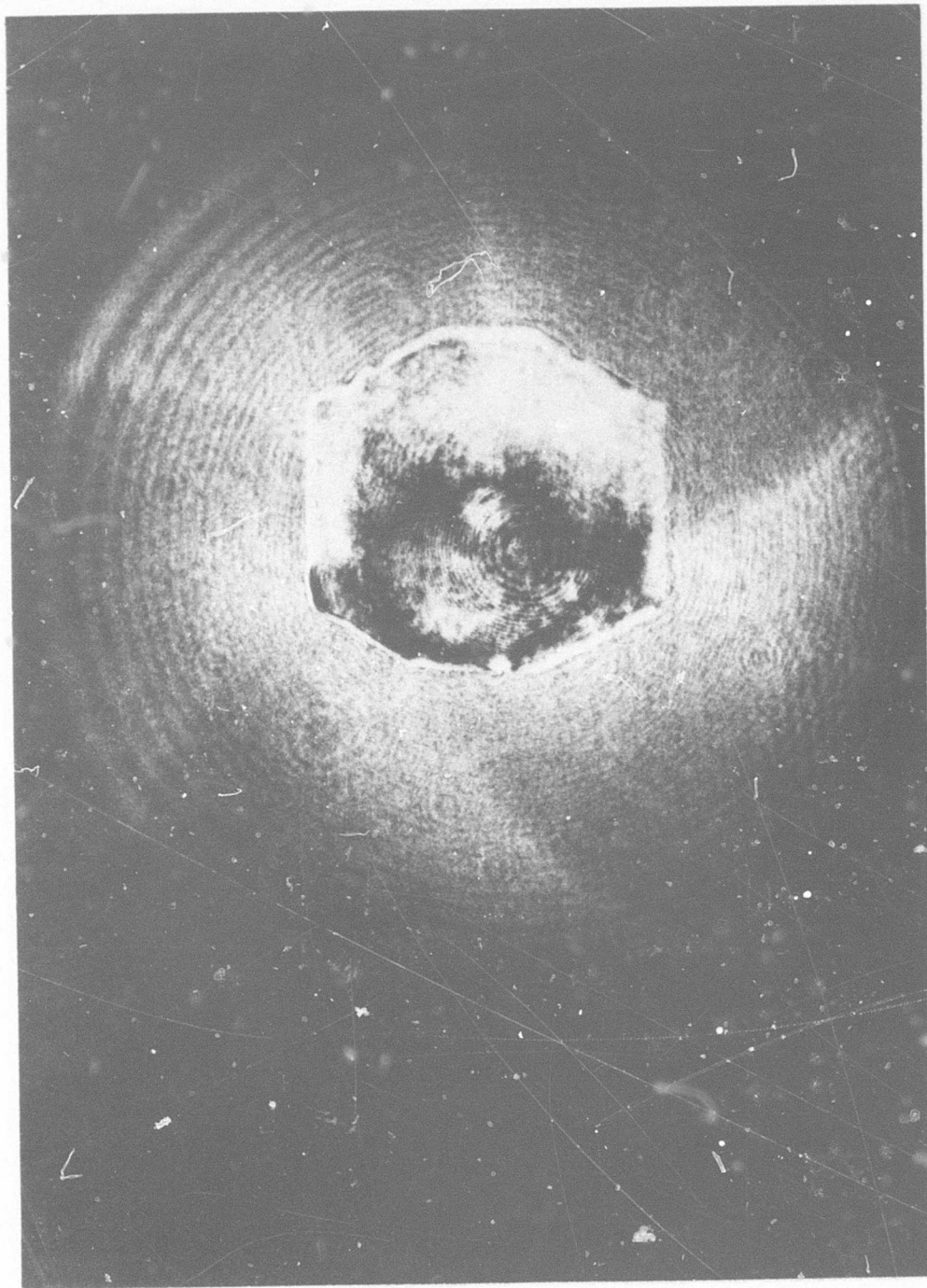


Figure 26 Mirror Surface Interferometer Pattern
Within One Fringe

b. **Mirror Pivot**

To best meet the requirements, a ball and socket pivot at the mirror center of gravity was selected. This design is illustrated in Figure 23.

The requirement of a two-axis gimbal at the mirror center of gravity more or less dictated the ball and socket pivot. The size needed to be minimal to avoid degradation of the plano mirror surface.

To avoid the problem of static "break-away" friction in combination with the subsequent lower magnitude of sliding friction, neoprene pads were clamped between the pivot ball and the socket shoes. These clamped washers acted as a torsional spring connection between the pivot and the mirror with some hysteresis, which provided a degree of damping to the dynamic system. The dynamic characteristics of the mirror/driver system followed the classical dynamic amplification factor curve for a second-order system with a ξ of 0.014, as indicated by Figure 27.

The degree of compression of the neoprene pads was controlled to give a sufficiently high lateral spring constant to maintain the mirror in place in the optical system under the vibration environment. Static loading tests, performed in accordance with the Engineering Test Plan, showed the axial deflections expected under the peak linear vibration environment of 20 g at 105 Hz would cause a translational mirror displacement in the optical system of approximately 0.0002 in. This was considered to be satisfactory.

2. **MIRROR DRIVER**

The primary requirements for the mirror driver included:

1) Driving Capabilities

- (a) Natural frequency of the mirror/driver system of approximately 500 Hz or higher
- (b) Sufficient amplitude of mirror motion.

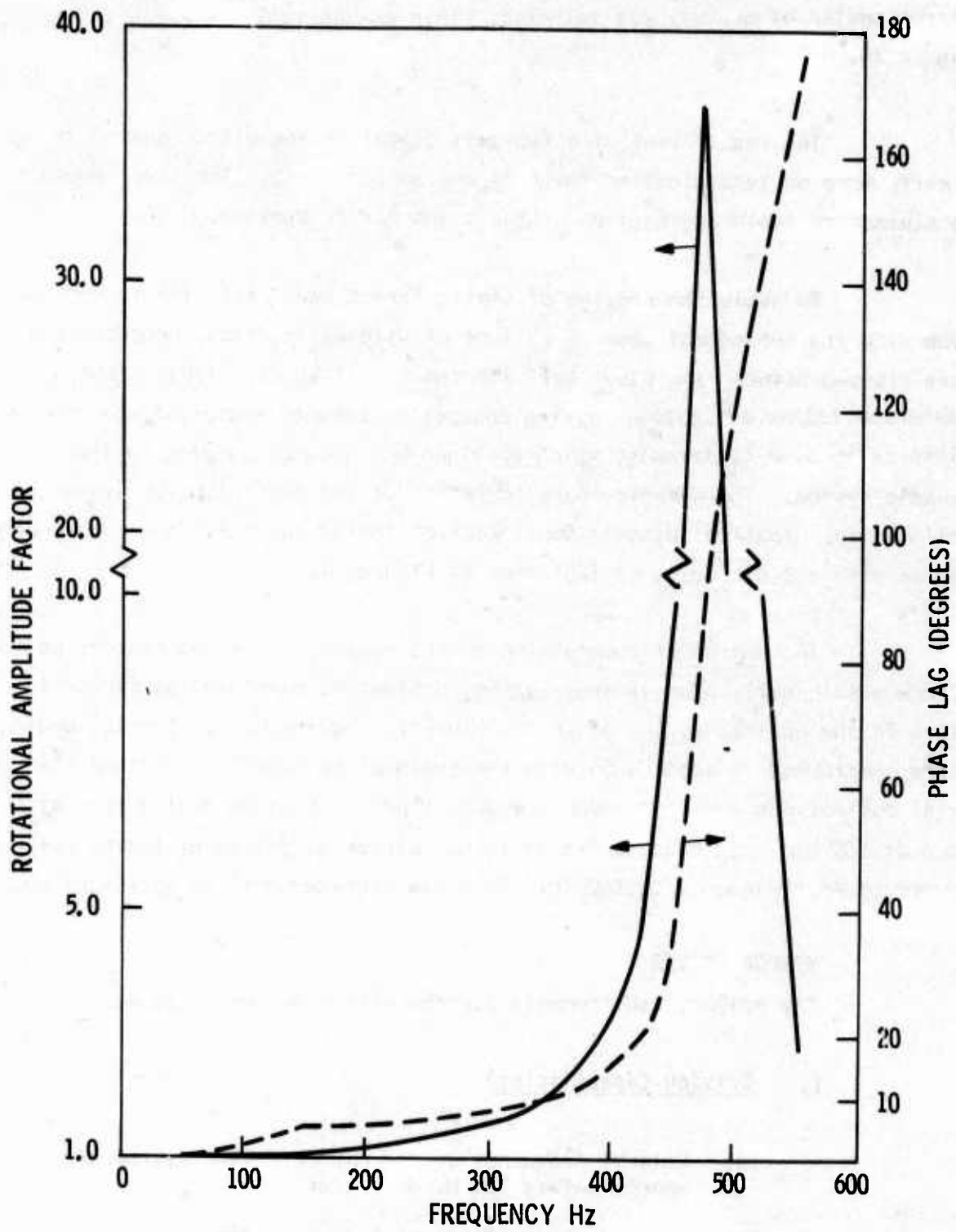


Figure 27 Mirror/Driver System Dynamic Characteristics

2) Characteristics

- (a) Linearity with frequency and amplitude
- (b) Low hysteresis
- (c) Stable characteristics with respect to temperature and time
- (d) Long life.

3) FLIR Modification Integration Considerations

- (a) Form factor
- (b) Weight.

The primary candidate drivers for the stabilization folding mirror were

- Magnetic torquers
- Piezoelectric benders
- Voice coils.

Because the magnetic torquers were relatively large and heavy and had a poor form factor for fitting into the FLIRs, primary consideration was given to the piezoelectric bender and the voice coil. The piezoelectric bender was selected as the mirror driver. The physical arrangement to drive the mirror about two axes is illustrated in Figure 28.

a. Driving Capabilities

To provide the required stabilization mirror performance, the drivers required a spring constant of 400 pounds/inch with a 0.0010 in. travel. An optical analysis of the narrow-field-of-view system of the AN/AAQ9 XA2 indicated a mirror motion of ± 0.572 microradian to accomplish an exact image position correction for a line-of-sight vibration of

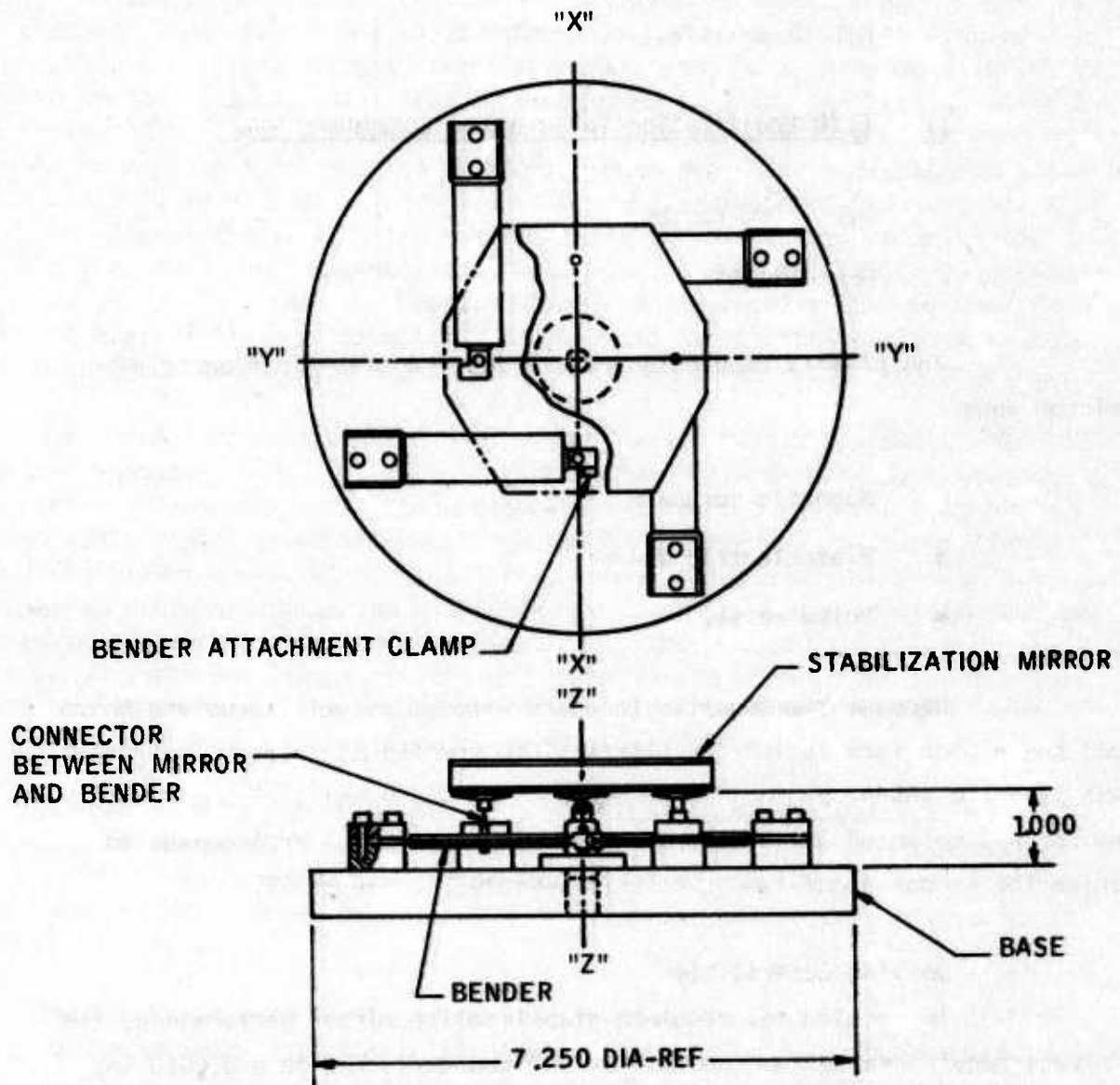


Figure 28 Laboratory Breadboard Stabilization Mirror Unit

±150 microradians. In cases where the mirror rotational axis is not normal to the optical system axis, a larger physical mirror motion about the canted axis is necessary to obtain the required effective optical system mirror motion. The relationship of the magnitude of the applied rotation about the canted axis to the effective mirror rotation in the optical system is:

$$\alpha = \frac{\alpha'}{\sin \beta}$$

where

- α = applied rotation about canted mirror rotational axis
- α' = effective mirror rotation in optical system
- β = angle between optical axis and the canted mirror rotational axis.

In the laboratory breadboard, which simulates the optical system of the AN/AAQ9 XA2, β is approximately 67 degrees. This results in a required rotation about the canted mirror rotational axis of ±0.62 microradian for complete image position stabilization.

Both the piezoelectric bender and the voice coil could provide these mirror driving capabilities. The voice coil has potentially the capability for significantly larger amplitude of travel than the piezoelectric benders. However, the voice coil has the following operating disadvantages:

- Heat is generated in the coils which must be attached to the mirror
- Accurate alignment must be held between the coils and the magnet
- Dirt must be excluded from the magnetic air-gap

By contrast, any heat liberated in the piezoelectric benders has no effect upon the mirror, no accurate alignment of the mirror position with the piezoelectric benders is required, and the drive system is relatively insensitive to dirt.

b. Characteristics

Because the stabilization system is planned to operate without feedback, the linearity and stability of the drivers is important. The voice coil drive force characteristics can be maintained by controlling the ampere flow of the current, rather than the applied voltage. The same current flow will generate the same force whether the coil is hot or cold. Also, the magnitude of the force generated is directly proportional to the current flow. However, non-linear can be encountered due to magnetic hysteresis and magnetic flux leakage.

The piezoelectric element also has a direct relationship between the applied voltage and the displacement, as indicated by the test data in Figure 29. It has a scale factor with temperature, being essentially linear at 0.25 percent/ $^{\circ}\text{C}$ from 0° to 44°C . This type of a scale factor correction is readily built into a system. Maximum achievable displacements of a piezoelectric device approach 0.010 in (double amplitude). However, there are many interactive factors affecting a design application. Consequently, singling out one parameter to list nominal maximum values without regard to other factors that may be involved in a design application can be relatively meaningless.

The ceramic used in the breadboard drivers had a frequency as well as amplitude dependence, as indicated by the test data shown in Figure 30. The magnitude of this dependency can be reduced by the selection of ceramic material with less hysteresis than the material used. It would be expected that a voice coil driver would also have a degree of frequency and amplitude dependence. The magnitude would be dependent upon the specific design.

Long life can be expected from both the voice coil and the piezoelectric driver. Current AESC flexural mode piezoelectric devices are designed for reliable service to 10^9 cycles. Voice coils do not require any mechanical flexure, except for the spring to establish the mirror/driver natural frequency; thus, longer life can be expected from the voice coil drive.

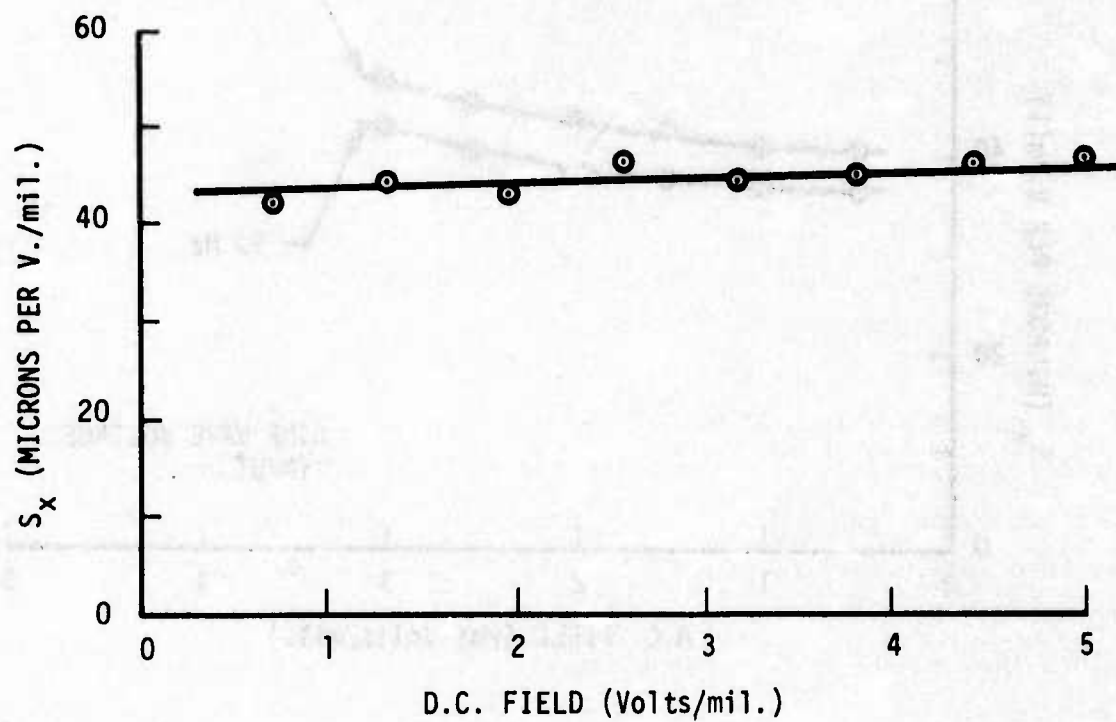


Figure 29 Displacement Sensitivity Versus D-C Electric Field Strength in Ceramic

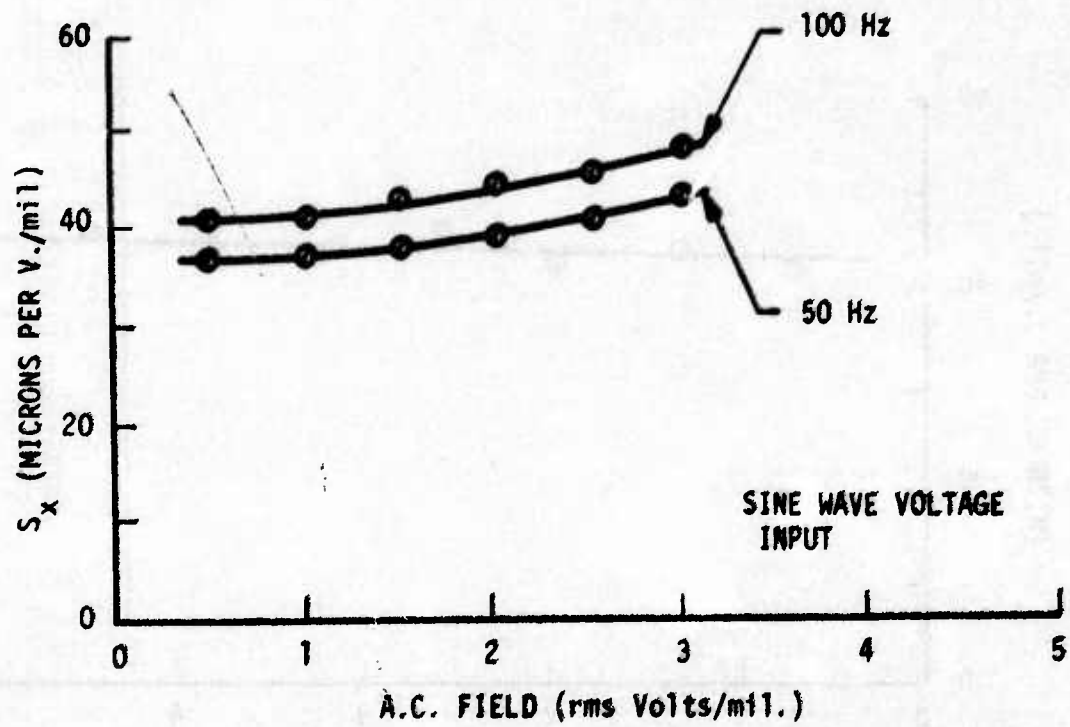
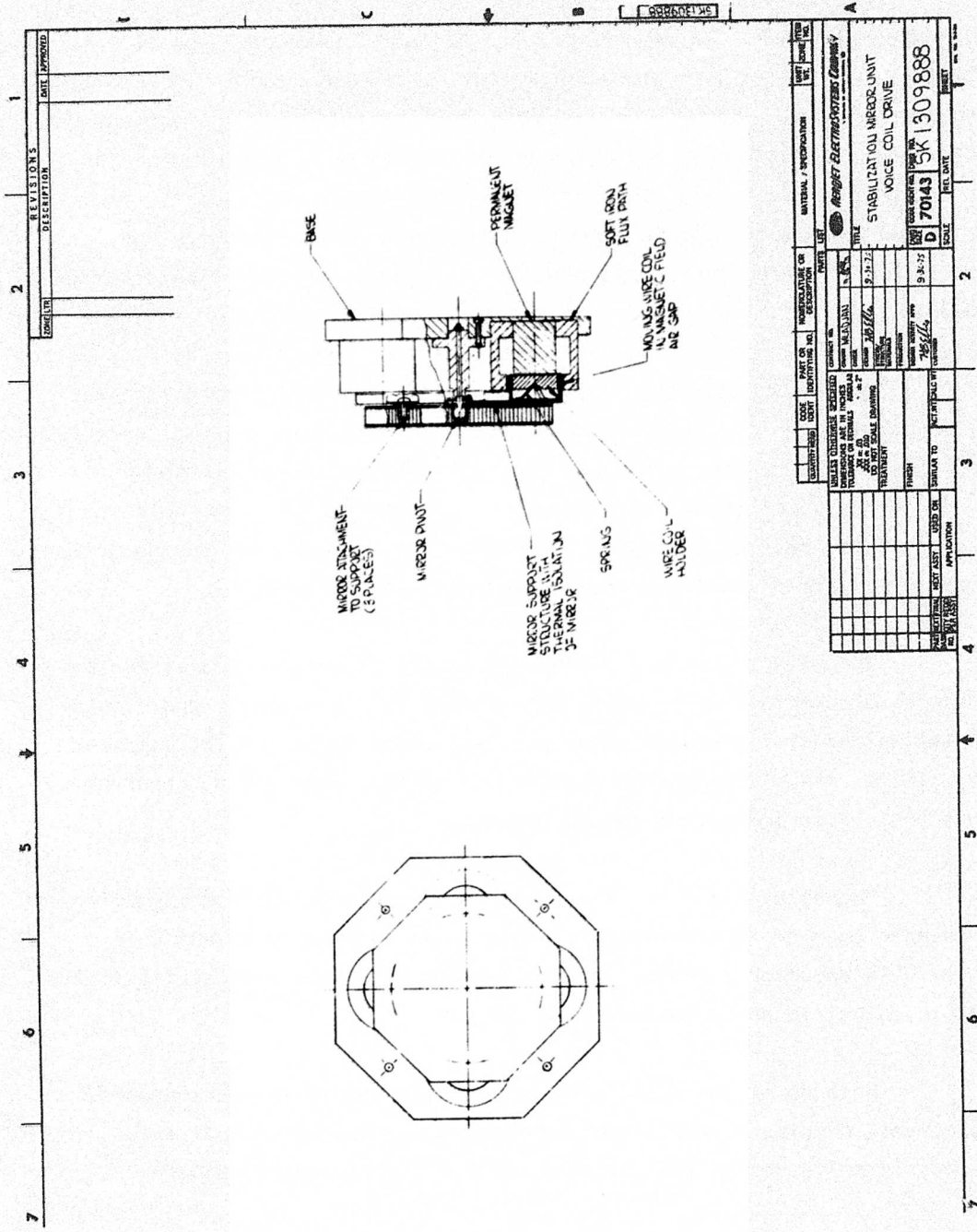


Figure 30 Figure Displacement Sensitivity Versus A-C Electric Field Strength in Ceramic



REV.	DATE	DESCRIPTION	BY	CHKD.
1				
2				
3				
4				
5				
6				
7				

REV.	DATE	DESCRIPTION	BY	CHKD.
1				
2				
3				
4				
5				
6				
7				

REV.	DATE	DESCRIPTION	BY	CHKD.
1				
2				
3				
4				
5				
6				
7				

REV.	DATE	DESCRIPTION	BY	CHKD.
1				
2				
3				
4				
5				
6				
7				

REV.	DATE	DESCRIPTION	BY	CHKD.
1				
2				
3				
4				
5				
6				
7				

REV.	DATE	DESCRIPTION	BY	CHKD.
1				
2				
3				
4				
5				
6				
7				

REV.	DATE	DESCRIPTION	BY	CHKD.
1				
2				
3				
4				
5				
6				
7				

REV.	DATE	DESCRIPTION	BY	CHKD.
1				
2				
3				
4				
5				
6				
7				

REV.	DATE	DESCRIPTION	BY	CHKD.
1				
2				
3				
4				
5				
6				
7				

REV.	DATE	DESCRIPTION	BY	CHKD.
1				
2				
3				
4				
5				
6				
7				

REV.	DATE	DESCRIPTION	BY	CHKD.
1				
2				
3				
4				
5				
6				
7				

REV.	DATE	DESCRIPTION	BY	CHKD.
1				
2				
3				
4				
5				
6				
7				

REV.	DATE	DESCRIPTION	BY	CHKD.
1				
2				
3				
4				
5				
6				
7				

REV.	DATE	DESCRIPTION	BY	CHKD.
1				
2				
3				
4				
5				
6				
7				

REV.	DATE	DESCRIPTION	BY	CHKD.
1				
2				
3				
4				
5				
6				
7				

REV.	DATE	DESCRIPTION	BY	CHKD.
1				
2				
3				
4				
5				
6				
7				

REV.	DATE	DESCRIPTION	BY	CHKD.
1				
2				
3				
4				
5				
6				
7				

REV.	DATE	DESCRIPTION	BY	CHKD.
1				
2				
3				
4				
5				
6				
7				

REV.	DATE	DESCRIPTION	BY	CHKD.
1				
2				
3				
4				
5				
6				
7				

REV.	DATE	DESCRIPTION	BY	CHKD.
1				
2				
3				
4				
5				
6				
7				

REV.	DATE	DESCRIPTION	BY	CHKD.
1				
2				
3				
4				
5				
6				
7				

REV.	DATE	DESCRIPTION	BY	CHKD.
1				
2				
3				
4				
5				
6				
7				

REV.	DATE	DESCRIPTION	BY	CHKD.
1				
2				
3				
4				
5				
6				
7				

REV.	DATE	DESCRIPTION	BY	CHKD.
1				
2				
3				
4				
5				
6				
7				

REV.	DATE	DESCRIPTION	BY	CHKD.
1				
2				
3				
4				
5				
6				
7				

REV.	DATE	DESCRIPTION	BY	CHKD.
1				
2				
3				
4				
5				
6				
7				

REV.	DATE	DESCRIPTION	BY	CHKD.
1				
2				
3				
4				
5				
6				
7				

REV.	DATE	DESCRIPTION	BY	CHKD.
1				
2				
3				
4				
5				
6				
7				

REV.	DATE	DESCRIPTION	BY	CHKD.
1				
2				
3				
4				
5				
6				
7				

REV.	DATE	DESCRIPTION	BY	CHKD.
1				
2				
3				
4				
5				
6				
7				

REV.	DATE	DESCRIPTION	BY	CHKD.
1				
2				
3				
4				
5				
6				
7				

REV.	DATE	DESCRIPTION	BY	CHKD.
1				
2				
3				
4				
5				
6				
7				

REV.	DATE	DESCRIPTION	BY	CHKD.
1				
2				
3				
4				
5				
6				
7				

REV.	DATE	DESCRIPTION	BY	CHKD.
1				
2				
3				
4				
5				
6				
7				

REV.	DATE	DESCRIPTION	BY	CHKD.
1				
2				
3				
4				
5				
6				
7				

REV.	DATE	DESCRIPTION	BY	CHKD.
1				
2				
3				
4				
5				
6				
7				

REV.	DATE	DESCRIPTION	BY	CHKD.
1				
2				
3				
4				
5				
6				
7				

REV.	DATE	DESCRIPTION	BY	CHKD.
1				
2				
3				
4				
5				
6				
7				

REV.	DATE	DESCRIPTION	BY	CHKD.
1				
2				
3				
4				
5				
6				
7				

REV.	DATE	DESCRIPTION	BY	CHKD.
1</				

A voice coil drive design was made to compare the voice coil with the piezoelectric mirror drive. To provide a fixed "power off" position for the mirror, a force-spring system was selected which resulted in the configuration shown in Figure 31. In this design, the ball-and-socket pivot was used to position the mirror in an optical system. The pivot was located at the mirror center of gravity and its supporting substructure, wire coils, etc., so that the mirror would not be affected by applied translational vibrations. In the design, the structure supporting the wire coils could not be directly attached to the mirror substrate because the thermal effects from the heat generated by the I^2R loss in the coils would degrade the optical quality of the piano mirror. Consequently, a light but stiff supporting structure was added, supporting the mirror at three points to minimize any thermal effects. Because the inertia of the mirror was substantially increased by the added weight of the coils of copper wire and the necessary structure to hold the wire coils and to thermally isolate the mirror, increased force in the drivers was necessary to maintain the mirror/driver natural frequency.

The size and weight of the voice coil magnets were dictated by the force requirements, resulting in magnets 2.0 in. in diameter and 1.5 in. long. The weight of the design shown was calculated to be 7.8 lb, compared with 2.3 lb for the piezoelectric design. Currently, there is no apparent way this basic size and weight can be reduced.

Magnetic shielding is expected to be required with a magnetic drive because even small magnetic fields can have an adverse effect upon the low-level FLIR detector signals. On the other hand, the electrostatic fields of the piezoelectric drive would have no effect.

Because of the size, weight, magnetic shielding requirements, and relatively complex mirror structure required by the voice coil drive, the piezoelectric drive design was selected for the laboratory breadboard.

The trilaminar bender configuration illustrated in Figure 32 was selected. The flexure mode element consists of a ceramic-aluminum-ceramic

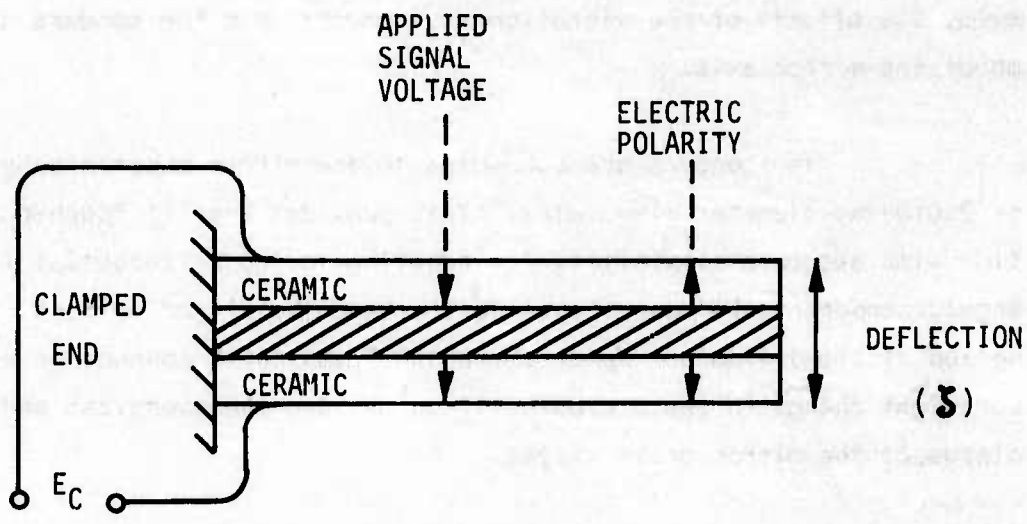


Figure 32 Simplified Side View of Trilaminar Bender

sandwich. It was designed with the requisite electrical characteristics needed to result in a flexure of the bar upon application of a voltage to the two-terminal input. With the application of a positive voltage, the bender will deflect in one direction. With the application of a negative voltage, it will bend in the other direction. By using a set of two benders to drive a mirror axis, the effects of any vibration environment upon the benders are balanced about the mirror axis.

The benders are connected to the mirror substrate by short lengths of 0.010-in.-diameter piano wire. This provides a stiff "push-pull" connection with adequate flexibility for adapting to the differential lateral and angular movements between the bender bar and the mirror motions. The combination of the trilaminar benders and the "push-pull" connection eliminates any boresight change in the mirror position between the energized and non-energized status of the mirror drive system.

The three-layer (trilaminar) bender bar, mounted as a cantilever, can be fabricated with highly reproducible results. Two prepolarized ceramic bars, electroded on their major surfaces after accurate lapping to prescribed thickness, are attached on opposite surfaces of precision-milled metal center-ply. They are attached by conductive epoxy, which is heat-cured under pressure.

Only minor long-term changes in the piezoelectric properties are expected. Since the two bender elements are from the same lot, they are expected to be subject to quantitatively similar changes in properties. Because the two elements in the laminated bender oppose each other, similar changes in properties tend to balance, resulting in negligible overall performance changes.

The details of the method of clamping the bender were found to have a marked effect upon the bender performance. Tests were made to investigate the effects of various clamping techniques, and a firmly cantilevered beam configuration was found to give the best performance.

3. FLIR MOTION SENSOR

For satisfactory performance, the FLIR line-of-sight displacements must be measured by an angular displacement sensor. The sensor must have a wide bandwidth with a linear response, a small phase shift (preferably none), and low broadband noise.

Angular displacement sensors are available that are essentially linear from 10 Hz to 1 kHz, and have a phase shift of 8.5 degrees at 10 Hz, dropping to 0.85 degree at 100 Hz, and 0.085 degree at 1000 Hz. The broadband noise from 10 Hz to 1000 Hz is less than 1 microradian. Satisfactory line-of-sight stabilization was measured with this sensor. At 105 Hz sinusoidal vibration input, 27 dB attenuation (broadband) was obtained, which would reduce a 150-microradian vibration amplitude to 7 microradians. The line-of-sight stabilization spectrum is shown in Figure 33.

The integrating rate gyros used for initial breadboard tests did not have these required characteristics. Although the output signal linearity could be maintained above the gyro rolloff frequency by compensation, such compensation increased the gyro noise as well as the signal. The gain versus frequency characteristics of the gyro compensation used with the integrating rate gyro are shown in Figure 34. When this gain was applied to the mechanical dynamic amplification of the mirror/driver system with a per unit critical damping of 0.014, the combined gain versus frequency noise amplifications became large, as shown in Figure 35. The resultant mirror stabilization noise with the integrating gyro was approximately 160 microradians rms with the spectrum shown in Figure 36. The integrating gyros used, however, did not represent the best obtainable. In fact, their angular momentum had been reduced significantly to increase torquing rate. This reduction also enhanced gyro noise. Thus, other integrating gyros could conceivably satisfy stabilization requirements.

4. ELECTRONICS

The stabilization system is shown by the system block diagram in Figure 37. In this system a stabilization mirror is located at a position in the telescope optics where the line-of-sight magnification is M . Thus, a

276-1195

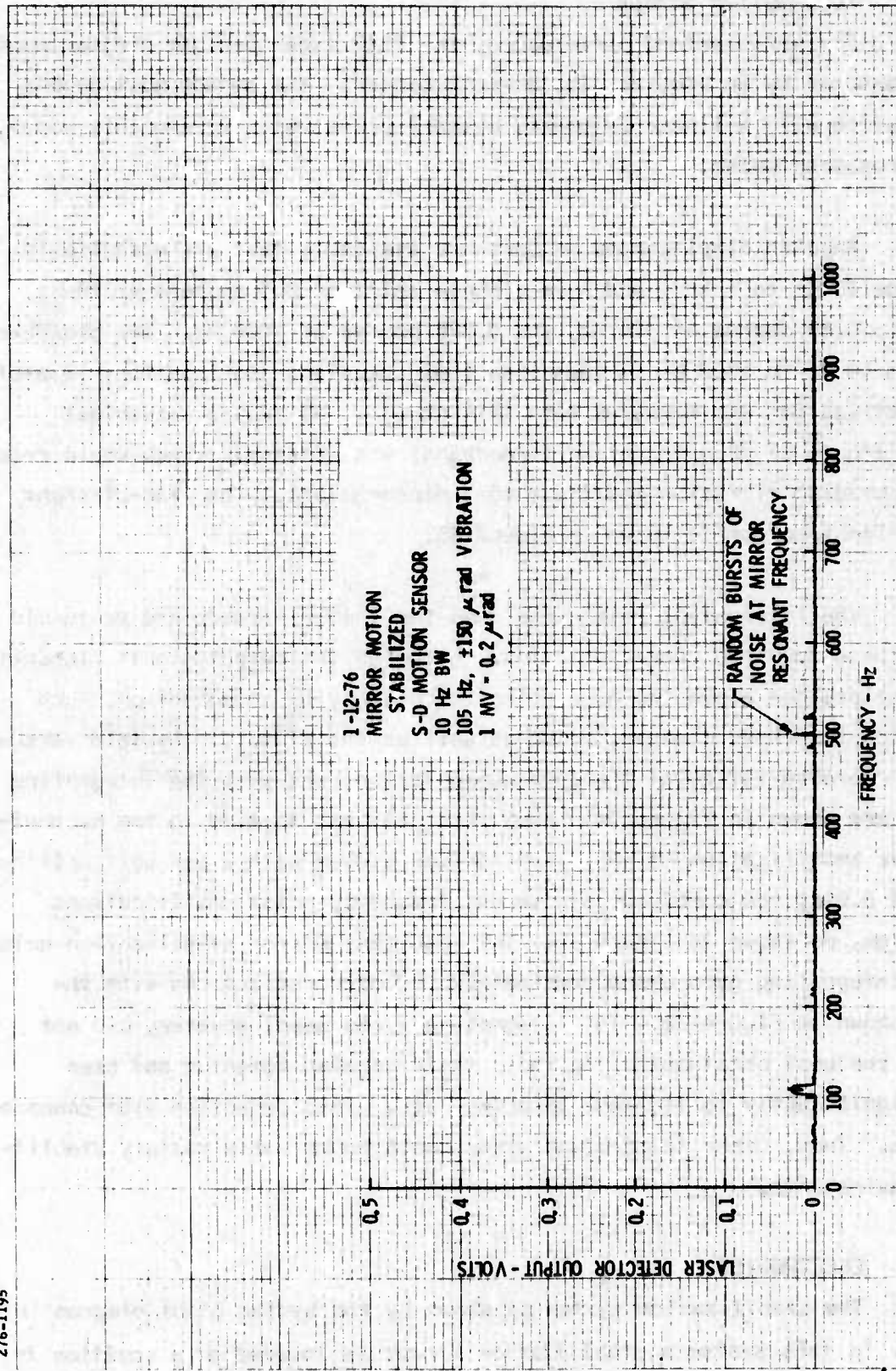


Figure 33 Line-Of-Sight Stabilization Spectrum With S-D Sensor

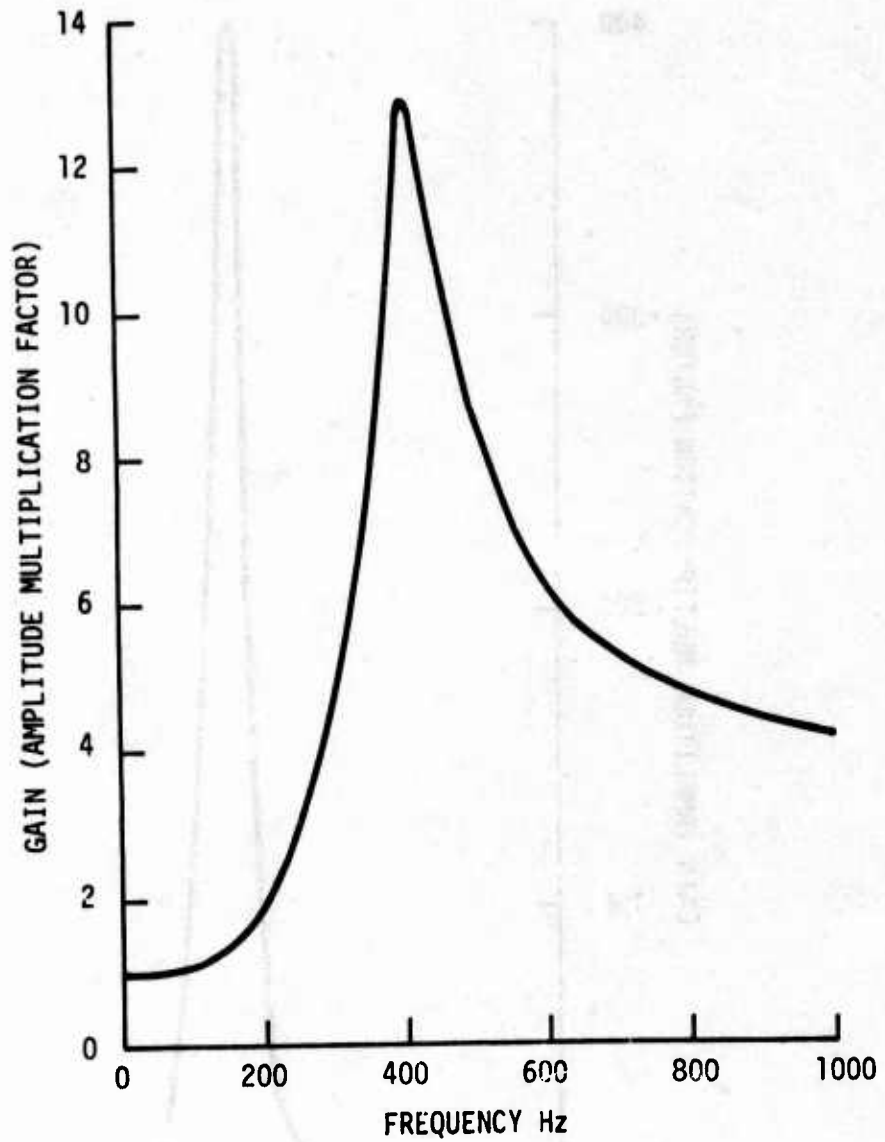


Figure 34 Gain Versus Frequency Characteristics Gyro Compensation

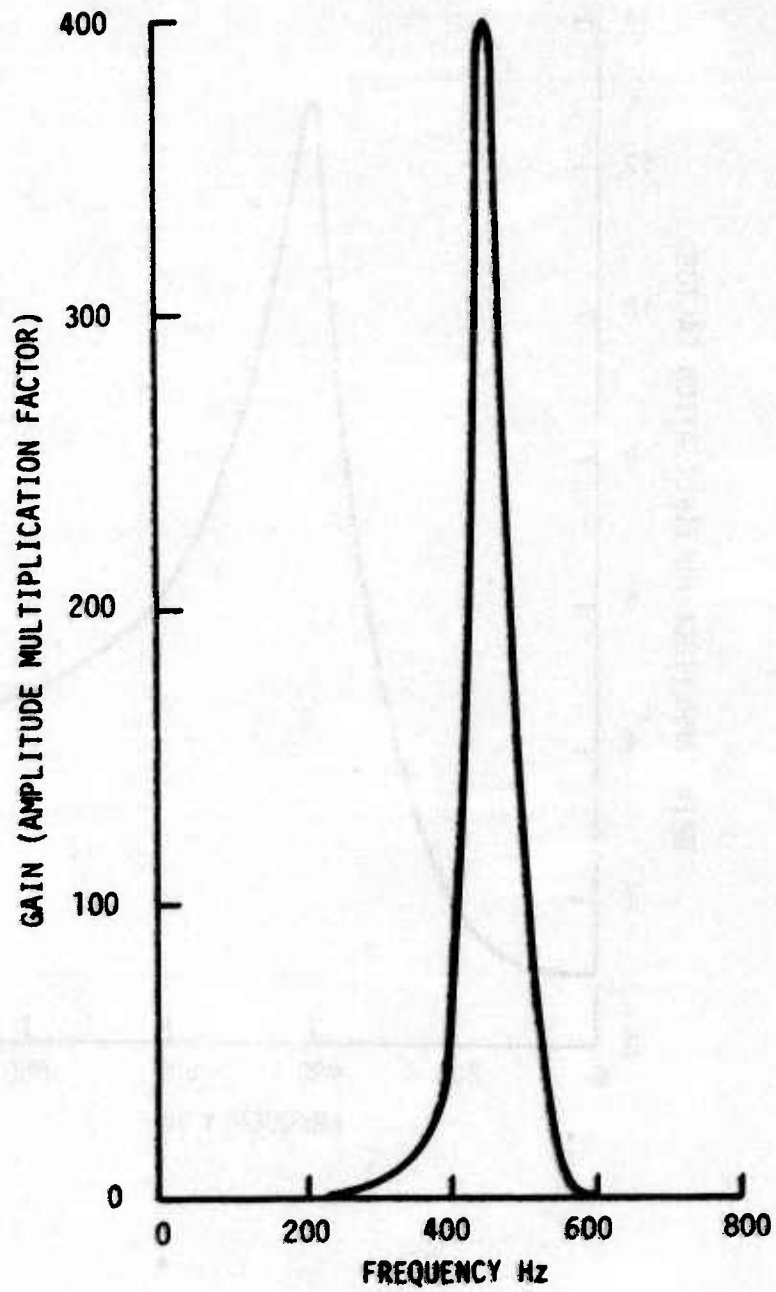


FIGURE 35 Combined Gain Versus Frequency Noise Amplification Characteristics

276-1196

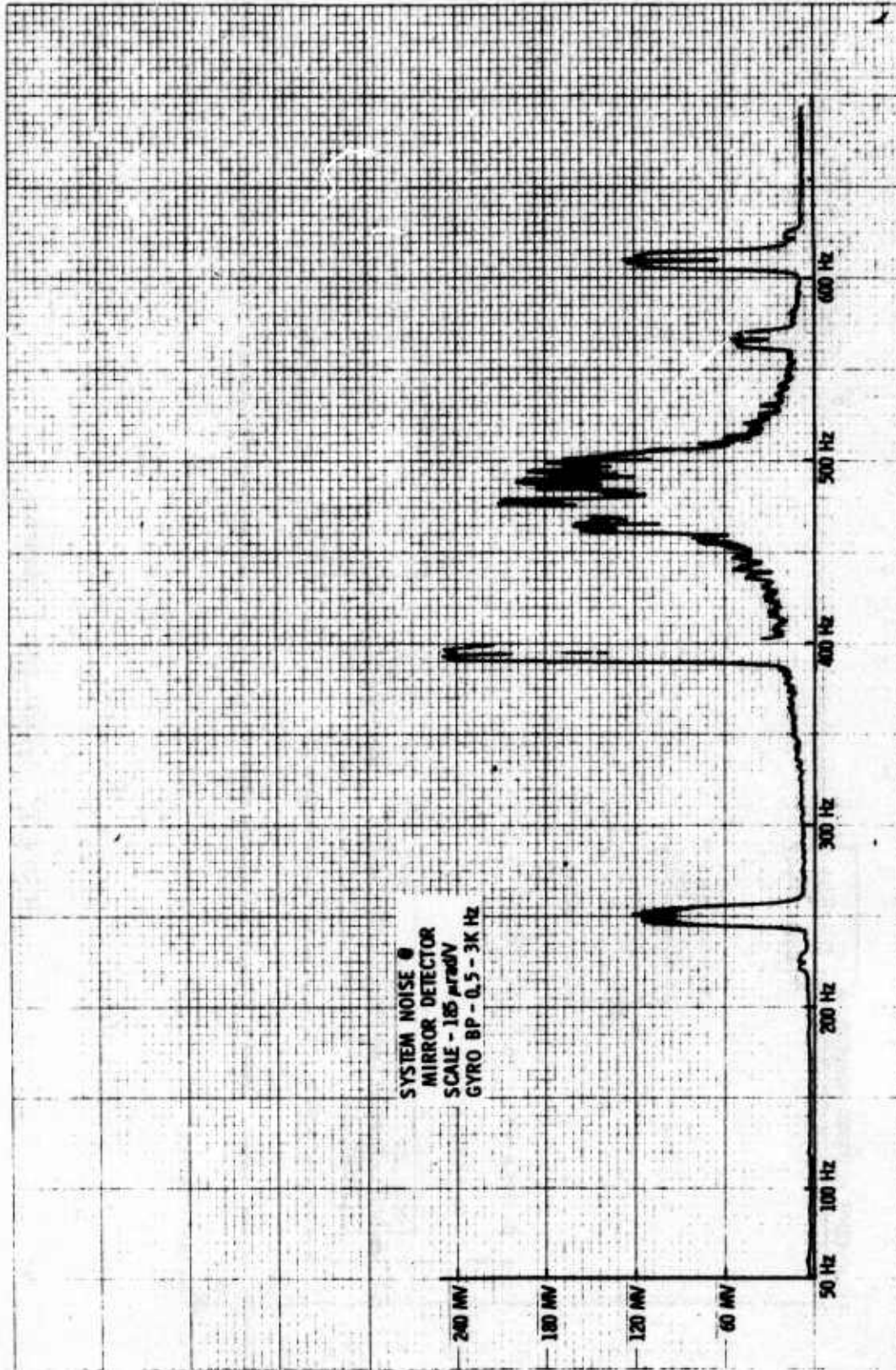


Figure 36 Mirror Stabilization System Noise Spectrum With Integrating Rate Gyro

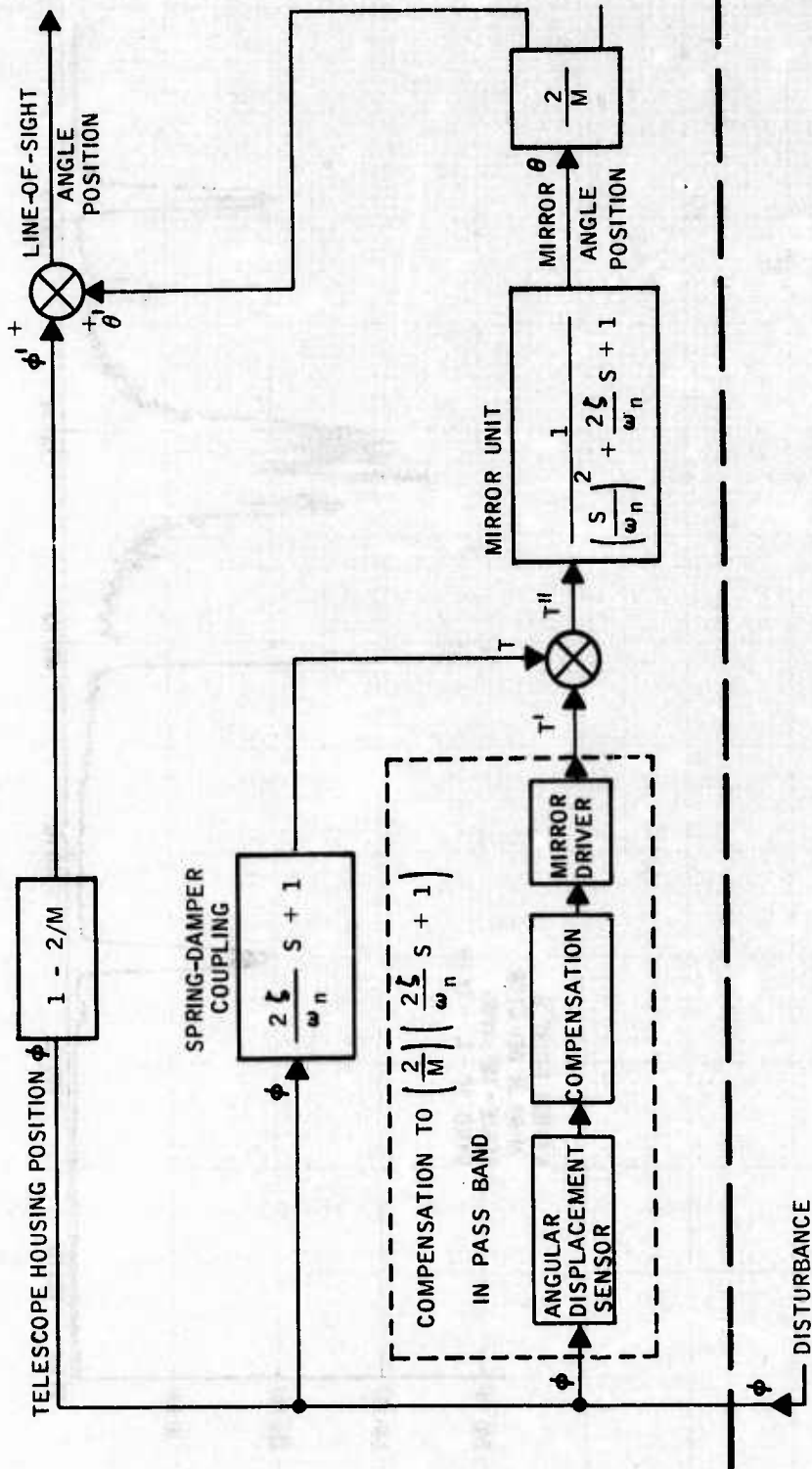


Figure 37 System Block Diagram

given stabilization mirror motion provides a $2M$ line-of-sight motion. Conversely, if the mirror angle is fixed in inertial space and the telescope housing is moved, the line-of-sight moves $(1 - 2/M)$ times the housing motion. Thus, to achieve line-of-sight stabilization, the mirror generated LOS motion (θ') must be equal and opposite to the housing generated motion (ϕ').

The mirror unit has a normal second order transfer function for a damped mass spring system between the applied torque and the mirror angular output. The torque (T'') applied to the mirror unit is the sum of the torque (T) due to the spring-damper coupling between the mirror and the telescope housing and the torque (T') applied to the mirror unit by the mirror driver. The driver torque (T') generated from the compensated output of an angular displacement sensor measuring the telescope housing position. The compensation network is selected to compensate for the spring-damper coupling, as shown, as well as for the frequency response anomalies in the electronics.

In this manner, the dynamic line-of-sight position stabilization is achieved. When a dc step disturbance is applied, the mirror angle position adjusts to the new telescope axis position with θ' becoming equal and opposite to ϕ' . This action holds the line-of-sight angle constant with varying telescope housing angles. Changes in telescope zoom ratio are compensated by changes in electronic gain in the compensation network.

In the laboratory demonstration system, the mirror magnification was 1. The maximum sinusoidal input frequency was 0.6 of the mirror unit natural frequency. The combination of the mirror unit, angular displacement sensor, mirror driver, and the physical dynamic coupling response in combination with the applied linear vibration frequency/amplitude schedule was such that a simple gain setting was the extent of the compensation required for the laboratory demonstration system.

Consequently, the electronics required for the laboratory demonstration test system included

- Scale factor amplifier between the angular displacement sensor and the driver power amplifier
- Driver power amplifier
- Power supply for the angular displacement sensor.

Laboratory equipment was used for these three functions in the breadboard demonstration system. The scale factor amplifier was a simple amplifier with an adjustable gain, which was adjusted to a fixed value for the tests. The driver power amplifier was a McIntosh MI-75.

The McIntosh MI-75 audio power amplifier was one of two amplifiers evaluated for this purpose. The other was a switching amplifier designed in-house. Both amplifiers were tested for linearity and phase shift over the frequency range of interest and at the required output voltage levels (approximately 500 volts peak). The McIntosh amplifier has a high-voltage tap on its output transformer enabling it to provide these high voltages directly. On the basis of these tests, the McIntosh was selected as the amplifier to be used in all subsequent testing of the mirror piezoelectric elements.

The McIntosh amplifier characteristics, shown in Figure 38, are suitable for the breadboard performance tests, down to a frequency of 50 Hz. Below this frequency the phase shift of the McIntosh will degrade the stabilization performance. A power amplifier with a suitable phase shift can readily be constructed.

<u>Frequency (Hz)</u>	<u>Gain (normalized)</u>	<u>Phase shift (degrees lead)</u>	<u>Maximum output (volts peak)</u>
10	0.25	16.0	250
25	0.75	7.5	375
50	1.00	3.2	500
100	1.00	1.2	500
200	1.00	0.2	500
300	1.00	0.1	500

Figure 38 McIntosh MI-75 Amplifier Characteristics

Section V

STABILIZATION PERFORMANCE VERIFICATION

Satisfactory performance of the laboratory breadboard stabilization mirror was verified in accordance with the Engineering Test Plan (AESC Report 5213-A). The line-of-sight stabilization tests achieved the 7-microradian objective over most of the frequency range, as indicated in Figure 1. The stabilization performance below 40 Hz was degraded because of the characteristics of the McIntosh MI-75 power amplifier. No significant boresight shift between stabilizing and nonstabilizing system status was apparent. Other tests indicated satisfactory insensitivity to the applied translational environment. The indicated mirror rotational movement (from mirror unbalance) was 2.8 microradian amplitude at the maximum vibrational environment of 20 g at 105 Hz. A 0.00025-in. axial displacement of the mirror surface at the optical axis was indicated at the maximum vibrational environment.

The test setup for measuring the line-of-sight stabilization is illustrated in Figure 39. The breadboard stabilized-mirror unit was mounted on a flexure bar. The applied linear motion of the shaker caused a rotational motion of the base of the unit. The amplitude of the angular vibration was directly proportional to the controllable axial vibration amplitude of the shaker. The angular displacements of the base of the breadboard stabilized-mirror unit were measured by an angular displacement sensor. The degree of stabilization was measured by the movement of the laser light beam which was reflected by the stabilized mirror into a spot motion sensor.

The mirror stabilization drive system and the mirror stabilization measuring system are shown by the block diagram in Figure 40. The mirror stabilization drive system consists of: a sensor power supply providing power to the angular positions sensor; a signal from the angular displacement sensor,

376-1467

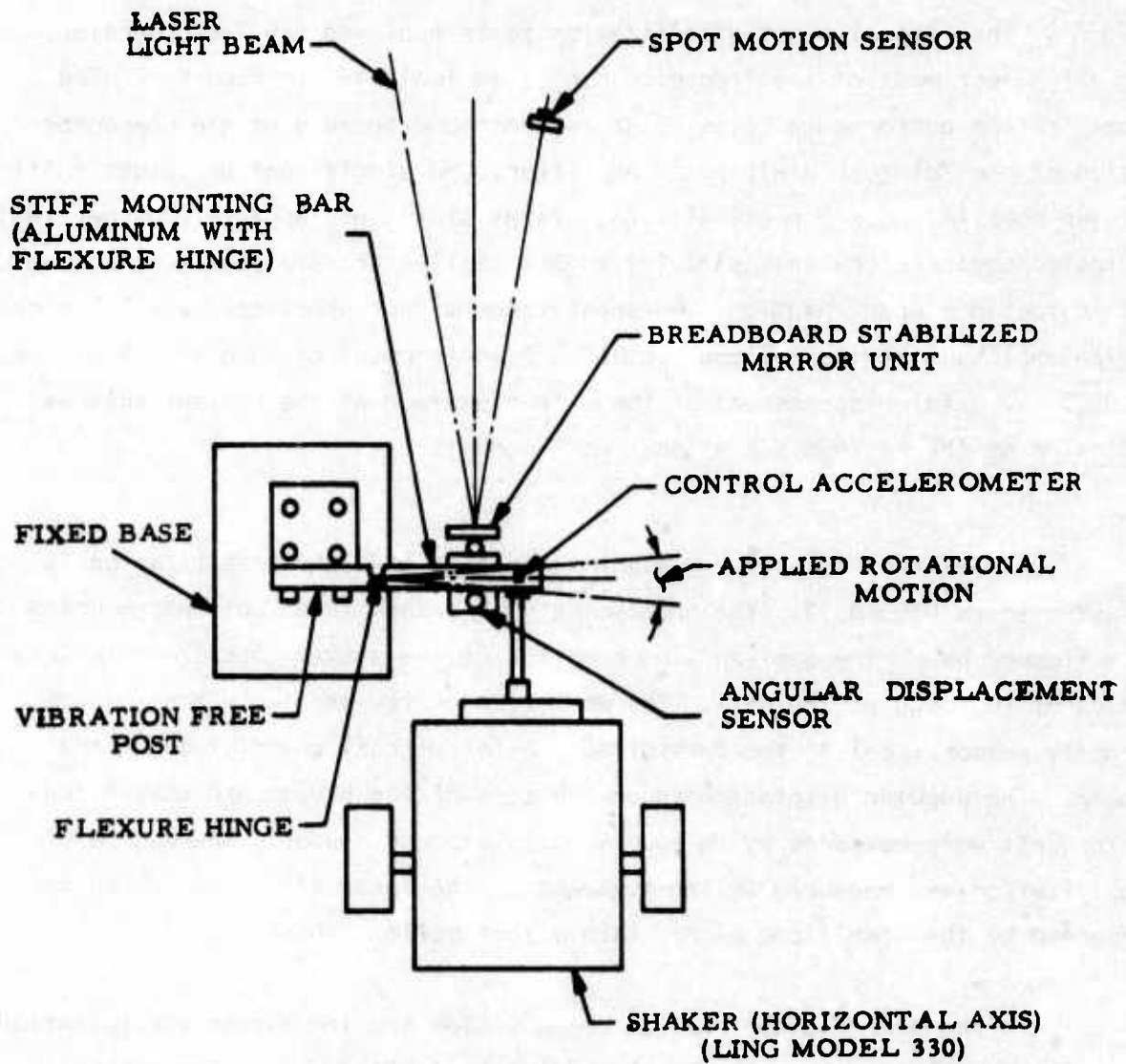


Figure 39 Breadboard Stabilization Mirror Stabilization Performance Tests

376-1466

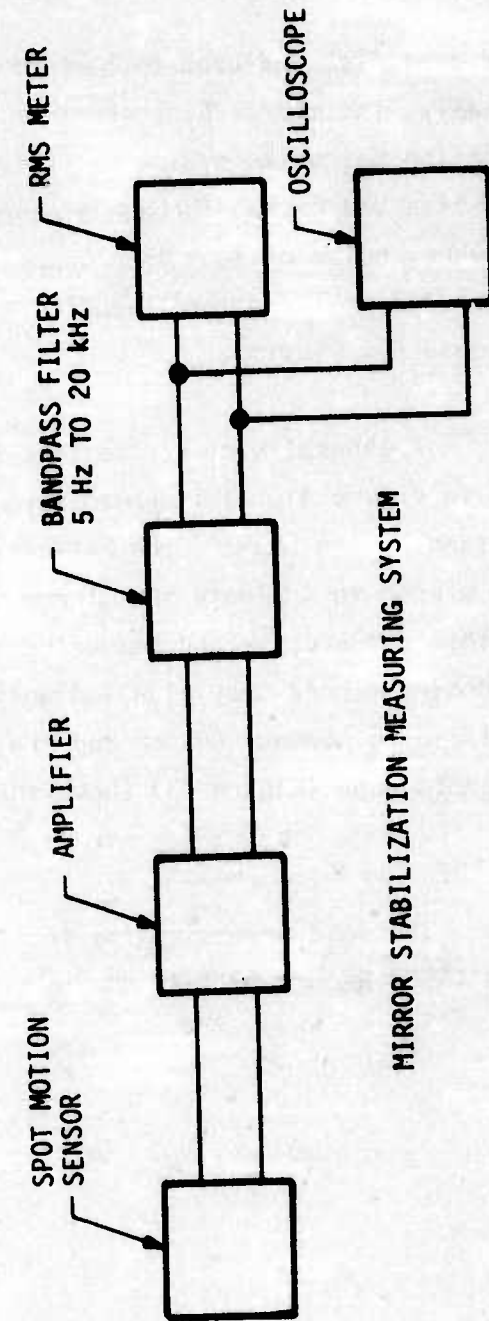
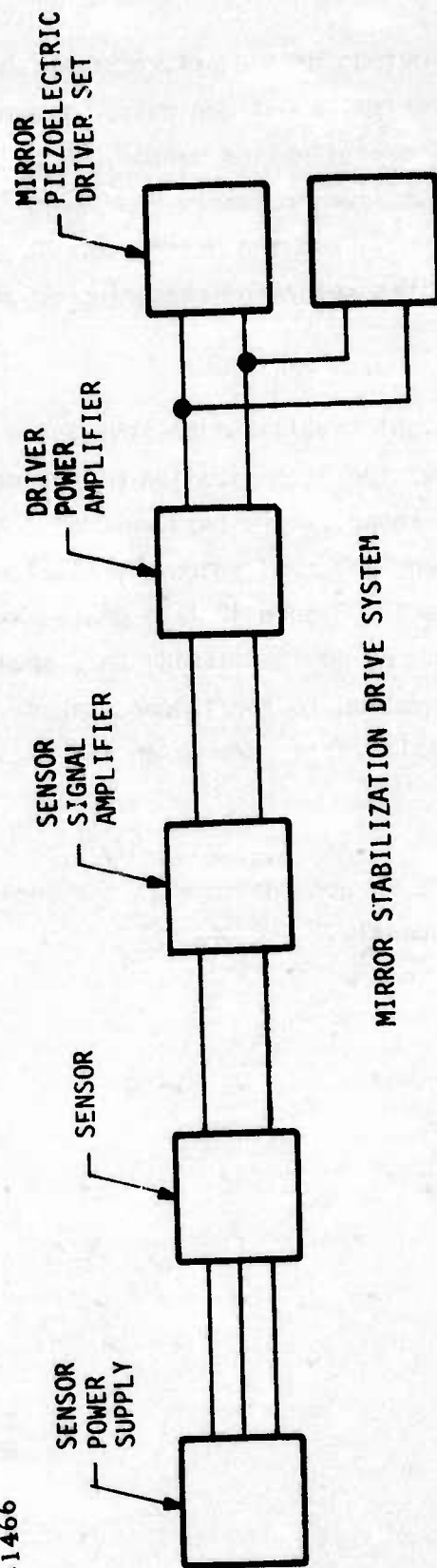


Figure 40 Test Setup Block Diagrams

which is amplified and used to control the output of the driver power amplifier; and, finally, the mirror piezoelectric driver set about one axis. The mirror stabilization measuring system consisted of a spot motion sensor, whose signal was amplified and passed through a bandpass filter to remove the laser-induced low-frequency noise of less than 5 Hz frequency, and the noise above 20 kHz. The filtered signal was then supplied to an rms meter for measuring or to an oscilloscope for viewing.

A general view of the line-of-sight stabilization test installation is shown in Figure 41. This photograph shows the stabilization mirror mounted to be driven by the shaker; the helium neon laser, whose beam was reflected from the mirror to indicate the mirror motion; and the laboratory electronics for the test setup drive and measuring systems. Figure 42 is a photograph of the breadboard mirror-stabilization unit mounted on the flexing bar, showing the angular displacement sensor and the connection to the linear shaker. Another photograph (Figure 43) shows the stabilization mirror on the flexure bar.

The data sheets of the tests made in accordance with the Engineering Test Plan (AESC Report 5213-A) are in the Appendix.

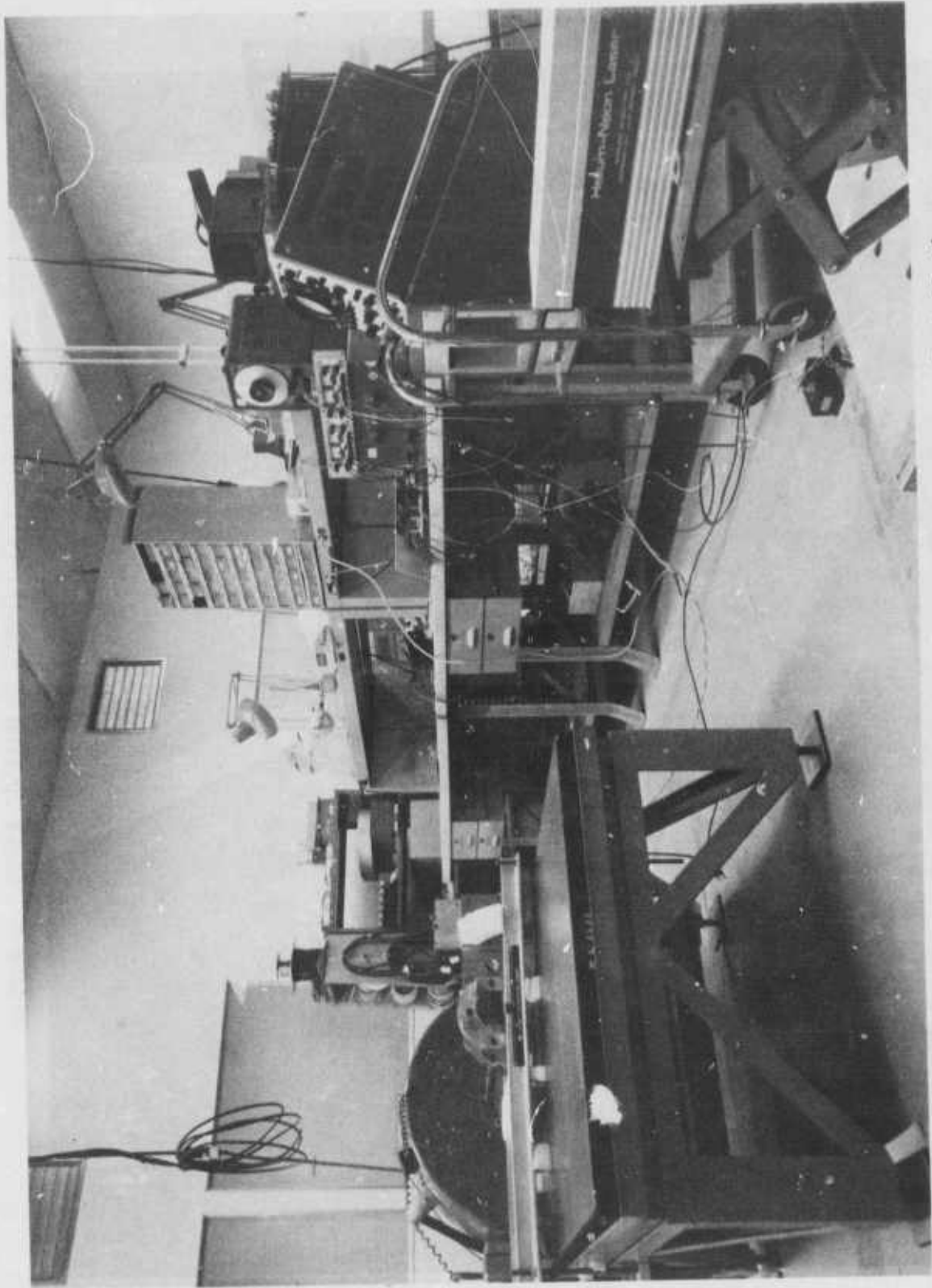


Figure 41 General View of Line-Of-Sight Stabilization Test Installation

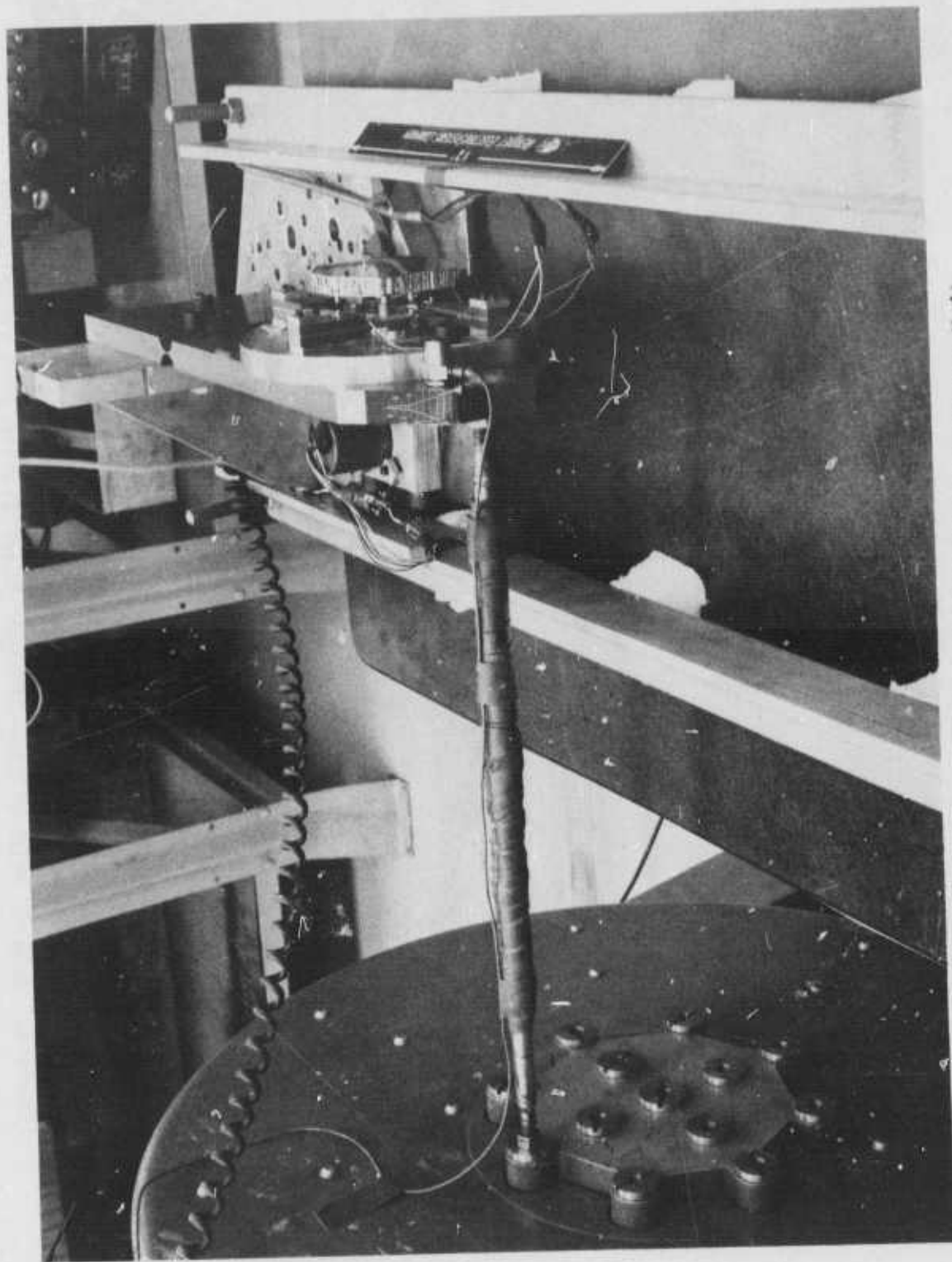


Figure 42 Close-Up View Of Stabilization Mirror Unit

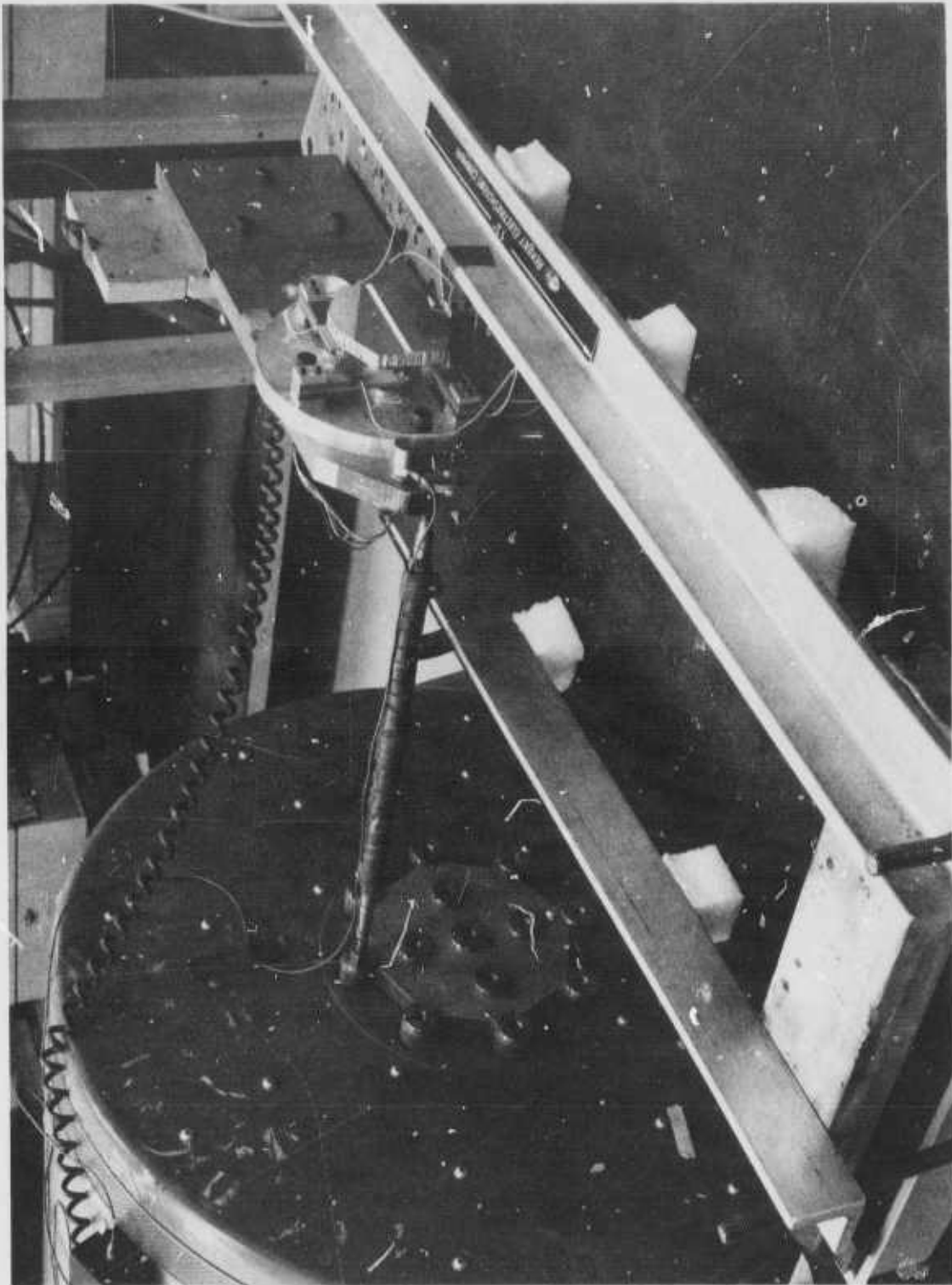


Figure 43 Close-up View of Stabilization Mirror Unit

Section VI

CONCLUSIONS AND RECOMMENDATIONS

Following are the main conclusions to be drawn from this program:

- a. A command-stabilized mirror represents the best method of improving stabilization for the two FLIR sensors, at minimum cost and redesign.
- b. Vibration reduction ratios of 26 dB can be achieved with real hardware providing resonances are avoided or compensated for.
- c. Stabilization levels of 7.5 microradians can be attained.
- d. The stabilization mirror system can be inserted in either of the two AN/AAQ9 FLIRS without optical degradation.
- e. Thermal and long-term drift characteristics of the stabilizing mirror do not create boresight offsets, nor are they expected to degrade isolation below 20 dB.
- f. Mirror configurations are ready for design efforts to apply them to specific FLIRS, and for hardware demonstration of such application.

It is recommended that a follow-on program be initiated to convert the breadboard developed and tested under this program into a prototype configuration, and that the prototype be tested to determine operational suitability.

Appendix

TEST DATA SHEETS
ENGINEERING TEST PLAN

APPENDIX

SECTION I

SENSITIVITY TO APPLIED VIBRATIONS

1. INDUCED MIRROR ANGULAR VIBRATIONS

The mirrors were balanced by applying known weights to the top and bottom of the mirror and measuring the amount of the mirror angular vibration when it was shaken. Metal was removed from the mirror as indicated to achieve the desired degree of balance. The data sheet for the final balance test is shown on page 86. The amount of mirror motion expected under a 105-Hz, 20-g linear vibration was calculated using the calculation sheet on page 87. When the indicated mirror motion under the 20-g environment was reduced to ± 2.8 microradians the method of balancing was considered proven. Since the degree of balance was adequate for the planned tests, no further balancing of the breadboard mirror was undertaken. The balancing method, however, is capable of achieving a significantly higher degree of mirror balance.

2. MIRROR POSITION TRANSLATION

To measure the amount of mirror position translation in the optical system under 20-g vibration, the mirror, mounted in its pivot, was statically loaded with a force equivalent to the effect of 20-g's acceleration on the mirror mass. The deflection of the mirror pivot was measured, indicating a 0.00025-inch deflection. The data are shown on page 88.

3. MIRROR UNIFORMITY TESTS

In these tests the laser beam was reflected from three locations on the mirror, during vibration, to determine if there were any differences in the mirror motion. No differences were identified, indicating that the mirror acted as a flat surface under the dynamic conditions imposed, as indicated by the test data on pages 89 and 90.

The three laser beam reflection positions were (a) on the right-hand edge of the mirror, (b) at the center of the mirror, and (c) at the left-hand edge. The mirror housing unit was subjected to 105-Hz, 150-micro-radian peak vibration input. The actual mirror motion was slightly less than this value, as the figures indicate. The top line in the oscilloscope photograph shows the laser beam motion at the detector. The bottom line is the output of an accelerometer on the flexing beam. The accelerometer output shows that the input vibration for all six photographs is the same. The results are the same for the stabilized and unstabilized cases.

The scale factor for the mirror motion was 91 microradians per cm. The accuracy of the measurement device was approximately 1 microradian.

SECTION II

LINE-OF-SIGHT STABILIZATION TESTS

1. SCOPE OF TESTS

Three groups of tests were performed, namely: Preliminary evaluation testing, Scheduled tests, and Additional tests. These are discussed in the following sections.

2. PRELIMINARY EVALUATION TESTS

Upon receipt of the S-D angular displacement sensor, a set of line-of-sight vibration attenuation test points was taken. Excellent stabilization performance was obtained as indicated by the test data presented in Figure 1. The test vibration frequencies were arbitrarily selected without any prior knowledge of system vibrational resonances. The test data is presented on page 85.

3. SCHEDULED TESTS

The line-of-sight stabilization tests performed involved reflecting a laser beam from the center of the mirror. The oscillograph records (pages 92 through 99) show the movement of the laser beam at the detector. The stabilized and unstabilized cases were taken at the same input vibration setting of the shake table, within a few seconds of each other. The test results are tabulated on page 91. The values of stabilized attenuation were calculated in terms of RMS detector volts. These values are plotted in Figure 1.

The frequencies which were selected give an approximate geometric progression. Because of customer interest, additional low-frequency tests were made, although the characteristics of the McIntosh MI-75 amplifier progressively degraded the stabilization performance at frequencies below 50 Hz. In a final system, phase compensation would extend this response to a lower frequency.

4. ADDITIONAL TESTS

a. **Increased Vibration Amplitude:** These tests were conducted in the same manner as the scheduled tests, and followed the completion of the scheduled tests.

The test point shown on page 100 was selected by increasing the vibration amplitude from the most severe scheduled point of 105 Hz and ± 150 microradians p-p until the laboratory equipment ceased to function properly because of amplifier saturation.

The mirror unit was subjected to extremely heavy vibration during the testing and the angular displacement sensor was jarred loose. It was replaced, and the point shown on page 101 is essentially a repeat of the previous test. The decreased performance was attributed to changes in the angular displacement sensor mount.

b. **Resonance Frequency Sweep:** These tests were conducted in the same manner as the scheduled tests, and followed the completion of the scheduled tests. The test unit was started at 600 Hz input frequency, which was progressively lowered. Records were taken at each frequency where a resonance of some type was noted. The resonance points were identified both by sound as well as by a sharp increase in the unstabilized mirror beam deflection amplitude.

Applied amplitudes were chosen, not in accordance with the mathematical model, but for convenience in scale factors for the oscilloscope display.

The test results are tabulated on page 102. Test points 9 through 13 are plotted in Figure 1. The oscilloscope traces are shown on pages 103 through 110.

**FLIR HIGH FREQUENCY STABILIZATION
STUDY PROGRAM**

Contract F33615-75-C-1128

**LINE-OF-SIGHT STABILIZATION DATA SHEET
S-D SENSOR INITIAL EVALUATION TEST**

Test Setup 746-B1

Detector Bandwidth 10 Hz - 20 KHz Hz

Test Point	Frequency Hz	g	Rotational Amplitude	Detector RMS Volts		Mirror Amplitude μ rad RMS		Stabilization Attenuation dB
				Stabilization		Stabilization		
				OFF	ON	OFF	ON	
1	20	.003" DA	$\pm 150 \mu$ rad	525 mv	90 mv			-15.3
2	25			535	84			-16.1
3	35			505	19			-28.5
4	50			492	20			-27.8
5	75			475	18			-28.4
6	105			477	23			-26.3
7	150	1.95	$\pm 73 \mu$ rad	262	25			-20.4
8	210		$\pm 38 \mu$ rad	122	28			-12.8
9	300		$\pm 18 \mu$ rad	29	62			+6.6

Test Date 1-12-76

Engineer C M Rutledge

FLIR HIGH FREQUENCY STABILIZATION
STUDY PROGRAM

Contract F33615-75-C-1128

MIRROR BALANCING DATA SHEET 6.1.1

Mirror Unit S/N-2 Axis Balanced Y-Y

RMS Volt Meter Ballantine Model 320A Position-Bender # 1 on Top

Band Pass Filter _____

Band Pass 20-1000 Hz

Rotational Vibration Mount SK 1309859

Applied Vibration: Frequency 105 Hz

Amplitude at Head 5.0 g

Amplitude at Mirror 3.2 g

Balancing Sequence Step No. 16

Point No.	Applied Weight		RMS Voltage	
	Ident.	Wt. (gm)	Top	Bottom
0	0	0	7.65	—
1	4	.155	20.0	—
2	1	.019	8.3	—
3	0	0	7.65	7.65
4	4	.155	—	19.7
5	1	.019	—	8.4
6	0	0	—	7.55
7				
8				
9				
10				
11				
12				

Test Date 7 Nov 1975

Data Recorded By HC Ellis

MIRROR BALANCING CALCULATION SHEET

Balancing Sequence Step No. YY-I

Balance Seq. No.	Top Bottom	Added Weight - grams		RMS Voltage		(d) Δ	(e) d/b	(f) ω	(g) c-f	(h) $g_B = g_T$	(i) e-ave I-B h/2	(j) Weight Unbalance grams i/j	Torque on Mirror at 1g gm-in	(k) Torque on Mirror at 20g T In lbs.	(l) $\omega = \sqrt{I}$ Mirror Angular Acceleration rad/sec	(m) Amplified Mirror Deflection at 105 Hz \pm /grad	
		(a) #	(b) Δ	(c) Weight	(d) Δ												
11	T	.155	.045	.110	18.5	8.45	18.0	8.45	8.45	8.45	8.45	8.45	8.45	8.45	8.45	8.45	8.45
	B	.155	.045	.110	20.2	18.0	20.2	18.0	18.0	18.0	18.0	18.0	18.0	18.0	18.0	18.0	18.0
12	T																
	B																
13	T																
	B																
14	T	.155	.045	.110	19.7	9.3	19.7	9.3	9.3	9.3	9.3	9.3	9.3	9.3	9.3	9.3	9.3
	B	.155	.045	.110	20.2	9.7	20.2	9.7	9.7	9.7	9.7	9.7	9.7	9.7	9.7	9.7	9.7
15	T	.155	.045	.110	20.2	9.6	20.2	9.6	9.6	9.6	9.6	9.6	9.6	9.6	9.6	9.6	9.6
	B	.155	.045	.110	20.3	9.7	20.3	9.7	9.7	9.7	9.7	9.7	9.7	9.7	9.7	9.7	9.7
16	T	.155	.045	.110	20.0	8.3	20.0	8.3	8.3	8.3	8.3	8.3	8.3	8.3	8.3	8.3	8.3
	B	.155	.045	.110	19.7	8.4	19.7	8.4	8.4	8.4	8.4	8.4	8.4	8.4	8.4	8.4	8.4
	T																
	B																
	T																
	B																
	T																
	B																

(1) weights applied 1.75 in from gimbal axis
 (2) Mirror inertia about pivot (with drivers) 2.20×10^{-4} in lb/sec² = I
 (3) $\chi = \frac{g}{(2\pi f)^2}$ deflection where $f = 105$ Hz

FLIR HIGH FREQUENCY STABILIZATION
STUDY PROGRAM

Contract F33615-75-C-1128

Data Sheet 6.1.2

MIRROR Z AXIS TRANSLATIONAL SHIFT

Mirror Unit S/N 1 Pivot Configuration 842 B3

Point No.	Applied Weight lbs.	Dial Indicator Reading 1/10,000 in.	Δ Weight lbs.	Increase Decrease	Δ Travel 1/10,000 in
0	-0-	0.0000	2.205	I	2
1	2.205	0.0002		D	2
2	-0-	0.0000		I	3
3	2.205	0.0003		D	2
4	-0-	0.0001		I	2
5	2.205	0.0003		D	2
6	0	0.0001			
AVE					2.2

$$\text{Spring Constant } k = \frac{\Delta W}{\text{Ave } \Delta \text{ Travel}} = \frac{2.205}{.00022} = \underline{10,020 \text{ lb/in}}$$

$$\text{Force of mirror } F @ 20 \text{ g } (58 \text{ g} \times 20) = \underline{2.56 \text{ lbs.}}$$

$$\text{Mirror Pivot deflection @ } 20 \text{ g } \frac{F}{K} = \frac{2.56}{10,020} = \underline{0.00025 \text{ in}}$$

Test Date 28 Oct 1975 Data Recorded By JHB Ellis

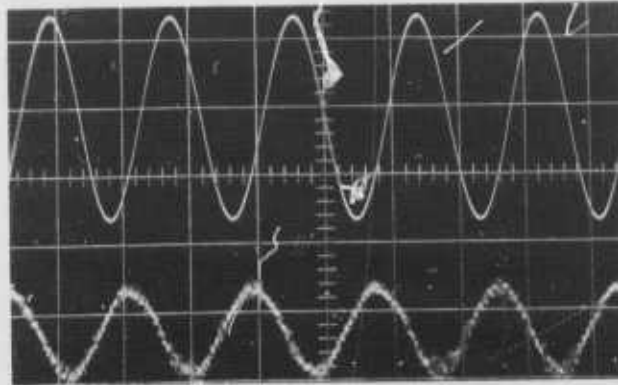
FLIR HIGH FREQUENCY STABILIZATION
STUDY PROGRAM

Contract F33615-75-C-1128

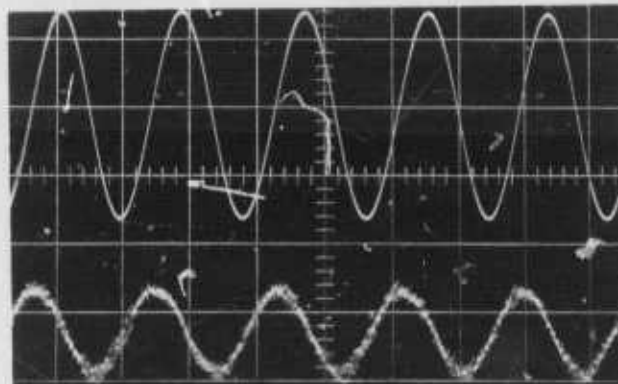
MIRROR UNIFORMITY

Test Set Up 863-G1 ; Frequency 105 Hz; Amplitude \pm 150 μ rad;

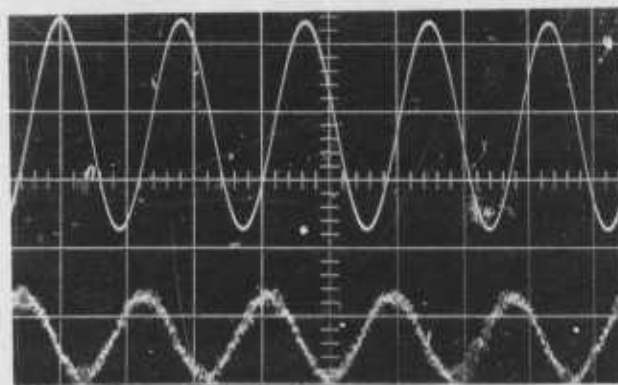
Detector Bandwidth 10 Hz Stabilization Status OFF



R Hand Edge
(West)



Center



L Hand Edge
(East)

Scale Factor μ rad/cm 91

Test Date 12-10-75

Engineer J.B. Ellis

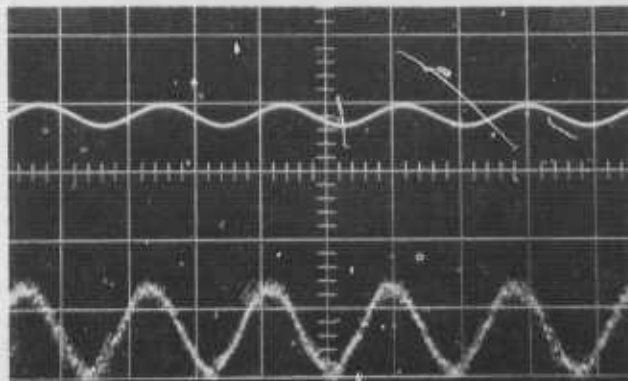
FLIR HIGH FREQUENCY STABILIZATION
STUDY PROGRAM

Contract F33615-75-C-1128

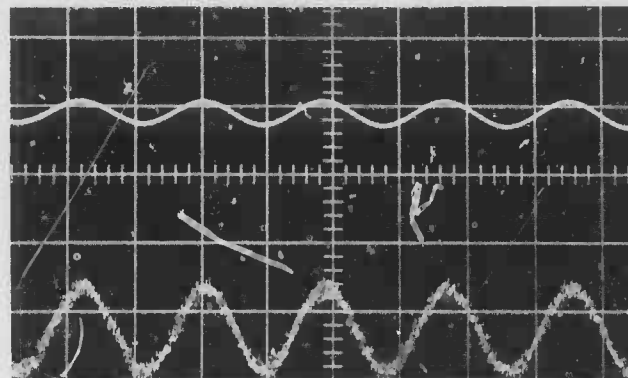
MIRROR UNIFORMITY

Test Set Up 863-G1 ; Frequency 105 Hz; Amplitude \pm 150 μ rad;

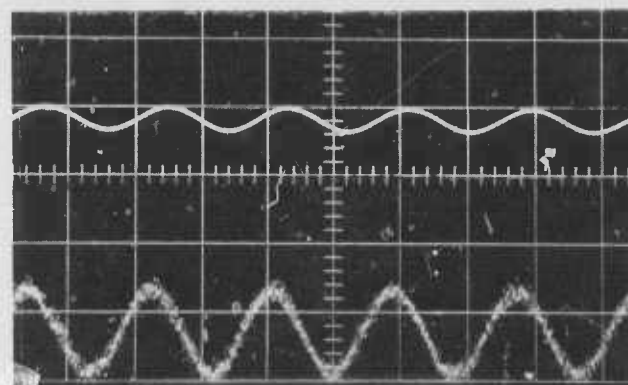
Detector Bandwidth 10 Hz Stabilization Status ON



R Hand Edge
(West)



Center



L Hand Edge
(East)

Scale Factor μ rad/cm 91

Test Date 12-10-75 Engineer HB Ellis

FLIR HIGH FREQUENCY STABILIZATION
STUDY PROGRAM

Contract F33615-75-C-1128

LINE-OF-SIGHT STABILIZATION DATA SHEET 6.2

Test Setup _____ Detector Bandwidth 5-20,000 Hz

Test Point	Frequency Hz	g	Rotational Amplitude	Detector RMS Volts		Mirror Amplitude μ rad RMS		Stabilization Attenuation dB
				Stabilization		Stabilization		
				OFF	ON	OFF	ON	
1	15	.085	Nominal $\pm 150 \mu$ rad p-p	.545	.167	104	32	-10.3
2	25	.13		.585	.056	112	11	-20.4
3	35	.21		.565	.049	108	9	-21.2
4	50	.42		.575	.041	111	8	-22.9
5	75	1.05		.675	.044	129	8	-23.7
6	105	1.9		.610	.029	117	6	-26.5
7	175	1.9	$\pm 54 \mu$ rad	.208	.040	40	8	-14.3
8	325	1.9	$\pm 14 \mu$ rad	.133	.021	25	4	-16.0

Test Date 3-10-76

Engineer C. Rutschow / ABella

FLIR HIGH FREQUENCY STABILIZATION
STUDY PROGRAM

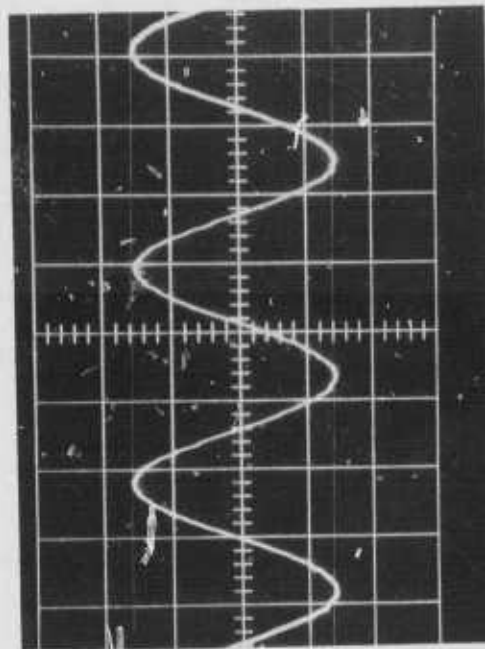
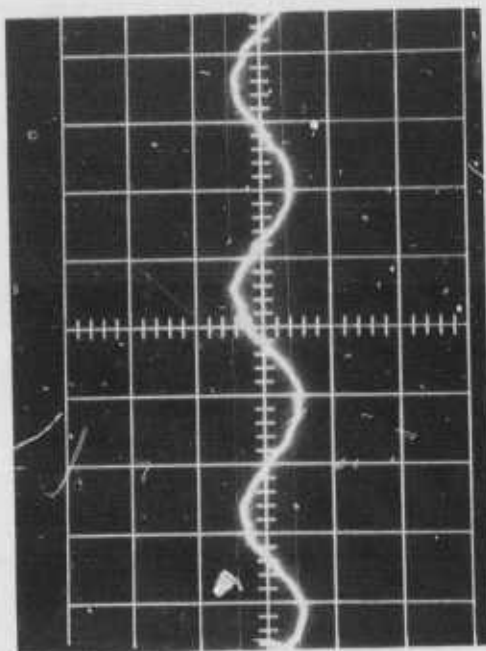
Contract F33615-75-C-1128

LINE-OF-SIGHT STABILIZATION DATA SHEET 5.2

Page 1 of 8

Test Setup 746-B1

Test Conditions: 15 Hz \pm 150 μ rad 5-20,000 Hz Detector Bandwidth



Mirror Stabilization ON

Mirror Stabilization OFF

Amplitude p-p (photo) (ON) .82 cm (OFF) 3.0 cm

Scale Factor μ rad/cm 95.5

Amplitude p-p (ON) 78 μ rad; (OFF) 287 μ rad

Attenuation $\frac{\text{ON}}{\text{OFF}}$.274 ; dB -11.3

Test Date 3-10-76 Engineer CR/ TB Ellis

FLIR HIGH FREQUENCY STABILIZATION
STUDY PROGRAM

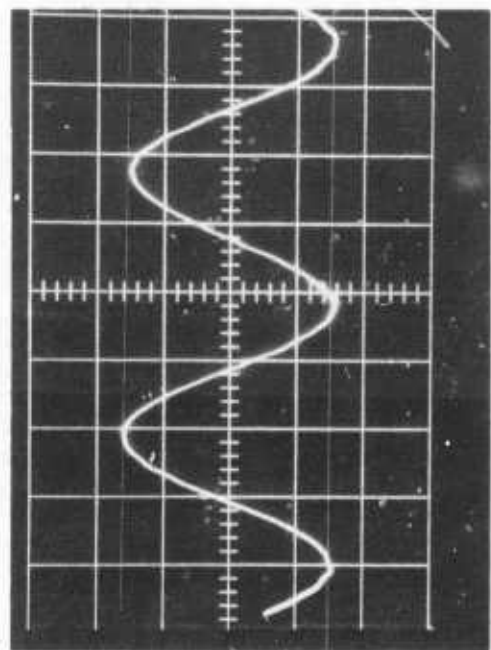
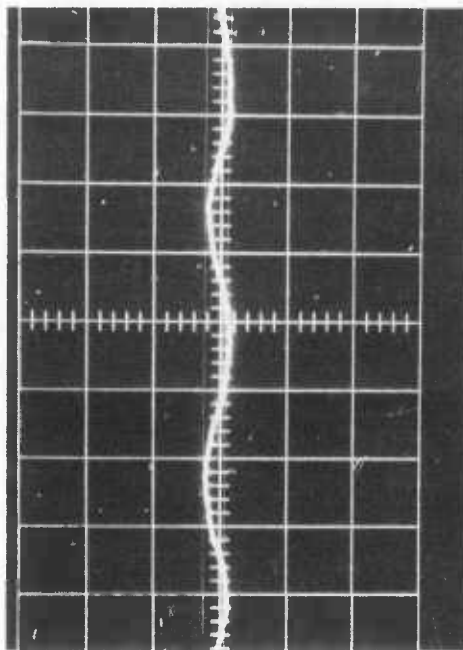
Contract F33615-75-C-1128

LINE-OF-SIGHT STABILIZATION DATA SHEET 6.2

Page 2 of 8

Test Setup 746-B1

Test Conditions: 25 Hz \pm 150 μ rad 5-20,000 Hz Detector Bandwidth



Mirror Stabilization ON

Mirror Stabilization OFF

Amplitude p-p (photo) (ON) .34 cm (OFF) 3.08 cm

Scale Factor μ rad/cm 95.5

Amplitude p-p (ON) 32 μ rad; (OFF) 294 μ rad

Attenuation $\frac{\text{ON}}{\text{OFF}}$.11 ; dB -19.2

Test Date 3-10-76 Engineer CR/ HBelli

FLIR HIGH FREQUENCY STABILIZATION
STUDY PROGRAM

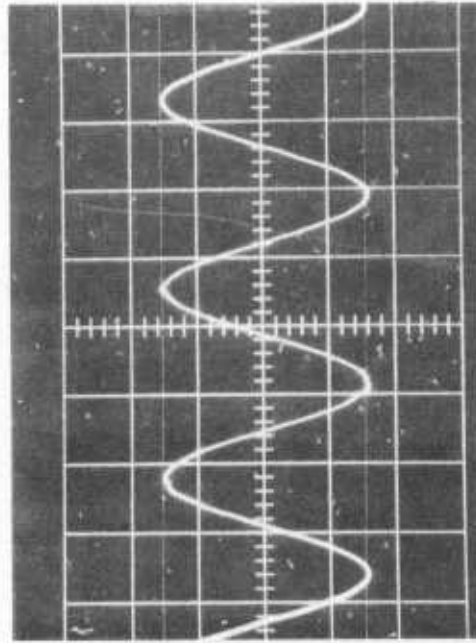
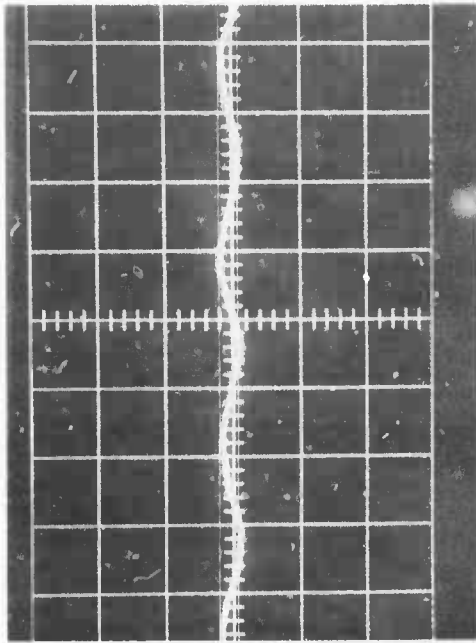
Contract F33615-75-C-1128

LINE-OF-SIGHT STABILIZATION DATA SHEET 6.2

Page 3 of 8

Test Setup 746-B1

Test Conditions: 35 Hz \pm 150 μ rad 5-20,000 Hz Detector Bandwidth



Mirror Stabilization ON

Mirror Stabilization OFF

Amplitude p-p (photo) (ON) .28 cm (OFF) 3.08 cm

Scale Factor μ rad/cm 95.5

Amplitude p-p (ON) 27 μ rad; (OFF) 294 μ rad

Attenuation $\frac{\text{ON}}{\text{OFF}}$.091 ; dB -20.8

Test Date 3-10-76 Engineer CR/ HBElli

FLIR HIGH FREQUENCY STABILIZATION
STUDY PROGRAM

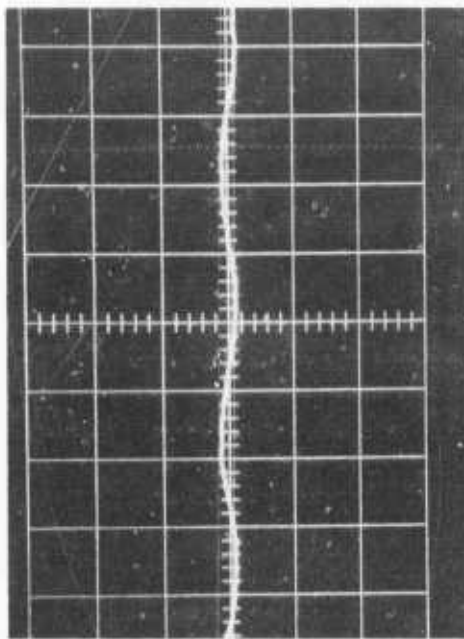
Contract F33615-75-C-1128

LINE-OF-SIGHT STABILIZATION DATA SHEET 6.2

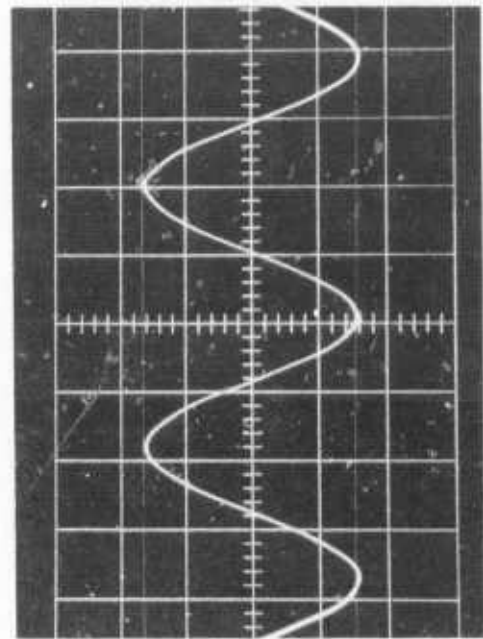
Page 4 of 8

Test Setup 746-B1

Test Conditions: 50 Hz \pm 150 μ rad 5-20,000Hz Detector Bandwidth



Mirror Stabilization ON



Mirror Stabilization OFF

Amplitude p-p (photo) (ON) .224 cm (OFF) 3.20 cm

Scale Factor μ rad/cm 95.5

Amplitude p-p (ON) 21 μ rad; (OFF) 305 μ rad

Attenuation $\frac{\text{ON}}{\text{OFF}}$.07 ; dB -23.1

Test Date 3-10-76 Engineer CR/ JBB/ELG

FLIR HIGH FREQUENCY STABILIZATION
STUDY PROGRAM

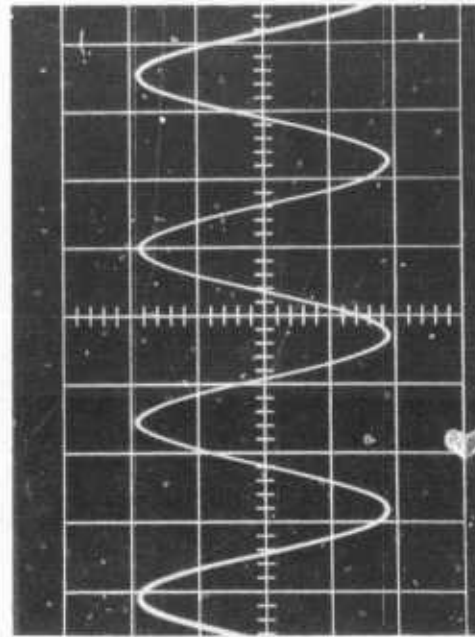
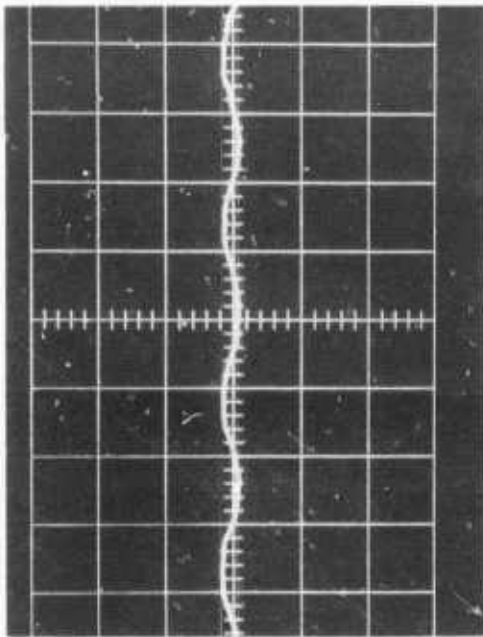
Contract F33615-75-C-1128

LINE-OF-SIGHT STABILIZATION DATA SHEET 6.2

Page 5 of 8

Test Setup 746-B1

Test Conditions: 75 Hz \pm 150 μ rad 5-20,000 Hz Detector Bandwidth



Mirror Stabilization ON

Mirror Stabilization OFF

Amplitude p-p (photo) (ON) .20 cm (OFF) 3.72 cm

Scale Factor μ rad/cm 95.5

Amplitude p-p (ON) 19 μ rad; (OFF) 356 μ rad

Attenuation $\frac{\text{ON}}{\text{OFF}}$.0538 ; dB -25.4

Test Date 3-10-76 Engineer CR / HBelli

FLIR HIGH FREQUENCY STABILIZATION
STUDY PROGRAM

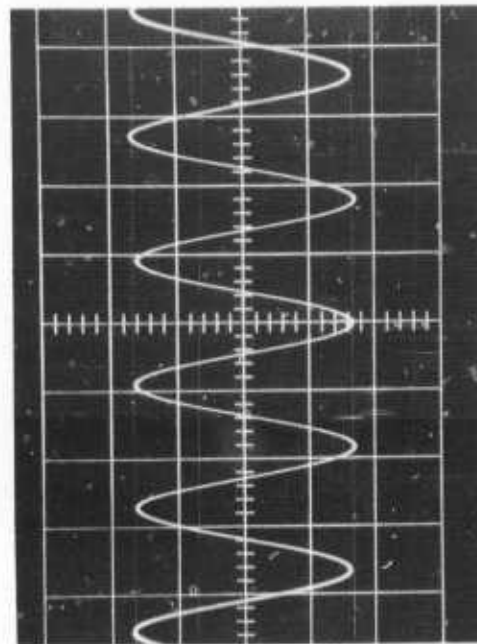
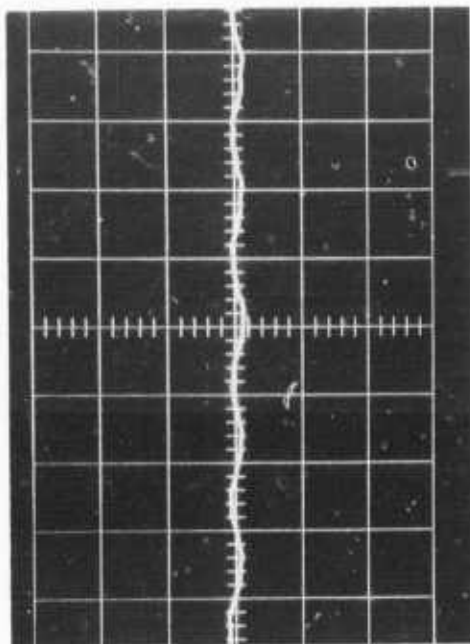
Contract F33615-75-C-1128

LINE-OF-SIGHT STABILIZATION DATA SHEET 6.2

Page 6 of 8

Test Setup 746-B1

Test Conditions: 105 Hz \pm 150 μ rad 5-20,000 Hz Detector Bandwidth



Mirror Stabilization ON

Mirror Stabilization OFF

Amplitude p-p (photo) (ON) .16 cm (OFF) 3.32 cm

Scale Factor μ rad/cm 95.5

Amplitude p-p (ON) 15 μ rad; (OFF) 317 μ rad

Attenuation $\frac{\text{ON}}{\text{OFF}}$.048 ; dB -26.4

Test Date 3-10-76 Engineer CR/ TABELLA

FLIR HIGH FREQUENCY STABILIZATION
STUDY PROGRAM

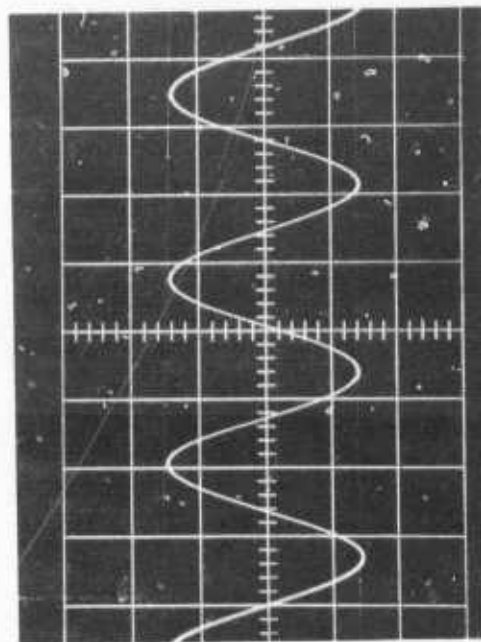
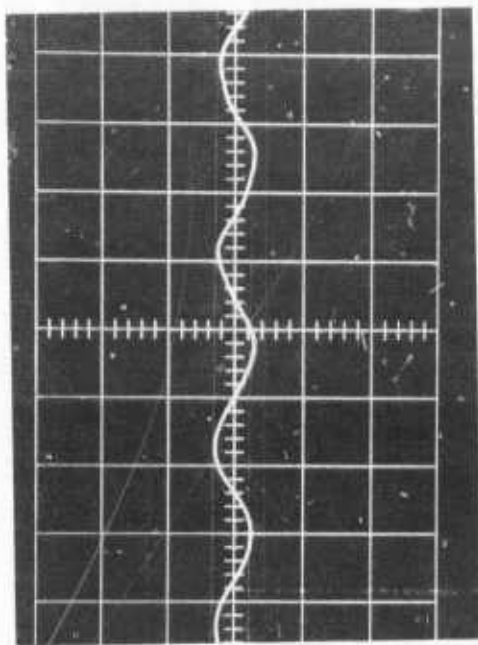
Contract F33615-75-C-1128

LINE-OF-SIGHT STABILIZATION DATA SHEET 6.2

Page 7 of 8

Test Setup 746-B1

Test Conditions: 175 Hz \pm 54 μ rad 5-20,000Hz Detector Bandwidth



Mirror Stabilization ON

Mirror Stabilization OFF

Amplitude p-p (photo) (ON) .54 cm (OFF) 2.83 cm

Scale Factor μ rad/cm 95.5

Amplitude p-p (ON) 51 μ rad; (OFF) 270 μ rad

Attenuation $\frac{\text{ON}}{\text{OFF}}$.191 ; dB -14.4

Test Date 3-10-76 Engineer CR / T. D. Ellis

FLIR HIGH FREQUENCY STABILIZATION
STUDY PROGRAM

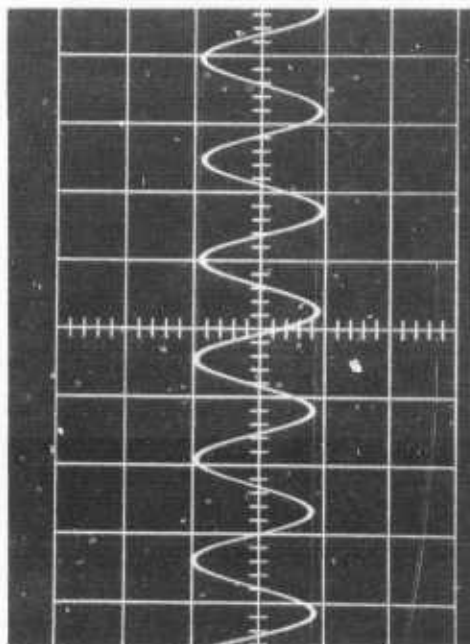
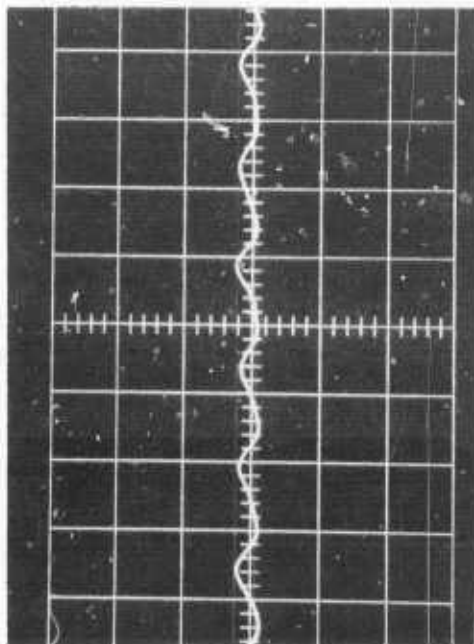
Contract F33615-75-C-1128

LINE-OF-SIGHT STABILIZATION DATA SHEET 6.2

Page E of 8

Test Setup 746-B1

Test Conditions: 325 Hz \pm 14 μ rad 5-20,000 Hz Detector Bandwidth



Mirror Stabilization ON

Mirror Stabilization OFF

Amplitude p-p (photo) (ON) .276 cm (OFF) 1.80 cm

Scale Factor μ rad/cm 38.2

Amplitude p-p (ON) 11 μ rad; (OFF) 69 μ rad

Attenuation $\frac{\text{ON}}{\text{OFF}}$.154 ; dB -16.3

Test Date 3-10-76 Engineer C.R. / TABELLA

FLIR HIGH FREQUENCY STABILIZATION
STUDY PROGRAM

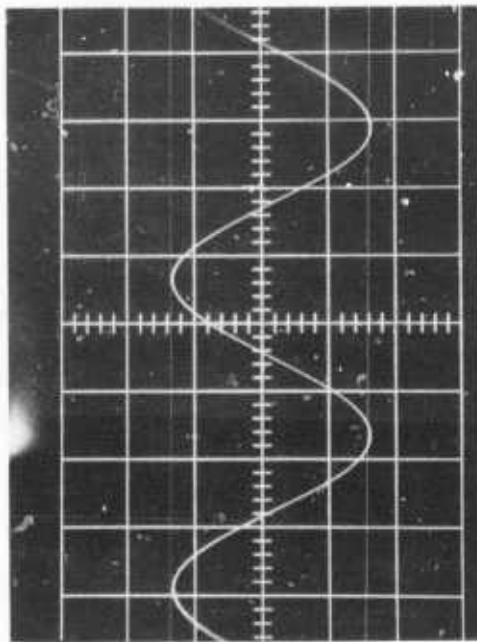
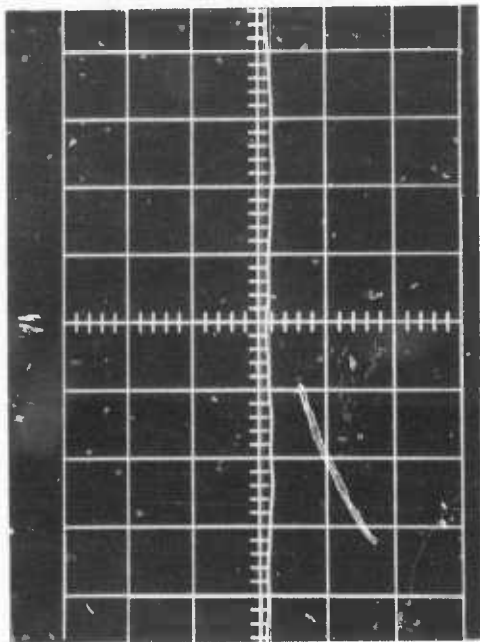
Contract F33615-75-C-1128

LINE-OF-SIGHT STABILIZATION DATA SHEET 6.2

Page 1 of 2

Test Setup 746-B1

Test Conditions: 105 Hz \pm 260 μ rad 5-20,000 Hz Detector Bandwidth



Mirror Stabilization ON

Mirror Stabilization OFF

Amplitude p-p (photo) (ON) .10 cm (OFF) 2.92 cm

Scale Factor μ rad/cm 191

Amplitude p-p (ON) 19 μ rad; (OFF) 558 μ rad

Attenuation $\frac{\text{ON}}{\text{OFF}}$.0343 ; dB -29.3

Test Date 3-10-76 Engineer CR1 HBELLS

FLIR HIGH FREQUENCY STABILIZATION
STUDY PROGRAM

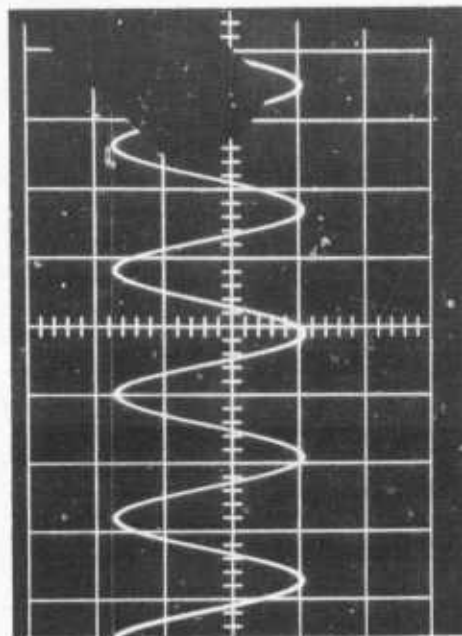
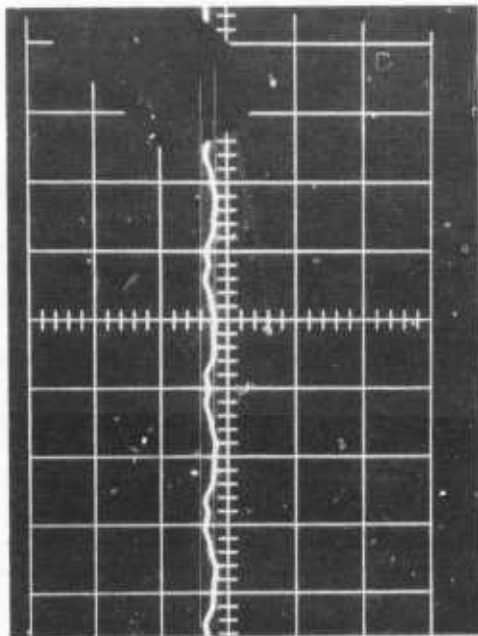
Contract F33615-75-C-1128

LINE-OF-SIGHT STABILIZATION DATA SHEET 6.2

Page 2 of 2

Test Setup 746-B1

Test Conditions: 105 Hz \pm 236 μ rad 5-20,000 Hz Detector Bandwidth



Mirror Stabilization ON

Mirror Stabilization OFF

Amplitude p-p (photo) (ON) .135 cm (OFF) 2.80 cm

Scale Factor μ rad/cm 191

Amplitude p-p (ON) 26 μ rad; (OFF) 534 μ rad

Attenuation $\frac{\text{ON}}{\text{OFF}}$.0485 ; dB -26.3

Test Date 3-10-76 Engineer CR1 JABELL

FLIR HIGH FREQUENCY STABILIZATION
STUDY PROGRAM

Contract F33615-75-C-1128

LINE-OF-SIGHT STABILIZATION DATA SHEET 6.2

Test Setup 746-B1 Detector Bandwidth 5-20,000 Hz

Test Point	Frequency Hz	g	Rotational Amplitude	Detector RMS Volts		Mirror Amplitude μ rad RMS		Stabilization Attenuation dB
				Stabilization		Stabilization		
				OFF	ON	OFF	ON	
9	89 R	1.9	Nominal P-P ±210 μ rad	.855	.043	163	8	-26.0
10	208 R	1.9	38	.185	.042	35	8	-12.9
11	249 R	1.9	27	.106	.140	32	27	-1.5
12	293 R	1.9 R	19	.127	.106	24	26	-1.6
13	303 R	.82	8	.278	.122	53	23	-7.2
14	501 R	.179	.6	.83	.40	158	76	-6.3
15	600	1.9	4.5	.168	.064	32	12	-8.4
16								

Test Date 3-10-76 Engineer CR/ NBELLE

FLIR HIGH FREQUENCY STABILIZATION
STUDY PROGRAM

Contract F33615-75-C-1128

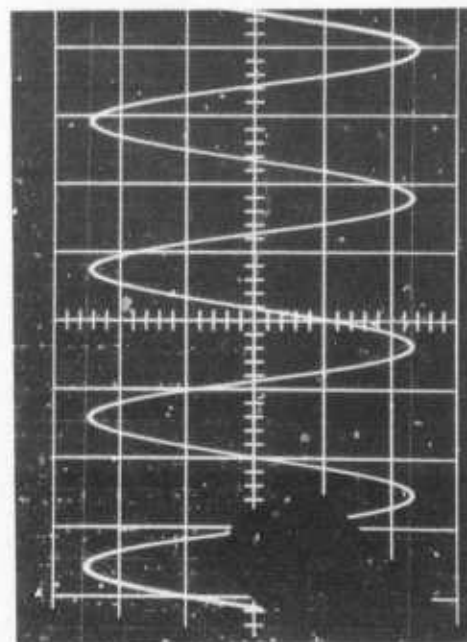
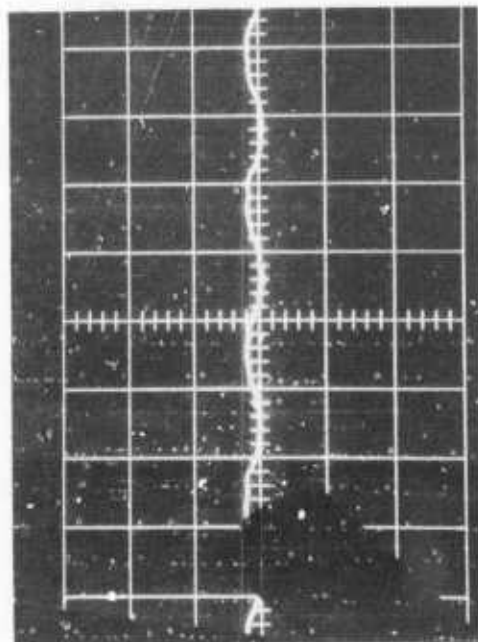
LINE-OF-SIGHT STABILIZATION DATA SHEET 6.2

Page 1 of 8

Point 9

Test Setup 746-B1

Test Conditions: 89 Hz \pm 213 μ rad 5-10,000 Hz Detector Bandwidth



Mirror Stabilization ON

Mirror Stabilization OFF

Amplitude p-p (photo) (ON) .25 cm (OFF) 4.78 cm

Scale Factor μ rad/cm 95.5

Amplitude p-p (ON) 24 μ rad; (OFF) 456 μ rad

Attenuation $\frac{\text{ON}}{\text{OFF}}$.0522 ; dB -25.6

Test Date 3-10-76 Engineer CR1 TBelli

FLIR HIGH FREQUENCY STABILIZATION
STUDY PROGRAM

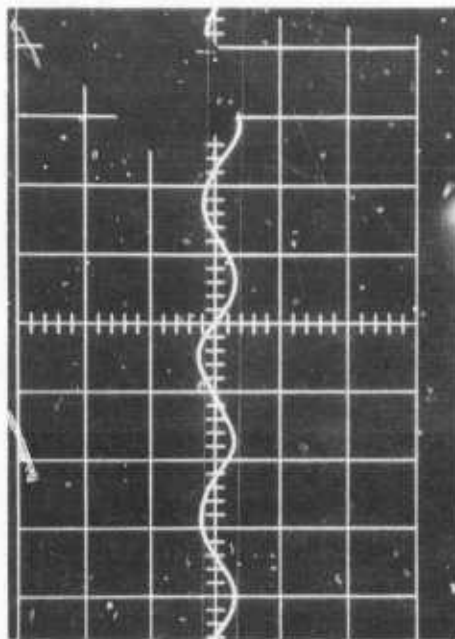
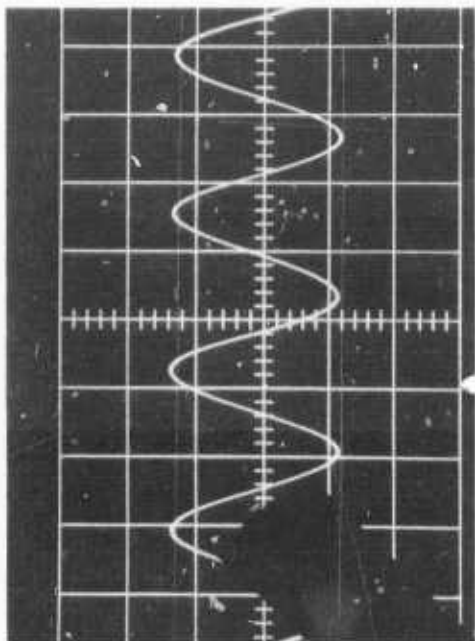
Contract F33615-75-C-1128

LINE-OF-SIGHT STABILIZATION DATA SHEET 6.2

Page 2 of 8
Point 10

Test Setup 746-B1

Test Conditions: 20K Hz \pm 38 μ rad 5-20,000 Hz Detector Bandwidth



Mirror Stabilization ON

Mirror Stabilization OFF

Amplitude p-p (photo) (ON) .54 cm (OFF) 2.46 cm

Scale Factor μ rad/cm 38.2

Amplitude p-p (ON) 21 μ rad; (OFF) 94 μ rad

Attenuation $\frac{\text{ON}}{\text{OFF}}$.22 ; dB -13.2

Test Date 3-10-76 Engineer CR/ HBS/LL

FLIR HIGH FREQUENCY STABILIZATION
STUDY PROGRAM

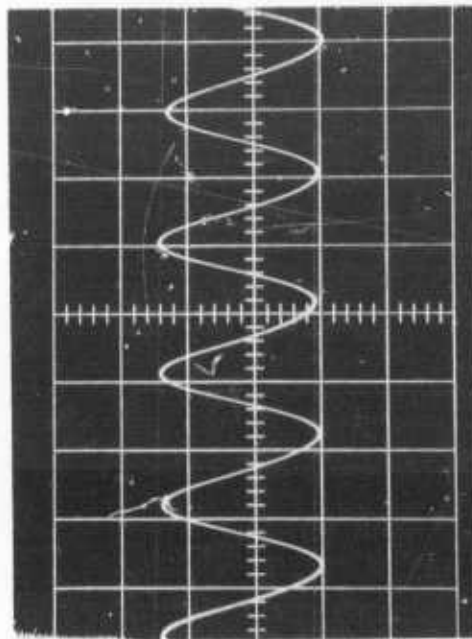
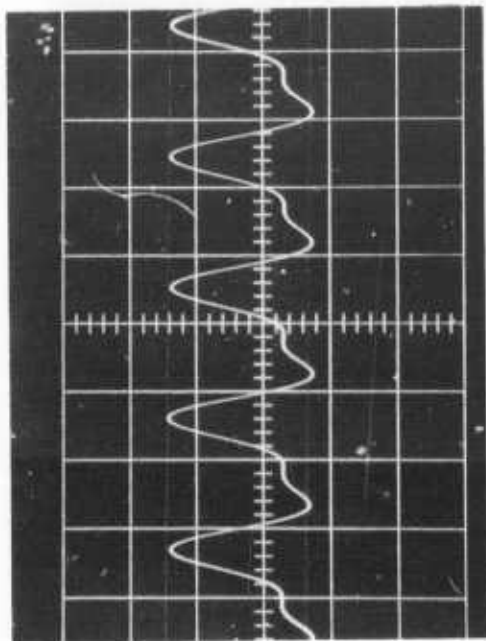
Contract F33615-75-C-1128

LINE-OF-SIGHT STABILIZATION DATA SHEET 6.2

Page 3 of 8
Point 11

Test Setup 746-B1

Test Conditions: 244 Hz \pm 27 μ rad 5-10,000 Hz Detector Bandwidth



Mirror Stabilization ON

Mirror Stabilization OFF

Amplitude p-p (photo) (ON) 2.08 cm (OFF) 2.28 cm

Scale Factor μ rad/cm 38.2

Amplitude p-p (ON) 80 μ rad; (OFF) 87 μ rad

Attenuation $\frac{\text{ON}}{\text{OFF}}$.914 ; dB -.8

Test Date 3-10-76 Engineer CR/ JHB Ellis

FLIR HIGH FREQUENCY STABILIZATION
STUDY PROGRAM

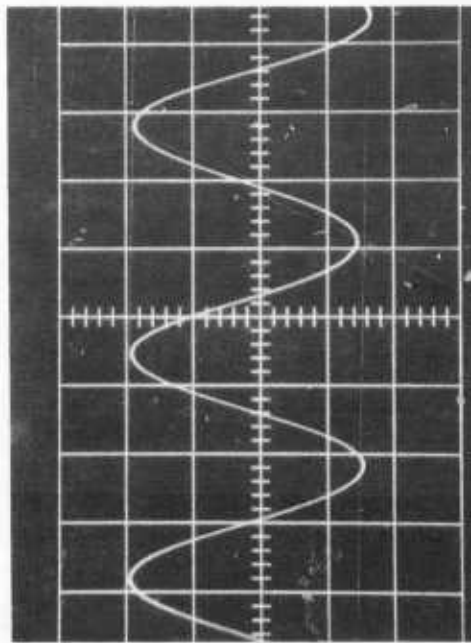
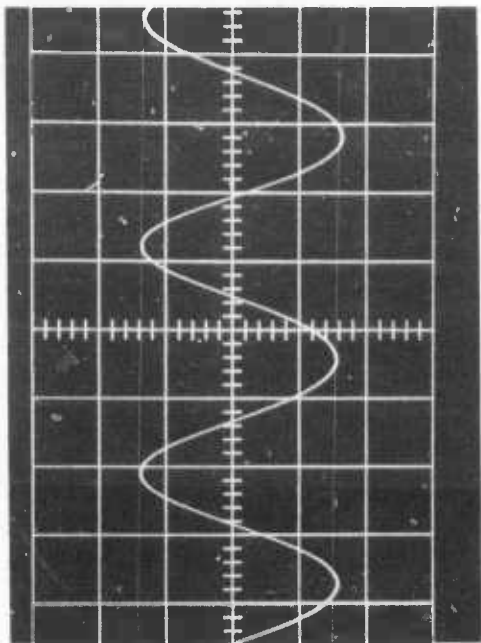
Contract F33615-75-C-1128

LINE-OF-SIGHT STABILIZATION DATA SHEET 6.2

Page 4 of 8
Point 12

Test Setup 746-B1

Test Conditions: 293 Hz \pm 19 μ rad 5-20,000 Hz Detector Bandwidth



Mirror Stabilization ON

Mirror Stabilization OFF

Amplitude p-p (photo) (ON) 2.42 cm (OFF) 3.46 cm

Scale Factor μ rad/cm 19.1

Amplitude p-p (ON) 56 μ rad; (OFF) 66 μ rad

Attenuation $\frac{\text{ON}}{\text{OFF}}$.85 ; dB -1.4

Test Date 3-10-76 Engineer CR / TWELL

FLIR HIGH FREQUENCY STABILIZATION
STUDY PROGRAM

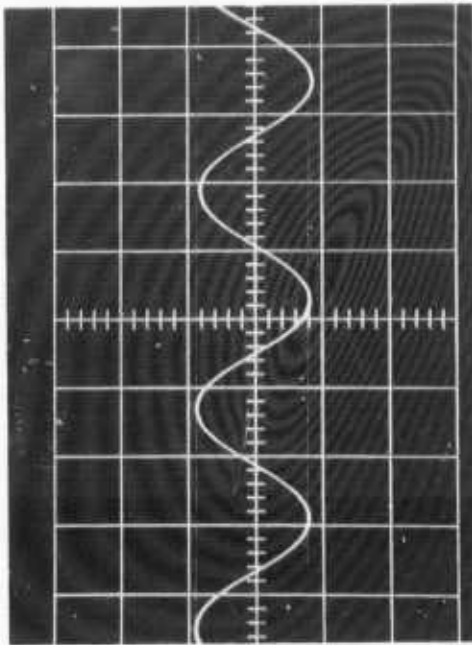
Contract F33615-75-C-1128

LINE-OF-SIGHT STABILIZATION DATA SHEET 6.2

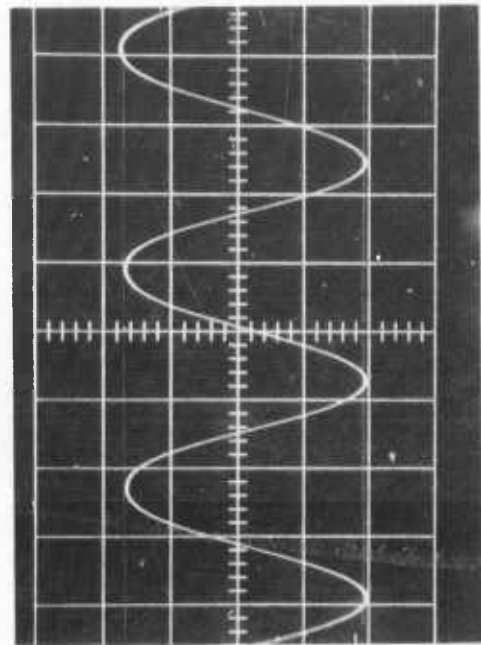
Page 5 of 8
POINT 13

Test Setup 746-B1

Test Conditions: 303 Hz \pm 8 μ rad 5-20,000 Hz Detector Bandwidth



Mirror Stabilization ON



Mirror Stabilization OFF

Amplitude p-p (photo) (ON) 1.68 cm (OFF) 3.60 cm

Scale Factor μ rad/cm 38.2

Amplitude p-p (ON) 64 μ rad; (OFF) 137 μ rad

Attenuation $\frac{\text{ON}}{\text{OFF}}$.467 ; dB -6.6

Test Date 3-10-76 Engineer CR/ JABELLA

FLIR HIGH FREQUENCY STABILIZATION
STUDY PROGRAM

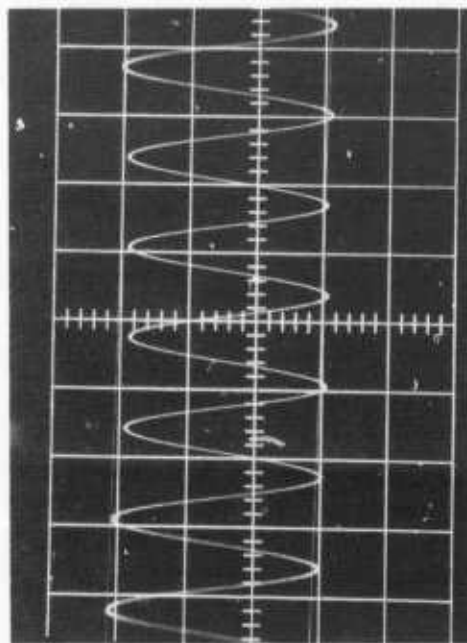
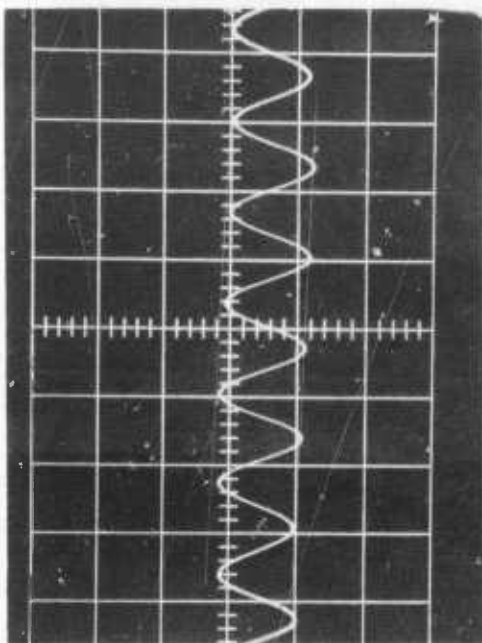
Contract F33615-75-C-1128

LINE-OF-SIGHT STABILIZATION DATA SHEET 6.2

Page 6 of 8

Test Setup 746-B1

Test Conditions: 365 Hz \pm 2.5 μ rad 5-20,000 Hz Detector Bandwidth



Mirror Stabilization ON

Mirror Stabilization OFF

Amplitude p-p (photo) (ON) 1.25 cm (OFF) 2.90 cm

Scale Factor μ rad/cm 19.1

Amplitude p-p (ON) 24 μ rad; (OFF) 55 μ rad

Attenuation $\frac{\text{ON}}{\text{OFF}}$.43 ; dB -7.3

Test Date 3-10-76 Engineer CR/ JAB/ELG

FLIR HIGH FREQUENCY STABILIZATION
STUDY PROGRAM

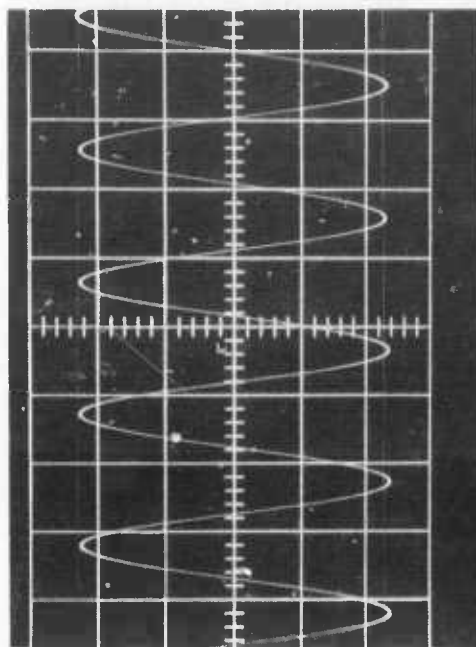
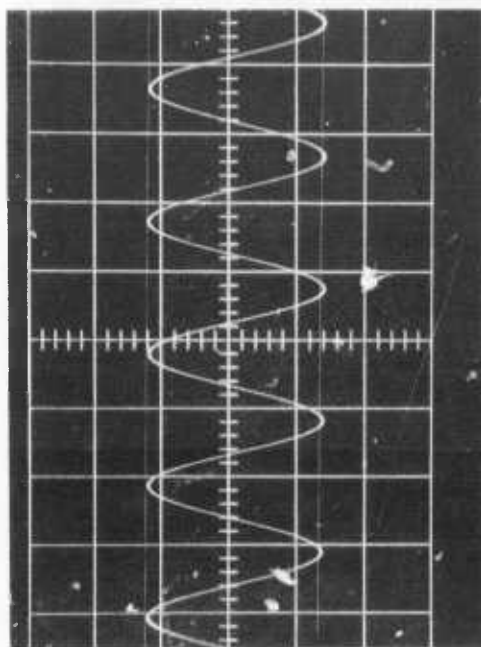
Contract F33615-75-C-1128

LINE-OF-SIGHT STABILIZATION DATA SHEET 6.2

Page 7 of 8
POINT 14

Test Setup 746-B1

Test Conditions: 501 Hz \pm .6 μ rad 5-20,000 Hz Detector Bandwidth



Mirror Stabilization ON

Mirror Stabilization OFF

Amplitude p-p (photo) (ON) 2.54 cm (OFF) 4.65 cm

Scale Factor μ rad/cm 95.5

Amplitude p-p (ON) 242 μ rad; (OFF) 445 μ rad

Attenuation $\frac{\text{ON}}{\text{OFF}}$.546 ; dB -5.25

Test Date 3-10-76

Engineer CR/ JABELL

FLIR HIGH FREQUENCY STABILIZATION
STUDY PROGRAM

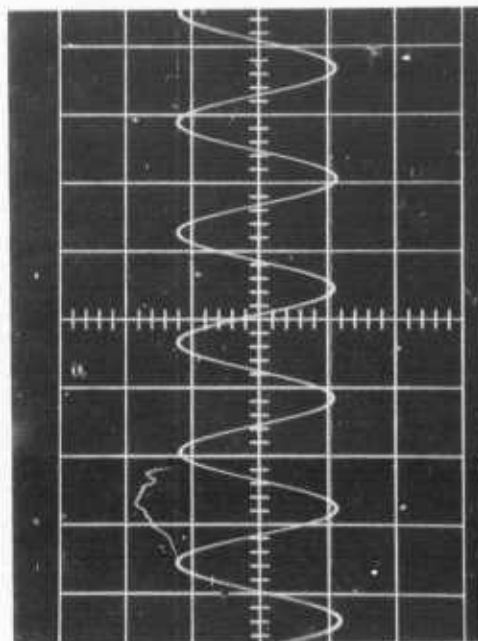
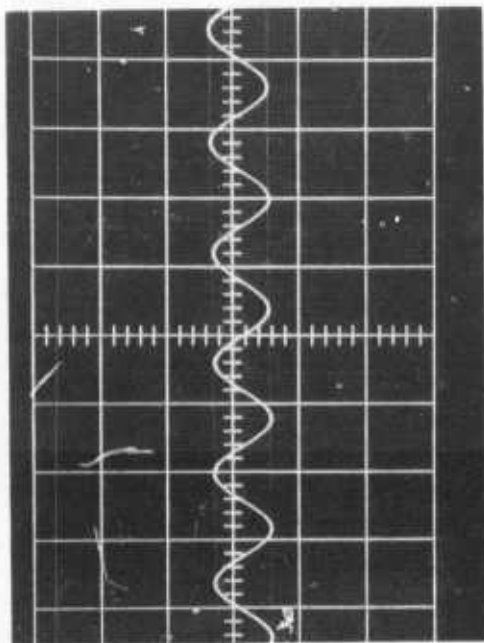
Contract F33615-75-C-1128

LINE-OF-SIGHT STABILIZATION DATA SHEET 6.2

Page 8 of 8
POINT 15

Test Setup 746-B1

Test Conditions: 600 Hz \pm 5 μ rad 5-24,000 Hz Detector Bandwidth



Mirror Stabilization ON

Mirror Stabilization OFF

Amplitude p-p (photo) (ON) .88 cm (OFF) 2.35 cm

Scale Factor μ rad/cm 38.2

Amplitude p-p (ON) 34 μ rad; (OFF) 90 μ rad

Attenuation $\frac{\text{ON}}{\text{OFF}}$.374 ; dB -85

Test Date 3-10-76 Engineer CR/ JWB/ellc

UNCLASSIFIED

AD BO 15295

AUTHORITY:

AFWAL

Tr 18 Sep 81



UNCLASSIFIED